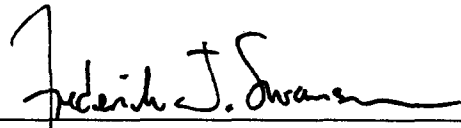# AN ABSTRACT OF THE THESIS OF

Steve Wondzell for the degree of __Doctor of Philosophy__ in
Forest Science presented on January 27, 1994.
Title: Flux of Ground Water and Nitrogen Through the Floodplain of a Fourth-Order Stream.

Abstract approved: _____

Frederick J. Swanson

Changes in the concentrations of dissolved ammonia (NH_4^{+1}), nitrate (NO_3^{-1}), organic nitrogen (DON) were monitored along ground water flow paths to determine the importance of the ground water system to the stream nitrogen budget. The study site was located on a wide floodplain along a fourth-order stream in the Oregon Cascades. A network of wells was installed during the summers of 1989 and 1990. Water table elevations and nitrogen chemistry was sampled seasonally and within individual storm events.

Subsurface flows were dominated by the flow of advected channel water through the gravel bar. Flow rates were correlated to stream discharge during base-flow periods, but did not increase during storms. In contrast, ground-water flows through the aquifer beneath the floodplain were small during base flow, but nearly doubled during storm events. The mean residence time of water stored within the aquifer was long, exceeding 10 days for the gravel bar and 30 days for the floodplain. Even though precipitation inputs to the aquifer during storms equaled 12% of the water stored in the gravel bar and 23% of the water stored in the floodplain, the mean residence time of water remained long.

Subsurface flow through the aquifer adjacent to the stream was a net source of nitrogen to the stream in all seasons of the year and during storms. Flows of water through the conifer forested floodplain supplied most of the nitrogen per unit length of stream - accounting for approximately two-thirds of the estimated flux, most of which is DON. The gravel bar was colonized by red

alder, a nitrogen fixing tree, and on a unit area basis, supplied 2.5 times more nitrogen to the stream than did the floodplain. I estimate that 2 kg ha^{-1} yr^{-1} are leached from riparian forests into the aquifer, and transported to the stream. The study site covered only one-half of the valley floor. Assuming that similar fluxes occurred from the opposite side of the valley, I estimate that 17 g of nitrogen yr^{-1} m^{-1} channel length are input to the stream. The stream is approximately 10 m wide, thus these inputs equal 1.7 g N m^{-2} streambed yr^{-1}.

FLUX OF GROUND WATER AND NITROGEN

THROUGH THE FLOODPLAIN OF A FOURTH-ORDER STREAM

by

STEVE WONDZELL

A THESIS
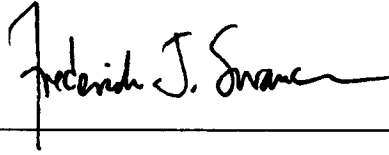
submitted to

Oregon State University

in partial fulfillment of

the requirements for the

degree of

Doctor of Philosophy

Completed January 27, 1994

Commencement June 1994

APPROVED:

Frederick J. Swanson

Professor of Forest Science in charge of major

Head of Department of Forest Science

Dean of Graduate School

Date thesis is presented _____ January 27, 1994 _____

Typed by Steve Wondzell for _____ Steve Wondzell _____

ACKNOWLEDGMENTS

TABLE OF CONTENTS

LIST OF FIGURES

LIST OF TABLES

FLUX OF WATER AND NITROGEN THROUGH
THE FLOODPLAIN OF A FOURTH-ORDER STREAM

CHAPTER 1:
GENERAL INTRODUCTION

Introduction

Interest in valley-floor ground-water systems has increased dramatically over the last decade due to a growing awareness that riparian areas may play important roles in catchment hydrogeochemistry (Bencala et al. 1984, Grimm and Fisher 1984, Stanford and Ward 1988, Pinay and Decamps 1988, Ford and Naiman 1989, Triska et al. 1989, Triska et al. 1990, Hornberger 1991). However, the effects of biochemical transformations occurring in these locations on the forms and concentration of dissolved nutrients in stream water is poorly understood. These effects depend on both the rates of these processes and the rate of flow between the stream and the shallow aquifer.

The subsurface hydrology of shallow aquifers in mountain valleys is complex, with water from a variety of sources flowing within a complex flow net. For this study, it was important to separate water in the shallow aquifer by source, and to be able to identify the zones within the aquifer that were dominated by water from each source. Unfortunately, neither simple descriptions of these systems nor a widely accepted terminology for individual components of flow within the aquifer exists. In this thesis I define two zones - the hyporheic zone and the ground-water zone. The **hyporheic zone**, as used here, includes both the surface hyporheos and the interactive hyporheos, defined by Triska et al. (1989) as zones where interstitial water was >98%, and <98% but >10% **advected channel water**, respectively. Implicit in this definition is the fact that water in stream channels can flow into the shallow aquifer for some distance by advection along gradients in potential energy before being returned to the stream

channel. Further, the hyporheic water is usually a mix of ground water and advected channel water, but may be pure advected channel water in some locations. Because stream water is exchanged between the surface and subsurface environment along flow paths through the hyporheic zone, this process is commonly called **exchange flow**.

I define the **ground-water zone**, like Triska et al. (1989), as the zone in which the water consists of <10% advected channel water. Like Triska et al. (1989), I did not distinguish between water from deeper regional aquifers and water draining from adjacent hillslopes. Although the term "ground water" is commonly used to denote any water found below the surface of the earth, its use here is quite specific, as defined above. Thus the terms "water", "subsurface" or "aquifer" - as in "water flow" or "subsurface hydrology" - have been used, rather than the general term "ground water" throughout this thesis. Please note that in all cases these terms refer to **saturated flow**, unless stated otherwise.

The hyporheic zone has long been known to be biologically active (Coleman and Hynes 1970). Nitrogen in the stream water is transported by exchange flows into the hyporheos where it may be transformed by biochemical processes (Grimm & Fisher 1984, Stanford and Ward 1988, Duff and Triska 1990). The hyporheic zone is typically well aerated (Triska et al. 1989), which allows mineralization of organic carbon (Triska et al. 1990) and nitrification of ammonium (NH_4^+-N). Inorganic forms of nitrogen may be taken up by plants, immobilized by microorganisms, or returned to the stream wherever advected channel water is discharged from the aquifer. In contrast ground water is often anaerobic and either organic-N or NH_4^+-N is the dominant form of dissolved nitrogen. Nitrate (NO_3^--N) is not abundant because it is usually removed from ground water via denitrification (Coats et al. 1976, Rhodes et al. 1985, Peterjohn and Correll 1984, Pinay and Décamps 1988). Where ground water and advected channel water mix, NH_4^+-N supplied in the ground water is rapidly nitrified (Triska et al. 1990).

The objective of this study was to quantify the flux of nitrogen in water flowing through the shallow aquifer beneath a riparian forest and between this

aquifer and the adjacent stream ecosystem along a fourth-order stream in the H.J. Andrews Experimental Forest, Oregon. The specific objectives of this study were: *1) to identify the factors that regulate both the direction and rate of water flow in this shallow aquifer; and 2) to quantify the flux of nitrogen between the riparian forest and stream ecosystem via subsurface flow.*

This thesis is organized in 4 chapters. Chapter #1, an overall introduction to the research project, provides a conceptual model of how, in mountainous landscapes, geomorphic variation controls the flow of water between a stream and its adjacent shallow aquifer. I then tie this model to the development of riparian vegetation communities and the distribution of red alder (*Alnus rubra* Bong.) along stream networks in the Cascades of Oregon. Finally, I use this conceptual model to develop specific hypotheses as to how subsurface hydrology and nitrogen cycling interact to influence stream nitrogen budgets.

Chapter #2 focuses on the subsurface hydrology of the study site. In this chapter, I describe the parameterization of MODFLOW (McDonald and Harbaugh 1988) to estimate the flux of advected channel water and ground water through the shallow aquifer at my study site. I also develop regression equations to relate the water fluxes predicted by this model to stream discharge, and contrast water fluxes during base flows to that occurring during a storm event. Chapter #3 describes the patterns observed in dissolved nitrogen concentrations among seasons and within storm events for wells located with each landform at the study site. Finally, Chapter #4 builds on the preceding two chapters, using long-term records of stream discharge to estimate total water flux for each season of a "typical" water year. I then combine the estimates of annual water flux with the mean concentrations of dissolved nitrogen to estimate both the seasonal and annual flux of nitrogen from the aquifer beneath the riparian forest ecosystem into the adjacent stream.

Conceptual Model

An understanding of geomorphic processes has been useful for classifying landforms within mountain stream valleys and for synthesizing information on forest-stream interactions at a variety of scales (Vannote et al. 1984, Frissell et al. 1986, Swanson and Sparks 1990, Grant et al. 1990, Gregory et al. 1991). This work has focused on surface and above-ground features, but largely ignored forest-stream interactions that occur as a result of the flow of water between the aquifer and the stream. I use this classification to develop a conceptual model describing both the location and extent of the hyporheic and ground-water zones and to predict the fluxes of both advected channel water and ground water through these zones.

Stream and Subsurface Hydrology

The flow of water is driven by gradients in potential energy, usually expressed as a difference in head across some distance. In a valley floor, the spatial pattern of head differences results from the pattern of landforms and channels, which control the direction, location, and rate of water flow between the shallow aquifer of a floodplain and the adjacent stream. There are two important sources of spatial variation to consider (Meyer et al. 1988, Sedell et al.1989, Swanson and Sparks 1990): the variation between stream reaches in the lateral extent of valley floor, the types of landforms present, and their spatial arrangement which I refer to as **lateral variation**; and the variation along the length of the stream network from headwater streams to rivers which I refer to as **longitudinal variation**, which follows the ideas of the stream continuum theory of Vannote et al. (1980) and Minshall et al. (1983).

Lateral variation. Stream reaches have been broadly categorized by the degree to which hillslope processes (eg. landslides), bedrock, and other features constrain both the width of the valley floor and the lateral migration of the active stream channel (Schumm 1977, Grant et al. 1990, Gregory et al. 1991). In constrained reaches the width of the active valley floor is less than twice the width of the active channel and floodplain and terrace deposits are limited. A narrow gorge where water might flow directly over bedrock or over a thin veneer of coarse sediments would be an example of a constrained reach. In unconstrained reaches valley floors are wider, and can exceed 100 m in width in third- to fifth-order streams, even in steep, mountainous areas.

In unconstrained reaches, head differences that drive subsurface flows may develop from geomorphic influences at three distinct spatial scales: 1) the individual channel-unit scale; 2) a sub-reach (or inter-channel) scale; and 3) the entire stream-reach scale. Of course, geomorphic influences would be limited to the individual channel-unit scale in constrained stream reaches because valley-floor landforms are lacking.

At the scale of individual channel units (Grant et al. 1990), sequences of alternating pools and riffles change the longitudinal gradient of the stream, producing gradients in potential energy that result in the advective flow of channel water downward into the streambed, and horizontally into the streambank. Variation in the depth of sediment or in the saturated hydrologic conductivity can also result in the advective flow of channel water into the hyporheic zone at this scale. These processes have been described by Vaux (1962) and Harvey and Bencala (1993).

At the sub-reach scale within the floodplain, the preferential, subsurface flow of water in either relic (buried or inactive) or secondary channels seems to dominate subsurface flow paths (described in this study, Chapter 2). I predict that longitudinally continuous deposits of coarse sediment, such as gravel and cobbles in relic channels, have much higher saturated hydraulic conductivities than do intervening areas of finer textured sediment. If these channels are connected to the main stream at their lower end, outflow from the channel will

create potential gradients within the aquifer resulting in flow of channel water from the stream or ground water from the floodplain into the relic channel. Similarly, if these channels are connected to the mainstream at their head, but are blocked before re-entering the stream, the flow will be the reverse of that described above. The potential gradients created by the influence of relic and secondary channels results in the advective flow of channel water over horizontal distances of ten or more meters into the floodplain, facilitating the development of laterally extensive hyporheic zones.

At the scale of the entire stream reach, the slope of the aquifer along the length of the valley in unconstrained stream reaches maintains a potential gradient that results in a net down-valley flow of subsurface water. Thus, I predict that aquifers should be recharged with advected channel water at the heads of unconstrained reaches, where the valley floor widens. Conversely, subsurface water should be discharged to the stream at the lower end of an unconstrained reach, where the valley floor once again becomes constricted.

The combined effects of processes operating at these three spatial scales result in complex patterns of subsurface flow of water within the floodplain of mountain stream valleys. These patterns of flow are further complicated by the distinct differences in the wet and dry seasons of the Pacific Northwest. I predict that seasonal changes in the input of water to the aquifer from tributary channels, precipitation, and from the adjacent hillslopes could have major effects on flow paths, residence times, and the distance to which advected channel water recharges the shallow aquifer beneath the floodplain. Harvey and Bencala (1993) showed that advective flow of channel water into the subsurface at the channel-unit scale ceased when the catchment was wet and flux of ground water from adjacent hillslopes was large. Similarly, increased inputs of ground water via saturated or unsaturated flow from adjacent hillslopes may reduce or even eliminate advection of channel water into the subsurface at either the sub-reach or reach scales described above.

Longitudinal variation. I predict that the potential influence of the hyporheic zone on stream water chemistry should vary along the stream continuum. The limiting hydrologic factors should be: 1) the rate of flow between the stream and subsurface, relative to the stream discharge, and 2) the residence time of the water in the subsurface. The rate of flow between the stream and subsurface should, in turn, be limited by the area of the wetted streambed through which water must flow, the hydraulic conductivity of the streambed, and the potential gradient between the channel and the subsurface. The ratio of the wetted streambed area to stream discharge should predict how the wetted streambed area may limit the effect of the hyporheic zone on stream water chemistry. Data from G. Lienkaemper (unpublished) collected from the Lookout Creek catchment (Fig. I.1) clearly illustrate this point (Table I.1). Assuming that the conductivity of the streambed is constant for steep-gradient, gravel- and cobble-bedded streams of first- through fifth-order within the catchment, for a given potential gradient, the relative rate of flow between the stream and subsurface should be greatest in first-order streams due to the large area of wetted streambed relative to discharge. Larger streams should have lower relative rates of flow because stream discharge is many times greater and the wetted streambed area across which exchange must take place is proportionally smaller.

The influence of the hyporheic zone on stream chemistry will also be a function of the rate of biochemical transformations occurring in the hyporheic zone and the residence time of the water in the subsurface. In the geologically young landscape of the Cascade Mountains, first-order streams are usually highly constrained, with poorly developed floodplains and riparian vegetation (Swanson et al. 1982a). These streams often flow directly over bedrock, or over a thin veneer of gravel and cobbles, and the extent of the hyporheic zone is restricted to the sediment of the immediate channel bed.

This conceptual model would predict that the residence time of water in the hyporheic zone of first-order mountain streams should be short, due to the small size of the hyporheic zone and the high saturated conductivity of the gravelly and cobble sediment. Further, inputs of ground water to the stream

Fig. I.1. H. J. Andrews Experimental Forest (Lookout Creek catchment)
showing the stream network, and the location of the study site along
McRae Creek. Inset shows the location of the H.J. Andrews
Experimental Forest within Oregon.
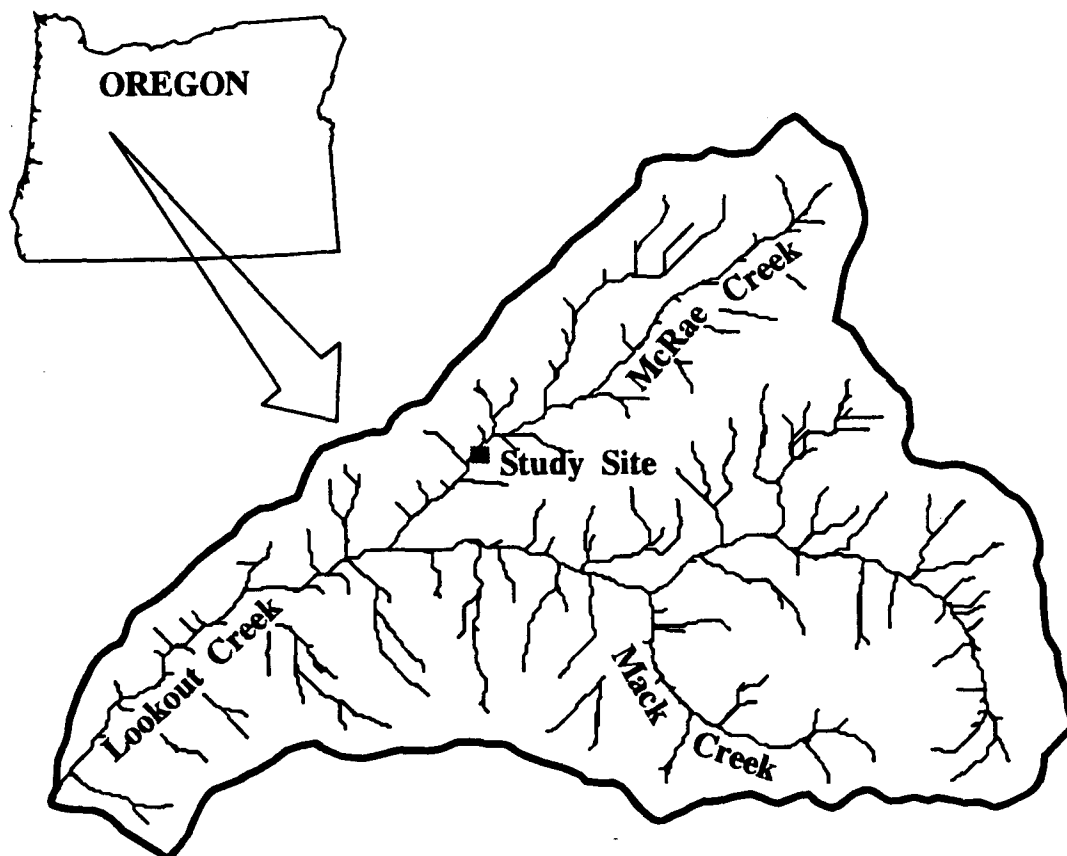
Table I.1. Calculated wetted stream bed area per unit length of stream, stream discharge, and area to discharge ratio for representative streams of each order in the Lookout Creek Catchment. Wetted surface area is equal to the wetted perimeter times a unit channel length. (G. Lienkaemper, USDA Forest Service, unpublished data).

Order	Wetted Surface Area (m^2)	Stream Discharge (m^3/s)	Ratio: Area to Discharge
1	2.36	0.005	487.60
2	4.36	0.026	167.37
3	8.34	0.369	22.59
4	12.10	1.558	7.77
5	15.30	3.256	4.70

channel from the adjacent hillslopes would be large. Consequently, I predict that the chemistry of stream water in first-order streams would be dominated by biochemical transformations occurring in the soil, or other terrestrial portions of headwater catchments, rather than in the hyporheic zone (Wallis et al. 1981). This prediction is supported by the nitrogen budget constructed for the first-order stream draining Watershed 10, H. J. Andrews Experimental Forest (Triska et al. 1984) which showed that ground water accounted for 70% of the total nitrogen input to the stream channel.

Constrained reaches of larger streams (fourth- through fifth-order) are geomorphically similar to first-order streams in that they are also highly constrained, with poorly developed riparian vegetation (Swanson et al. 1982a). These streams often flow directly over bedrock, or over a thin, patchy veneer of gravel and cobbles, and the hyporheic zone is restricted to the sediment of the immediate channel bed. However, most of the stream water in higher-order stream reaches consists of inputs of stream water from upstream reaches - water that originally entered the channel network higher in the catchment. Extending the stream continuum theory (Vannote et al. 1980, Minshall et al. 1983), the chemistry stream water will be little effected by biochemical processes occurring adjacent to these larger streams because of the volume of stream water flowing in the channel.

In contrast, unconstrained reaches of third-order and larger streams have wide valley floors where floodplains and associated riparian vegetation are well developed. I predict that the greatest extent of the hyporheic zone would occur in unconstrained stream reaches where the wetted streambed area is large and where valleys contain relatively extensive sediment deposits. Although the hyporheic zones may reach their maximum extent along the largest streams and rivers, their influence on water chemistry would be swamped by the effect of upstream inputs in streams where discharge is high. On the basis of this conceptual model, I would predict that the relative influence of the hyporheic zone on stream-water chemistry would be greatest in the unconstrained stream reaches of the smallest streams within the network. First- and second-order streams are typically incised

in deep V-shaped valleys so that unconstrained stream reaches are first found along third-order streams on the west slope of the Cascade Mountains in Oregon.

The texture of sediment deposited within the valley floor also determines the extent of the hyporheic zone and the rate of water flows between the hyporheic zone and the stream. The hyporheic zone only extends a few tens of cm from the streambed in fine-textured sediment (Cummins et al. 1975, Triska et al. 1989) but tens to hundreds of meters in coarse-textured sediment (Triska et al. 1989), and in one extreme case, 2 km from a boulder bedded river channel (Stanford and Ward 1988). Streambed materials in high gradient mountain streams tend to be a poorly graded mix of cobbles, gravel and sand with high saturated hydraulic conductivities. Therefore, the hyporheic zone may well be extensive.

Nitrogen Cycling

Influence of hillslope ground water drainage. A water budget constructed for the first-order stream draining Watershed 10, H. J. Andrews Experimental Forest indicates that 65% of the precipitation (160 cm yr^{-1}) is exported as stream flow (Sollins et al. 1980, Waring & Schlesinger 1985). This water transported approximately 330 kg $ha^{-1}yr^{-1}$ of inorganic and organic solutes (Swanson et al. 1982b) from the adjacent hillslopes to the stream. Because of the development of the drainage network, 53% of the area of the Lookout Creek catchment drains directly into first-order streams (Table I.2). Data from Watershed 10 would indicate that the stream water chemistry should be dominated by the solutes dissolved in hillslope drainage water.

Much of the total channel length of third- through fifth-order steams is also constrained and subsurface water flows directly to the stream channel. However, the magnitude of hillslope ground water inputs is small relative to the total volume of water flowing in the channel, and should have relatively little influence on the stream water chemistry. For example, assuming a constant unit

area discharge, ground-water inputs from hillslopes adjacent to the channel of fifth-order lower Lookout Creek should account for only 4% of the total annual discharge from the catchment (Table I.2).

Little of the total channel network in the Lookout Creek basin lies in unconstrained stream reaches, and most of that is restricted to third-order or larger streams. Sediment within wide valley floors contain shallow aquifers. Water and dissolved solutes draining from adjacent hillslopes must enter these aquifers before reaching the stream channel. The residence time of water in the ground water system are long and the dissolved nutrients transported in the ground water can be biochemically transformed. Thus as stream order increases, stream water chemistry should reflect the chemical signature of channel water imported from upstream rather than the effect of biogeochemical processes occurring in the aquifer within the riparian zone of unconstrained stream reaches.

Nitrogen dissolved in ground water draining from the soils of upland old-growth Douglas-fir forests is the primary source of nitrogen for first-order streams, supplying more than 70% of the total nitrogen input to a stream (Triska et al. 1984). The forest canopy is continuous over small streams, consequently primary productivity in is light limited, the uptake of dissolved nitrogen by photoautotrophs is low and approximately 75% of total nitrogen inputs are lost to downstream transport (Triska et al. 1984). The upland forest canopy is not continuous over the channel of third-order and larger streams. Because of the increased availability of sunlight, nitrogen transported in the stream water from headwater reaches is rapidly depleted. Because nitrogen inputs from these sources are relatively small, primary productivity becomes nitrogen limited (Gregory 1979).

Interaction between the stream and floodplain. In small, mountain streams, most bacteria and algae are not suspended within the water, but on sediment surfaces (Hynes 1970, Vannote et al. 1980, Wallis et al. 1981, Minshall et al. 1983). Many studies have shown the importance of benthic communities to

Table I.2. The proportion of the total channel length with the stream network, and the proportion of the total chatchment area within the Lookout Creek catchment draining directly to the channel in streams of each order. Mean annual discharge for stream of each order. (G. Lienkaemper, USDA Forest Service, unpublished data).

Order	Proportion of Channel Length (%)	Proportion of Catchment Area (%)	Mean Annual Discharge (l s^{-1})
1	53	66	5
2	23	16	26
3	13	10	369
4	5	4	1558
5	6	4	3256

biochemical transformations (Hynes 1970, Dahm 1980, Bott et al. 1984, Loch et al. 1984, Pringle and Bowers 1984, Pringle 1987). However, subsurface epilithic communities also play important roles in stream ecosystems (Hynes 1983, Mickleburgh et al. 1984, Grimm and Fischer 1984, Loch et al. 1984). The chemical transformations involved in the cycling of nitrogen within ecosystems are primarily mediated by living organisms, consequently, it seems reasonable to expect that the rates of many biogeochemical transformations on nitrogen should be a function the surface area of sediment and the residence time of water in contact with these surfaces.

In high gradient mountain streams where the streambed is armored by stones and cobbles, the total surface area of sediment on the streambed is small in comparison to that of the subsurface environment where interstitial spaces between large cobbles are typically filled with sand and gravel. Therefore the flow of water between the stream and the subsurface, and the residence time of the water in the subsurface may be major factors regulating nitrogen cycling within stream ecosystems. The conceptual model presented above suggests that the relative importance of the hyporheic and ground-water zones would be greatest in unconstrained reaches of intermediate sized streams (third- to fourth-order). If the subsurface is a critical location for nitrogen transformations, flow of channel water through the hyporheic zone could reduce spiraling lengths (Elwood et al. 1983, Newbold et al. 1983) and contribute to the tight cycling of nitrogen in this transport-dominated environment.

If additional sources of nitrogen were available to the stream, they could be a major factor regulating stream productivity. Red alder, a nitrogen fixing, early successional species (Worthington 1965, Bollen and Lu 1968), colonizes frequently flooded or recently disturbed surfaces along the margins of larger streams. Flows of advected channel water beneath these alder stands could potentially leach nitrogen from the riparian zone and transport it to the stream. The sites along constrained stream reaches colonized by alder are typically narrow and discontinuous, seldom exceeding a few meters in width. In contrast, the valley floor is wide in unconstrained stream reaches and a variety of

landforms, including floodplains and terraces develop between the stream and adjacent hillslopes. During peak flow water may spread laterally across the floodplain, re-occupy old channels, and even cut new channels. Thus, physical interactions between the stream and adjacent terrestrial ecosystems in unconstrained stream reaches frequently result in disturbance. In these locations gravel bars are extensive, often exceeding 10 m in width. Lateral bars are present along either or both sides of the channel for much of its length, and it is common to find bars within the active stream channel. In most cases, these gravel bars are dominated by red alder.

Studies using the acetylene reduction method estimate that red alder may fix as much as 60 to 70 kg N ha^{-1} yr^{-1} (Tripp et al. 1979, Bormann and Gordon 1984). Studies based on stand age suggest that the accumulation rates of nitrogen in the forest floor and mineral soil beneath red alder stands are high, ranging from 85 kg ha^{-1} yr^{-1} (Cole et al. 1978) to 320 kg ha^{-1} yr^{-1} (Newton et al. 1968). Bormann and DeBell (1981) estimated a mean annual accumulation rate of 100 kg ha^{-1} yr^{-1}, with 15% accumulating in the forest floor, 35% in the surface soil horizons between 0 and 20 cm, 30% accumulating between 20 and 50-cm depth, and the remainder stored in biomass. However, these estimates were made in deep, well drained forest soils. In contrast, the soils of the gravel bars colonized by alders are young and poorly developed, with very high contents of cobble, gravel and coarse sand, without appreciable accumulation of organic material on the surface and with relatively shallow depths to the aquifer.

Rates of nitrogen fixation have not been estimated for riparian environments, but there is no reason to expect that they would be dramatically different than in uplands. Further, since the soils of the gravel bar environments are poorly developed it seems reasonable that leaching losses would be greater in this environment than in deep, well developed, upland soils. Thus, stands of red alder may represent a significant source of nitrogen to the stream ecosystem.

Objective and Hypotheses

The objective of this study was to quantify the effect of subsurface flows on the transport of nitrogen between the riparian forest and adjacent stream ecosystem. I choose a study site along a fourth-order unconstrained reach of a mountain stream, where I predict that subsurface flows have their maximal influence on the nitrogen budget of the stream. The conceptual model presented above predicts that the relative magnitude of subsurface flows would be largest in this location and that nitrogen fixed by red alder in this location may be a significant source of nitrogen to the stream. However, neither the rates of subsurface flows through either the hyporheic or ground-water zone nor the transport of dissolved nitrogen have been quantified. The specific hypotheses tested were:

Hypothesis 1: The shallow aquifer beneath the floodplain is maintained year round by both advected channel water and ground water draining from hillslopes. Recharge of the shallow aquifer underlying the riparian forest with advected channel water dominates subsurface flow paths during the summer dry season when tributary and hillslope inputs are minimal. Ground water from the adjacent hillslopes dominate subsurface fluxes through the shallow aquifer during the wet winter season. Thus, subsurface flow paths reflect the relative magnitude of water input from each source.

Hypothesis 2: Relatively rapid changes in subsurface flow paths occur during storm events. The residence times and flow paths of water flowing through the aquifer are long during the dry summer months. In contrast, during storm events, large pulses of water flow into the aquifer from tributary channels and adjacent hillslopes and shorten the mean residence time of water stored there. These inputs also limit the distance to which advected channel water can flow into the aquifer, thereby reducing the extent of the hyporheic zone during the winter.

Hypothesis 3: Riparian forests and the associated shallow aquifer act as net sinks for nitrogen transported in the stream water during the summer dry season. During the summer, both stream and subsurface water is warm and

vegetation is actively growing and photosynthesizing. Rates of nitrogen uptake and denitrification are expected to be high during this period. Additionally, mean residence times are expected to be longer during the summer, leading to an expansion of anaerobic environments and extending the length of time that dissolved nitrogen can be transformed or taken up.

Hypothesis 4: During the winter wet season the riparian zone is a net source of nitrogen to the stream. Since microbial processes slow at cold temperatures, and since most of the vegetation is dormant during the winter, nitrogen is less likely to be transformed during the winter months. Further, the soils of the riparian zone are flushed with water from precipitation and the water table rises, exposing more of the soil profile to leaching. Thus, both the hyporheic and ground-water zones are expected to leak nitrogen during the winter months, especially when peak discharges move large volumes of water through the aquifer.

Hypothesis 5: Red alder-dominated gravel bars are the primary source of nitrogen from the floodplain to the stream ecosystem. Stands of red alder growing on recently disturbed sites along third- to fourth-order stream channels fix large quantities of nitrogen. Their location corresponds to areas in which the rate and magnitude of subsurface flows and the size of the hyporheic zone are largest relative to stream discharge. Due to the poorly developed soils, leaching losses of this fixed nitrogen are high and advected channel water flowing through these sites is enriched in nitrogen, especially NO_3^--N. Since the advected channel water is highly oxygenated, denitrification losses are small, and most of the nitrate is flushed to the stream. Conifers dominate other sites on the floodplain, but due to shallow rooting and greater depths to the water table, the terrestrial system is relatively isolated from the ground water and is not a significant source of nitrogen to the stream.

Hypothesis 6: Nitrogen transformations occurring in the aquifer over the course of the year result in a net increase in the nitrogen load of water draining from the fourth-order watershed.

CHAPTER 2:
SUBSURFACE WATER FLOW THROUGH THE FLOODPLAIN OF A FOURTH-ORDER MOUNTAIN STREAM: SEASONAL AND STORM DYNAMICS

List of Terms and Abbreviations

Much of the terminology used in ground-water modeling is specialized, and some of the terms used in this thesis may be specific to MODFLOW and not widely used among hydrologists. Further, this thesis is.inter-disciplinary in scope, and some of the terms, like stress period, will have a different meaning to ecologists than to hydrologists. Consequently, the meanings of some terms may not be immediately obvious. I have not coined new terms, but rather followed the terminology used by the original authors of MODFLOW (McDonald and Harbaugh 1988), which has found its way into at least some of the ground-water modeling literature (for example, see Anderson and Woessner 1992). Essential terms and abbreviations are defined below.

Advected Channel Water - subsurface water that has flowed into the aquifer from the stream channel along head gradients. Contrast with **Ground Water**.

GHB cell - General Head Boundary cell. These cells are used to specify **general** conditions at the edge of the model domain (**boundary**) where flow into (or out of) the model is a function of a specified **head** and a conductance. These cells are an infinite, external source (or sink) of water for the model. The flux into the model is equal to the difference between the specified head of the external source and the head in the GHB cell, multiplied by the conductance. The conductance equals the saturated hydraulic conductivity multiplied by the cross sectional area through which flow occurs and divided by the distance.

Thus:

$$Q_{GHB} = CONDUCTANCE_{GHB}(HEAD_{GHB}-HEAD_{CELL}) \quad \text{and}$$

$$CONDUCTANCE_{GHB} = k_{GHB}(HEIGHT \times WIDTH)/LENGTH$$

Ground water - the water from either deep, regional aquifers or water draining from soils on the adjacent hillslopes. Advected channel water is **not** considered ground water.

MR - Mean of Residuals: $\qquad \sum_{i=1}^{n} \dfrac{(y_i - \hat{y_i})}{n}$

MAR - Mean of the Absolute Value of Residuals: $\qquad \sum_{i=1}^{n} \dfrac{|(y_i - \hat{y_i})|}{n}$

MODFLOW - MODular three-dimensional, finite-difference, ground water FLOW model written by McDonald and Harbaugh (1988). The model is highly flexible due to its modular structure. For example see STR1.

Nodal Spacing - Distance between the centers of adjacent elements (or grid cells) in the model. MODFLOW uses a block-centered grid, thus the nodes are located at the center of each grid cell.

Steady State Simulation - Flows of water into and out of each cell are equal. Thus, there is no change in water table levels within the modeled aquifer. Under steady state conditions there is no need for multiple stress periods or time steps because the model solution is not time dependent.

STR1 - Stream Module, version 1 (Prudic 1989). This module simulates flow between a stream and an underlying grid cell. As for GHB cells, flow is a function of the difference between the specified head of water in the stream above the cell and the head of the subsurface water in that cell, multiplied by the conductance through the streambed. The conductance of the streambed is equal to the saturated hydraulic conductivity times the area of the streambed divided by the thickness of the stream bed.

Stress Period - **Period** of time during which boundary conditions are constant (boundary conditions can be changed between stress periods). When

boundary conditions are changed, water table levels will not be in equilibrium with flows into or out of the model - thus creating a **stress** on the modeled system. A stress period generally consists of many time steps, and during each time the step water water will flow between cells and water table levels may change.

Transient Simulation - Transient simulations are composed of a sequence of Stress Periods. Because boundary conditions can be changed between stress periods, fluxes into and out of the model, and water table levels in each cell, are likely to change. A transient simulation usually uses the head distribution predicted from a steady state model run to specify the initial head for each cell in the model domain. In subsequent stress periods, boundary conditions are changed, thereby changing fluxes into and out of the model domain. The model then calculates the flows of water between grid cells as well as the changes in water table levels for each cell at each time step.

Introduction

The subsurface hydrology of shallow aquifers in mountain valleys is complex, with water from a variety of sources flowing within a complex flow net. It is commonly assumed that precipitation and subsequent drainage of water from adjacent hillslopes are the primary inputs to floodplain aquifers (Wallis et al. 1981), and that ground water flows in a down-valley direction or at an angle towards the stream. Ground-water is discharged to the channel through either the bank or streambed so that most stream reaches in mountain valleys are influent - or gain water over their length from ground water discharge. These patterns of flow have been shown in many studies (for example: Wallis et al. 1981, Larkin and Sharp 1992, McDowell et al. 1992, Jordan et al. 1993). Thus, as noted by Hynes (1983), it may be surprising that several studies (Triska et al. 1989, Harvey and Bencala 1993) have documented the flow of water from stream channels, into the streambed and laterally into the adjacent aquifer, even in influent stream reaches.

The factors that control the flow of channel water into the streambed (Vaux 1962, 1968, Savant et al. 1987), and laterally for short distances into the stream bank (Harvey and Bencala 1993), have been described. However, advected channel water may flow more than 10 m from the stream channel in some locations (Triska et al. 1984, Castro and Hornberger 1991). The factors that control flows over these larger distances are largely unexplored. Further, little is known about how changes between dry and wet seasons, or between baseflow and stormflow periods, affect flow patterns. Meyer et al. (1988) assumed that the advection of channel water into the subsurface will increase with increasing stream discharge, but there is little evidence to support this idea. Variation in streambed topography are the primary factor driving exchange flows (Vaux 1962, 1968, Savant et al. 1987, Harvey and Bencala 1993). Yet, as flow increases and water levels rise, the effect of topographic variation is drowned out (Grant et al. 1990, Gregory et al. 1991). Further, Harvey and Bencala (1993) showed that increased drainage of ground water from adjacent side slopes during

snow melt prevented advection of channel water into the floodplain. Clearly, the complexities of the subsurface flow through shallow aquifers in mountain stream valleys are poorly understood.

The objective of this study was to estimate the flux of both advected channel water and ground water through a shallow aquifer adjacent to a small mountain stream. This study was specifically designed to investigate changes in both the direction and rates of subsurface flows under the range of stream discharges observed for each season of the year, as well as the changes that occur when stream discharge increases during storms. Unfortunately, subsurface flows cannot be measured directly. Consequently, the approach used here was to calibrate the numerical flow model, MODFLOW (McDonald and Harbaugh 1988), to predict the head observed within a network of wells. The calibrated model was then used to estimate fluxes of both advected channel water and ground water through the subsurface.

I used this approach because a calibrated flow model can be used to synthesize field data and to explore the dynamics of ground water flow under changing conditions. This approach is not without problems, however. Flux estimates are proportional to hydraulic conductivity (k), which is inherently difficult to measure. This uncertainty is greatly exacerbated if independent flux estimates are not available to constrain the model predictions. Model predictions may also be influenced by scale effects that can not be simulated even using very fine spatial resolution. However, a variety of ground water flow models are widely available, several of which are well documented and have been applied a variety of ground-water flow problems. Although data needs are intensive, the approach is convenient in remote locations where detailed geohydrologic information is limited or lacking. A network of simple wells can be installed into shallow stream-side aquifers for little cost; heads can be easily measured within a well; wells can be easily surveyed; and slug tests can be used to estimate the saturated hydraulic conductivity at each well.

Methods

Site Description

The study site (Fig. I.1) is located along McRae Creek, a fourth-order stream within the Lookout Creek catchment and the H.J. Andrews Experimental Forest in the western Cascade Mountains of Oregon (44° 10' N, 122° 15' W). Most of the area is in primary Douglas-fir forest (*Pseudotsuga menziesii* (Mirbel) Franco.) and western hemlock (*Tsuga heterophylla* (Raf.) Sarg.) forest. A network of logging roads was constructed within the catchment and approximately 24% of the area has been clearcut and regenerated in Douglas-fir plantations since 1950. Primary logging roads continue to be maintained within the catchment to provide research access.

The drainage area above the study site is 1,400 ha, and elevation within the catchment ranges from 600 m at the study site to 1,600 m along the drainage divide. At elevations above 1,000 m snow accumulates during the winter; at lower elevations, snow falls during cold winter storms but is melted during warmer rain storms so that in most winters there is not a seasonal snow pack at the study site. Average annual precipitation is approximately 2,500 mm, falling mainly between November and March (Bierlmaier and McKee 1989). Stream discharge was highly variable over the study period, ranging from a low of 400 m^3 h^{-1} during September or October, to 2,200 m^3 h^{-1} during base flow periods throughout the winter, and with peak flows during fall and winter storms exceeding 20,000 m^3 h^{-1} .

The instrumented study site is 250 m long and 80 m wide. It is located along the eastern bank of an unconstrained stream reach in which the entire valley floor exceeds 100 m in width (Fig. II.1). Within this reach alluvial sediment has been reworked by lateral channel migration. A layer of rounded, stream-worked cobbles underlies the entire floodplain. However, the depth to this layer varies depending on the thickness of overbank deposits. A complex of landforms is

Fig. II.1. McRae Creek study site showing landforms, vegetation types, and well locations.
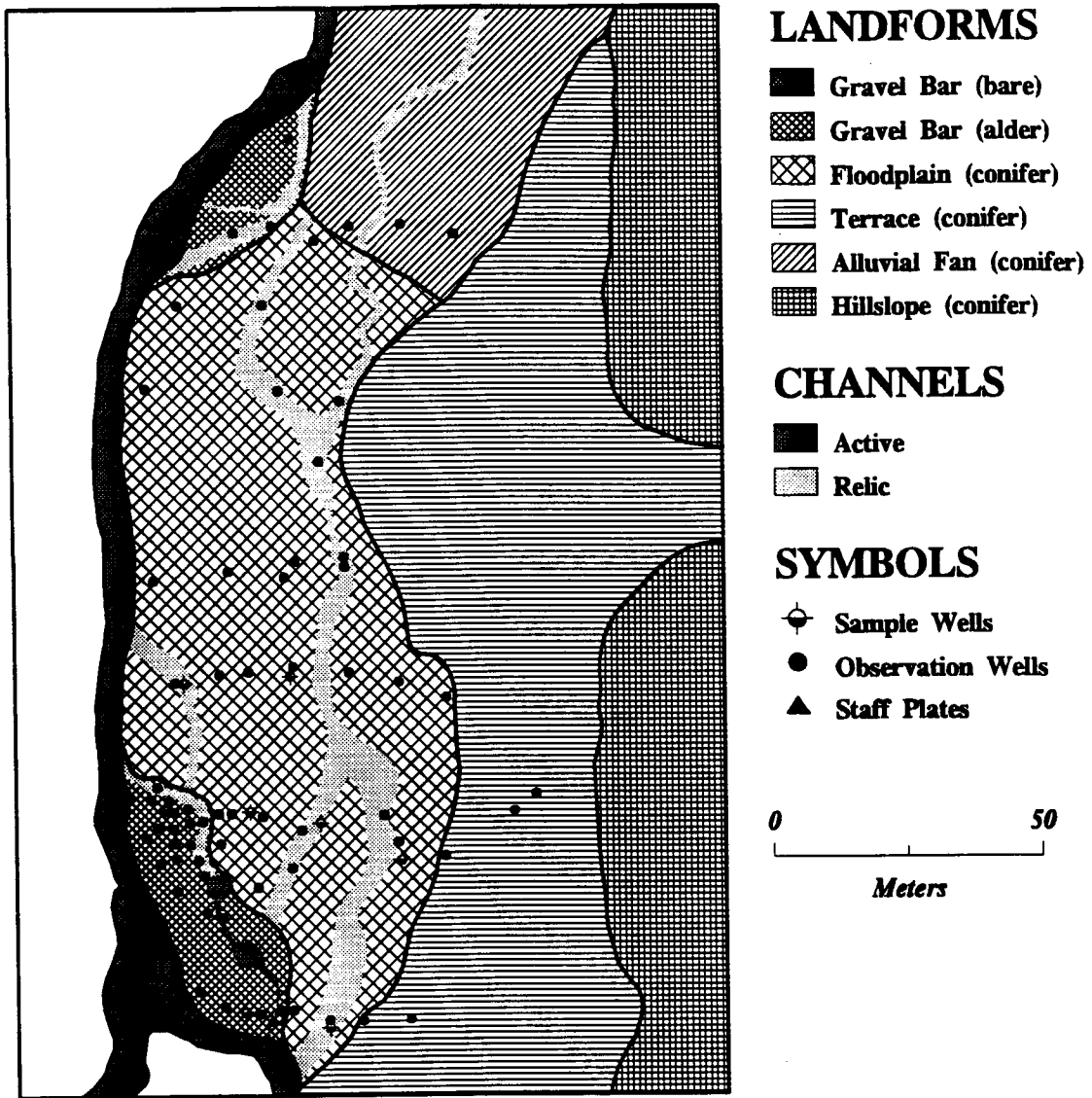
LANDFORMS

- ■ Gravel Bar (bare)
- ▨ Gravel Bar (alder)
- ▧ Floodplain (conifer)
- ▤ Terrace (conifer)
- ▨ Alluvial Fan (conifer)
- ▦ Hillslope (conifer)

CHANNELS

- ■ Active
- ▢ Relic

SYMBOLS

- ⚲ Sample Wells
- ● Observation Wells
- ▲ Staff Plates

0   50

Meters

present within the study site, including recently formed gravel bars, older floodplain surfaces, relic channels, and terraces.

The study site was staked on a 10 x 10 m grid, and used as a base for mapping the major surface features of the valley floor and boundaries between the valley floor and adjacent alluvial fans, terraces and hillslopes. Elevations for the stream boundary were surveyed by stretching a measuring tape down the center of the stream, surveying the elevation of the stream bed, and recording the depth of water at 1 m intervals. All elevations for the entire study site were referenced to an arbitrary bench mark. Maps of the landforms and well locations were digitized in ARC/INFO.

Well Network.

There is no road access to the study site so all wells had to be driven by hand. Because of the presence of large cobbles throughout the study site, the deepest wells penetrate only 2.5 m below the surface. There are no data on vertical gradients in head or hydraulic conductivity because wells are shallow, and the depth to confining layers is unknown.

A single transect of wells was established during late summer in 1989 as a pilot study to monitor changes in solute concentrations in ground water across a toposequence from the hillslope to the stream. Wherever possible, wells were placed into holes driven at least 50 cm below the surface of the water table at summer base flow. Holes were back filled with the soil originally removed, and if necessary, additional fill was taken from nearby soil pits or recent root-throw pits. Following installation of the wells, back fill was washed and entrained sediments were removed from the well casing by repeated pumping using a large diameter tube and a bilge pump. During the summer of 1990, five more well transects were added to provide a plan view of the water table within the study site. An additional 18 wells were established on, and adjacent to, the gravel bar during 1991 and 1992.

Well casings were made from varying lengths of PVC pipe. Most were 2.54 cm in diameter, but some were constructed from 3.81 or 7.62 cm diameter pipe. Well "screens" were made by drilling 0.32 cm diameter holes into the bottom 50 cm of each PVC pipe, at an approximate density of 1 hole cm^{-2}. The bottom of each casing was plugged with a solid rubber stopper to prevent sediment from entering the bottom of the casing. All wells were capped with PVC caps to prevent contamination with foreign materials, and caps were vented to prevent the build up of back pressure when water table elevations changed. The locations of all wells were mapped (Fig. II.1) and the elevation of the well head and the ground level at each well was surveyed.

Saturated hydraulic conductivities (k) were calculated from falling-head slug tests. A volume of water was poured into the well casing to raise the water level in the well. The rate at which water returned to equilibrium levels was measured using a pressure transducer and data logger. The data were analyzed using the method developed by Bouwer and Rice (1976) and further described by Bouwer (1989) and Dawson and Istok (1991). This method is appropriate for partially penetrating wells in unconfined, heterogenous, anisotropic aquifers. Most of the well casings were 2.54 cm in diameter, and while the test is valid for small diameter wells, the estimated value of k applies only to a small region around the well (Bouwer 1989).

Seasons were subdivided into periods of base flow or storm flow using hydrographs of either stream discharge or well records of water table elevations. Storms were further subdivided by the rising, crest, and falling legs of the stream hydrograph. Water table elevations were measured from the well network and from stage plates located in both the mainstream of McRae Creek and in the pools of flowing water in the relic channel at the back of the gravel bar (Fig. II.1). Water table elevations and stream stage were measured during base flow conditions for all seasons of the year and during four storms over the course of the study. It took 1 to 2 hours to measure the water depths in all wells. The frequency and timing of storm observations were based on the intensity of precipitation and changes in stream stage. Four to five observations were spaced

irregularly over a single day during intense storm periods to capture both the rising, crest and falling legs of the stream hydrograph and the associated rise and fall of the water table.

McRae Creek was not gauged so I used records from Mack Creek which is 4.5 km away, with a catchment area of 875 ha (Fig. I.1) and a similar elevation range. I assumed that the unit area discharges would be similar for the two catchments. Therefore, to estimate McRae Creek discharge, I multiplied Mack Creek discharge by the ratio in size between the two catchments (1.6).

Ground Water Flow Model

MODFLOW: USGS Finite-Difference Model

The USGS finite-difference model (McDonald and Harbaugh 1988) was purchased from S.S. Papadopulos & Associates, Inc., (7944 Wisconsin Ave., Bethesda, MD 20814). This package included the modified Block-Centered-Flow (BCF2) package (McDonald et al. 1991), the STream flow-Routing (STR1) package (Prudic 1989), and several post-processing programs: PostModflow (PM) to extract simulated heads or draw downs from a selected model layer or cross section; HeadCOMPare (HCOMP) to compare predicted heads to observed heads in a well; and FlowBUDGET (FBUDGET) to calculate a flow budget for any subregion of the model domain.

Model Assumptions

I used a 2-dimensional model because wells were shallow and calibration data were available only to describe the upper one to two m of the aquifer. In a 2-dimensional model saturated hydraulic conductivities and heads are constant with depth. The model was parameterized so that the thickness of the modeled aquifer was approximately 3 m during summer low flow. Observations of sediment layers in stream banks and soil pits at the study site showed that individual sediment layers were generally <2 m in thickness and did not exceed 3 m. Although deeper alluvial layers are most likely present at the study site, I assumed that there was no leakage through the bottom of the modeled aquifer because alternating layers of fine and coarse sediment characteristic of alluvial deposits would tend to restrict vertical flow to or from deeper layers. I assumed that evapo-transpirational losses from the aquifer could be ignored because the water table was more than 1 m below the ground surface during the summer, and

because Doug-fir and western hemlock trees are shallow rooted (Waring and Schlesinger 1985).

Because the stream channel was treated as a no-flow boundary, all subsurface flows through the model domain had to be routed out via the main channel. It is possible that some of the subsurface flows at the study site actually pass beneath the channel. However, it was not possible to calibrate a 3-dimensional model and extend the model domain so that the model could simulate subsurface flow beneath the channel. This will not influence the estimates of subsurface fluxes since these are based only on the flows of water into the model domain. However, estimates of both the mean residence time of the water in the subsurface, and the amount of nitrogen transported to the stream (Chapter #3) would be affected.

Model Design

The model domain was irregular in shape, approximately 105 m in length and 65 m across at its widest point. Initially, a regular grid with 5 m nodal spacing was used to discretize the model domain. The grid, consisting of 21 rows, 13 columns, and 227 active cells, was generated from ARC/INFO using the digitized coverage of valley floor landforms. The boundary at the head of the floodplain was an arbitrarily chosen line crossing the floodplain from the stream to the terrace, immediately upstream of the transect of wells PV05 to PV40-A (Fig. II.2). The head in each General Head Boundary cell (GHB - see definitions of terms) adjacent to wells PV05, PV19, PV31, and PV40-A (Fig. II.2) was extrapolated from the gradients between pairs of wells on the PX and PV transects (PX09 to PV05; PX18 & PX22 to PV19; PX30 to PV29 & PV31; and PX40 to PV40 A&B). I then interpolated the heads for the remaining GHB cells along the length of the boundary.

The physical boundary between the floodplain and terrace defined the right hand, or terrace boundary, of the model domain. The potential gradients were

Fig. II.2. Model Domain - entire simulated area. Dashed lines indicate grid
cells and are spaced at 2.5 m intervals. Landform shadings and well
symbols follow Fig. II.1. GHB cells along the head of the floodplain and
along the right boundary are shaded. Unlabeled wells on the gravel bar
are shown in Fig. II.3.
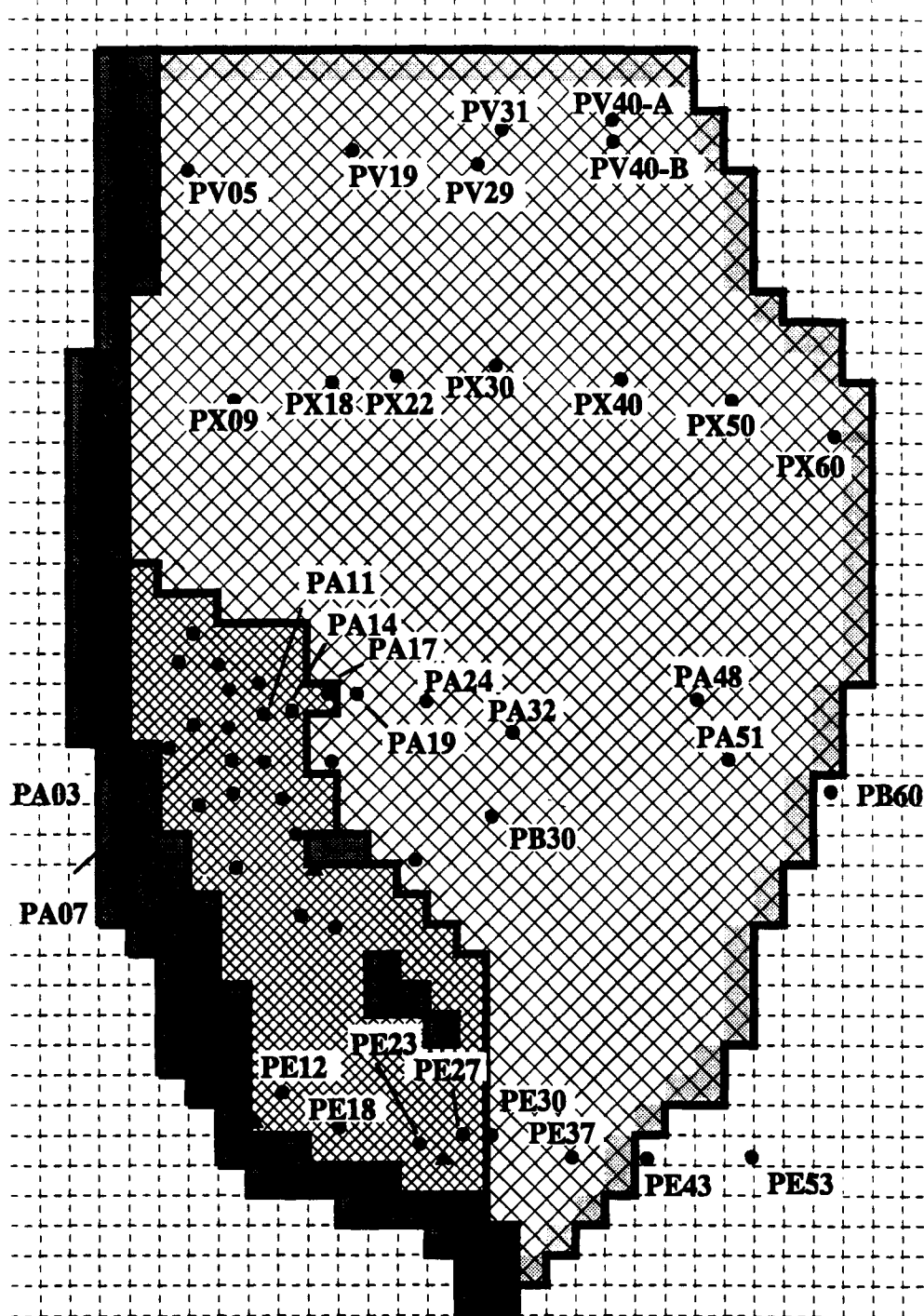
Fig. II.3. Model Domain - Gravel Bar only. Landform shadings and well symbols follow Fig. II.1.
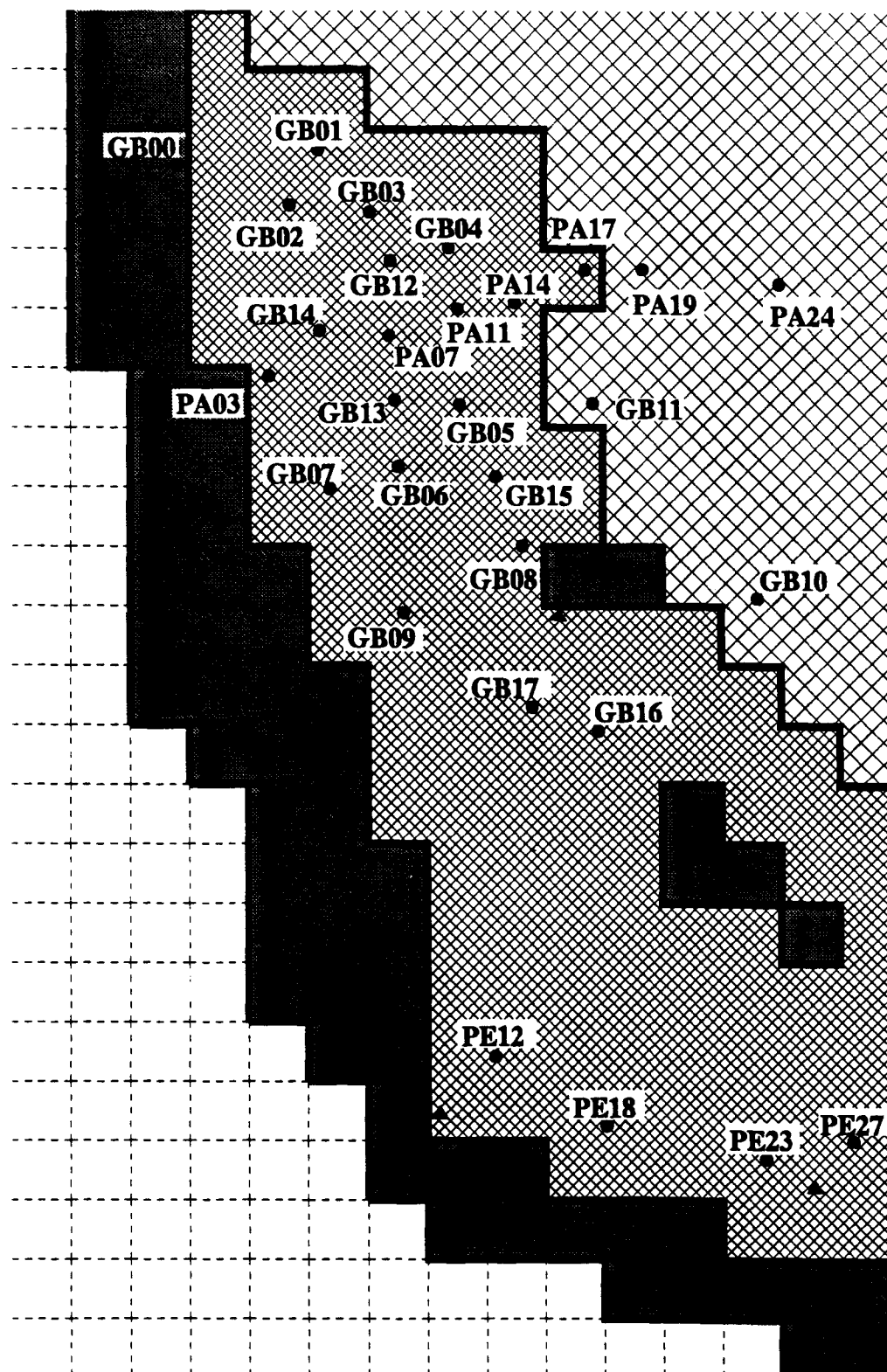
quite steep along this boundary and poorly sampled because it was nearly impossible to establish wells on the terrace. Wells PX60 and PE43 (Fig. II.2), located at the base of the terrace, defined the heads in their respective GHB cells. A linear gradient between wells PA51 (on the floodplain) and PA72 (on the terrace) was assumed in order to interpolate the head in the GHB cell at the terrace boundary between these two wells. I assumed that the head gradient along the boundary between these three GHB cells was linear and interpolated the heads for the intermediate GHB cells.

Finally, the stream channel was modeled as a no-flow boundary located along the west (or left) edge of the model domain (Fig. II.2 and II.3). Cells located beneath the stream channel were identified in the MODFLOW subroutine STR1. The water and stream bed elevations for each stream cell were calculated by averaging the stream survey data for all survey points within a single stream cell. I assumed that the change in stream water surface elevations for each stream cell matched the change in elevation observed on the staff gauge in the center of the stream reach. Therefore, water elevations for each stream cell were adjusted by the difference in stream elevation observed on the date and time at which the stream was surveyed and the day data were collected for each model run.

Point estimates of k for each well were used to define a saturated hydraulic conductivity for each cell in the model, using the Thiessen Polygon Method. The conductance of each GHB cell was then calculated using k values from adjacent model cells.

Model Calibration

MODFLOW (McDonald and Harbaugh 1988) was initially calibrated with head data recorded from the well network during a low flow period on 28 September 1992 when elevations of the water table were constant over a period of several days. Both the mean of the residuals (MR) and the mean of the absolute

value of the residuals (MAR) were used to calibrate the model. Positive (or negative) values of MR indicate that the predicted water table elevations are too high (or too low) throughout the model domain. Thus, this is a measure of the systematic error in model predictions. In contrast, the MAR is a measure of the fit of the model to the observed data. Clearly, it would be possible that the predictions from a model run would result in a MR near zero but with large MAR, therefore both were used to calibrate the model.

Predicted heads were much higher than observed heads for the first model runs which indicated that inputs of water from GHB cells along the floodplain and terrace boundaries were supplying too much water to the floodplain. Consequently the conductances between each GHB cell and the adjacent model cell were reduced until the MR was less than ±1 cm. In a subsequent series of trial-and-error model runs, the boundaries between zones of constant k, originally determined by the Thiessen Polygon Method, were adjusted to minimize the MAR. I was eventually able to reduce MAR to less than 10 cm, with a range of 0.3 to 30.0 cm (Fig. II.4). The predicted head in wells PV19 through PV40-B was slightly underestimated, whereas the head predicted in wells PE12 through PE37 was slightly overestimated. I was unable to find a combination of GHB conditions and k that would eliminate this error.

The model was further calibrated to data from 7 additional sample dates - 3 summer and 4 winter - that bracketed the range of stream and water table elevations observed over the study period (Fig. II.5). During summer, the range in elevations was less than 10 cm for both the stream and the water table. The model predictions fit the observed data very well over this range, with the MR ranging within ±2.0 cm of the observed values, and the mean of the MAR ranging from 12 to 14 cm. However, this cannot be construed as a rigorous test of the model because the subsurface flows for the date on which the model was first calibrated were similar to those observed on all other dates during summer low flow.

Observation for winter base flow were made during inter-storm periods several days in length, when either stream or water table elevations were not

changing rapidly. Observation were made under a wide range of conditions because of the timing of data collection, variations in intensity of the preceeding storm, and the time since that storm. The fluxes of water into the floodplain changed slowly during these periods, however, the slow rate of change in the observed ground water elevations suggested that the flow of ground water through the floodplain was in near equilibrium with the inputs to the floodplain. Consequently, it seemed reasonable to model the conditions observed during the winter base flow period as if steady state conditions existed.

Model calibration runs showed a reasonably good fit for data collected from the end of the longest inter-storm period, and a progressively worse fit under increasingly wet conditions. The model consistently underestimated the mean elevation of observed head by 8 to 16 cm. Comparisons of data from individual wells showed that predictions were quite close to observed elevations in wells on the gravel bar, but that heads were underestimated by 30 to 70 cm in wells along the terrace boundary.

These results suggested that the boundary conditions specified for GHB cells along the terrace-floodplain boundary did not account for the magnitude of ground water flux from the adjacent hillslope during wet, mid-winter conditions. The model was recalibrated to the data collected during the wettest winter base flow period by gradually increasing the specified head in the GHB cells until the MR for the wettest date was < 1 cm. After recalibration, the predicted heads fit the observed data well for for the three other dates during the winter base flow period (Fig. II.6). The MR for ranged between ±4.0 cm and the MAR ranged between 11 to 12 cm. The predicted fluxes from the terrace GHB source showed an abrupt, or step like increase between summer and winter that is an artifact of recalibrating the model to fit better the winter data. These results suggested that a more complex function that gradually increased ground-water flows from the terrace GHB cells in concert with increases in stream discharge should be used. However, judging from the magnitude and distribution of the residuals, the magnitude of error introduced into the model predictions was small, relative to

Fig. II.4. Comparison between observed and predicted heads for 24 observation
wells for 28 September, 1992, the date of the observations with which
MODFLOW was first calibrated. The dashed line indicates equality
between the predicted and observed values (the regression line is not
shown).

$$Predicted = 0.8985(Observed) - 0.0028$$

$$r^2 = 0.992$$

Fig. II.5. Range in stream water elevations at the McRae Creek stage plate and
water table elevations in two floodplain wells observed during base flow
periods between 1989 and 1993. Closed symbols designate the stream and
water table elevations on the observation dates used to calibrate
MODFLOW.
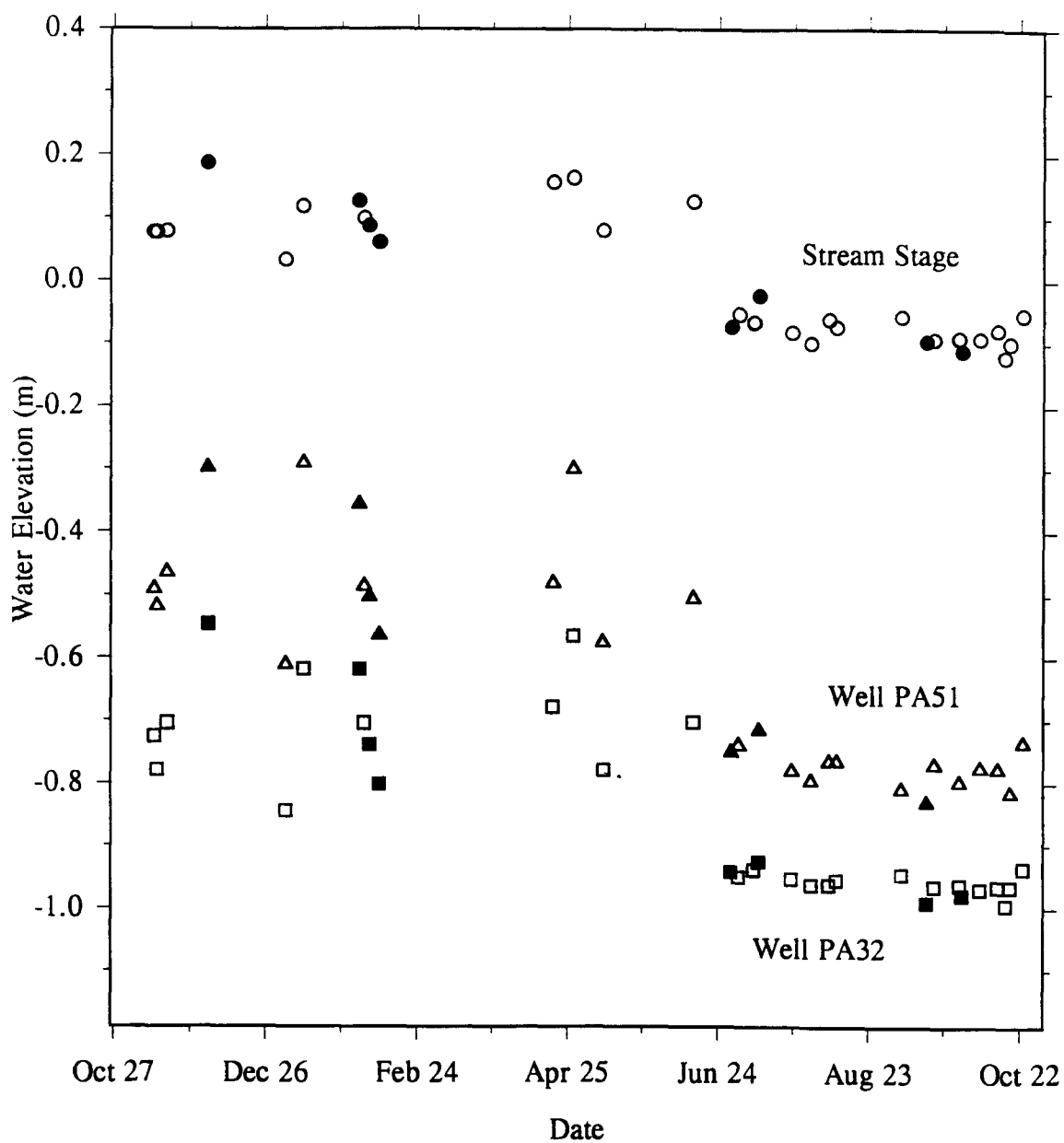
the sensitivity of the predictions to variations in either **k** or the saturated depth (described below). Consequently, no further adjustments were made to improve the calibration of the model.

Sensitivity Analysis

Discretization. The predicted fluxes of the model calibrated with a 5.00 m nodal spacing were compared to those with nodal spacings of 2.50 m and 1.25 m to test the sensitivity of the model to the spatial discretization. The MR and MAR calculated from simulations using the three nodal spacings were similar (Table II.1) and suggested that any of these nodal spacings were equally appropriate to simulate subsurface flows through the aquifer. However, the 1.25 m nodal spacing seemed to be an over-interpolation of the available data (Stoertz and Bradbury 1989), given the small number of observation wells within the study site. The 5 m nodal spacing resulted in too coarse a representation of landform boundaries at the study site. I therefore used a nodal spacing of 2.50 m for all subsequent model runs. This spacing provided a realistic representation of the landform and stream boundaries with a manageable number of cells.

Distribution of k. The water fluxes predicted by MODFLOW are sensitive to both the value and the spatial distribution of *k*. I used spatial distributions of *k* produced by kriging, inverse distance, inverse distance squared and minimum curvature interpolation available in SURFER (software distributed by Golden Software Inc.), and the Thiessen Polygon Method from ARC/INFO. I also used a "homogenous" distribution in which the values of *k* used for all cells within either the gravel bar or the floodplain were equal to the average conductivity measured from all the wells within that landform. The results of these model runs were compared to the results of the "hand-fit" distribution found by calibrating the model (Table II.2). In general, the model runs using all of the

Fig. II.6. Comparison between observed and predicted heads for 24 observation
wells for the eight dates for which the MODFLOW was calibrated. The
dashed line indicates the regression between the observed and predicted
values.

Predicted = 0.95(Observed) + 0.01

r^2 = 0.99
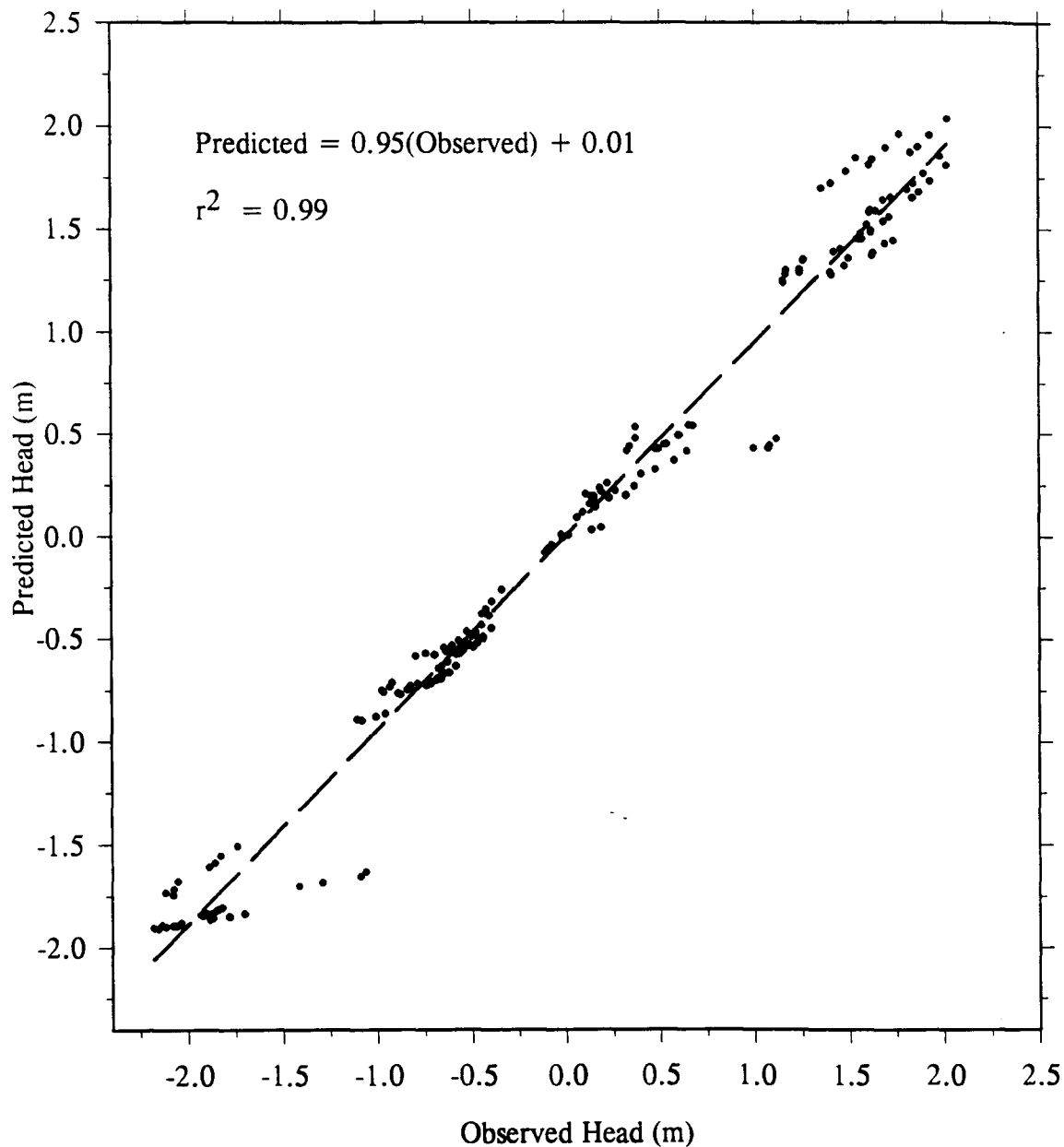
Table II.1. Model structure, mean residual, mean of the absolute value of the residuals, standard deviation, and estimated ground water fluxes from three sources at three different nodal spacings.

Nodal Spacing (m)	Col. (#)	Row (#)	Cell (#)	Mean Residual (m)	Mean Abs. Residual (m)	Standard Deviation	H_2O Flux Gravel Bar ($m^3 h^{-1}$)	H_2O Flux Floodplain ($m^3 h^{-1}$)	H_2O Flux Terrace ($m^3 h^{-1}$)
5.00	13	27	227	0.003	0.116	0.209	2.09	0.62	0.12
2.50	27	42	888	0.055	0.099	0.122	2.23	0.62	0.19
1.25	54	84	3551	0.040	0.117	0.162	2.06	0.67	0.25

Table II.2. Comparison of model runs using a variety of spatial interpolators for k.

Interpolation Method	Mean Residual (m)	Mean Abs. Residual (m)	Standard Deviation	H_2O Flux Gravel Bar $(m^3\ h^{-1})$	H_2O Flux Floodplain $(m^3\ h^{-1})$	H_2O Flux Terrace $(m^3\ h^{-1})$
Inverse Distance	0.213	0.282	0.286	1.50	0.91	0.23
Inv. Dist. Squared	0.215	0.287	0.284	1.43	0.88	0.23
Kriging	0.217	0.274	0.226	1.46	0.78	0.17
Minimum Curvature	0.189	0.292	0.308	1.37	0.60	0.18
Homogenous	0.153	0.262	0.288	2.33	1.27	0.21
Thiessen Polygons	0.213	0.287	0.280	1.64	0.67	0.21
Hand Fit Model	0.055	0.099	0.122	2.23	0.62	0.19

interpolation methods simulated the overall gradients of head within the model domain. The MR ranged between 0.2 and 0.3 m for these runs. The distributions of k produced by kriging, minimum curvature, inverse distance, and Thiessen polygon methods failed to reproduce the zones of greatest conductivity in the gravel bar and predicted lower flow rates of advected channel water than did the model runs using the homogenous or hand-fit distributions of k.

Effect of variation in k. Ground water fluxes computed from MODFLOW are based on Darcy's Law (Eq. 1) which states that flux (Q) is related to saturated hydraulic conductivity (k) by the following equation:

$$Q = -kA \frac{\Delta h}{\Delta l}$$

(Eq. 1)

where A is the cross sectional area through which flow occurs, h is the head and l is the distance. An independent flux measurement should be used to validate predictions from a calibrated model because measurements of k are intrinsically crude. Unfortunately, independent measurements of subsurface flows through the aquifer at the McRae Creek study site are unavailable. Consequently, the resulting flux estimates cannot be rigorously validated. Therefore, I tested the sensitivity of the model predictions to variations in k. The calibrated model had a mean hydraulic conductivity of 0.51 m^3 h^{-1} in the gravel bar and 0.15 m^3 h^{-1} in the floodplain. The values of k assigned to each cell were multiplied by 0.1, 0.5, 1.0, 2.0, 5.0, respectively, for each of five model runs. The conductances for each GHB cell were also adjusted accordingly. Clearly the predicted fluxes are very sensitive to variations in k (Fig. II.7).

Effect of variation in aquifer thickness. Subsurface flows predicted from MODFLOW are proportional to the cross-sectional area (A) of the aquifer through which flow occurs (Eq. 1). Unfortunately, the stratigraphy of valley

Fig. II.7. Sensitivity analysis to variation in k.

FLOOD PLAIN

Flux = 5.23 (k)

GRAVEL BAR

Flux = 3.91 (k)

Flux $(m^3\ h^{-1})$

Mean Conductivity $(m\ h^{-1})$
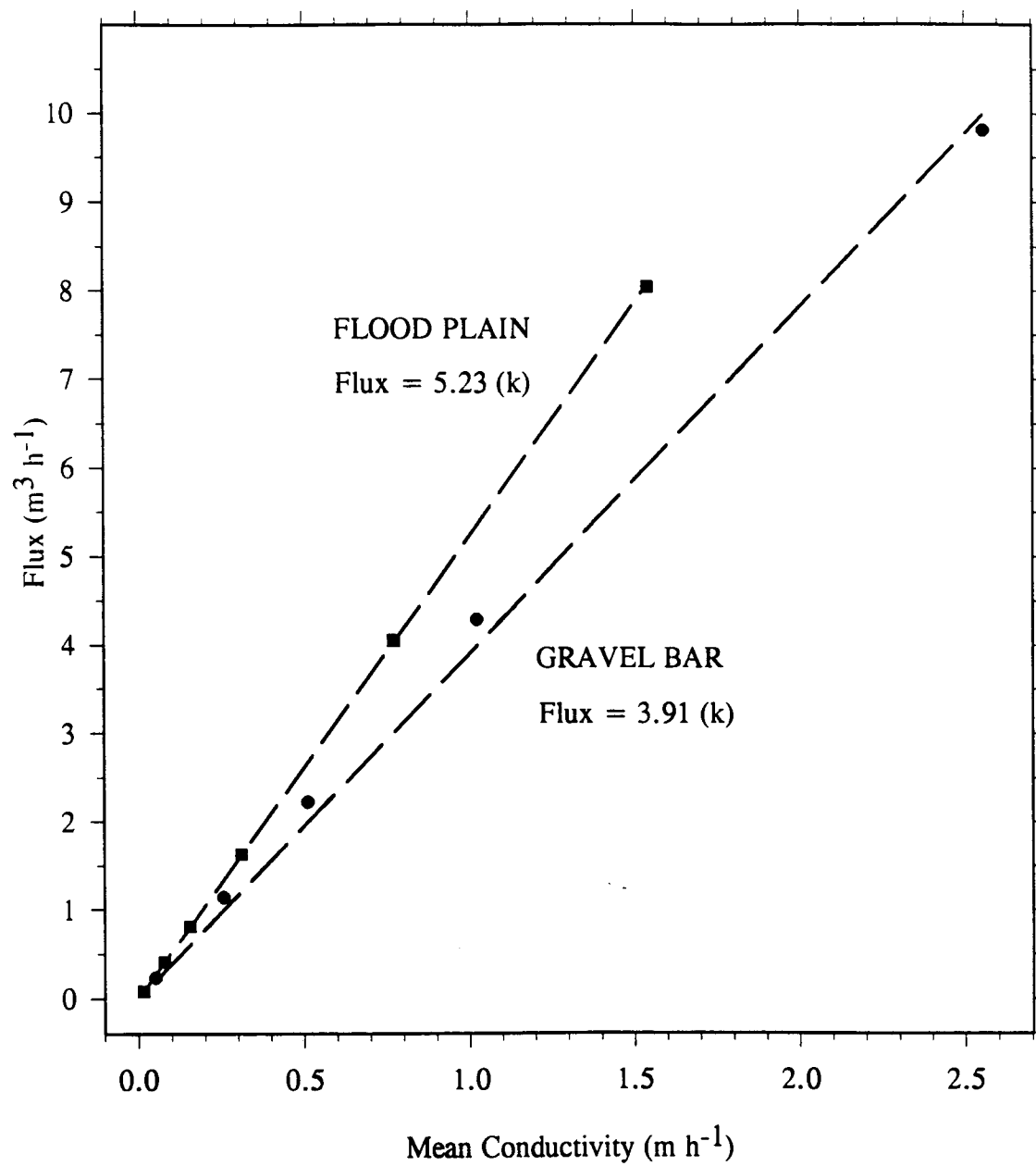
floor deposits has not been described and the site was not accessible by road. Large cobbles in the subsurface makes it impossible to drive wells to the bottom of the aquifer by hand. Thus no hydrogeologic data are available to define depths to impermeable layers for the model. Consequently I tested the sensitivity of the predicted flows to the variation in aquifer thickness by varying the depth to the bottom of the aquifer for a series of model runs. The conductances for each GHB cell were also adjusted accordingly. Clearly, predicted fluxes through the model domain are sensitive to variations in thickness (Fig. II.8).

Model Validation

The model was validated using a transient simulation of a 6-day storm. During this storm, 13.7 cm of precipitation were recorded at the H.J. Andrews Experimental Forest administration site, 7 km away. This precipitation equals an estimated input of 564 m^3 of water to the floodplain and an input of 113 m^3 of water to the gravel bar. These precipitation inputs were a known flux into the model domain, and were large relative to the 250 m^3 of subsurface flux that would have been expected during winter base flow conditions over the same time period. If the model severely underestimated subsurface fluxes, the predicted heads would be much higher than the observed heads, because the water table would rise as precipitation inputs were stored within the aquifer instead of draining to the stream. Also, the water table elevations would return to the steady state, or pre-storm condition, more slowly than was actually observed, because the drainage of water stored within the aquifer would be slowed. Conversely, if the model overestimated ground water fluxes, precipitation inputs would drain from the aquifer too rapidly, the predicted heads would be much lower than observed heads, and water table elevations would return to pre-storm conditions much faster than was actually observed. Consequently, the comparison between the predicted and observed changes in storage within the floodplain was a reasonable test of the model predictions.

Fig. II.8. Sensitivity analysis to variation in depth to confining layer.

GRAVEL BAR

Flux = 0.71 (Thickness)

FLOOD PLAIN

Flux = 0.27 (Thickness)

Flux ($m^3\ h^{-1}$)

Saturated Thickness (m)
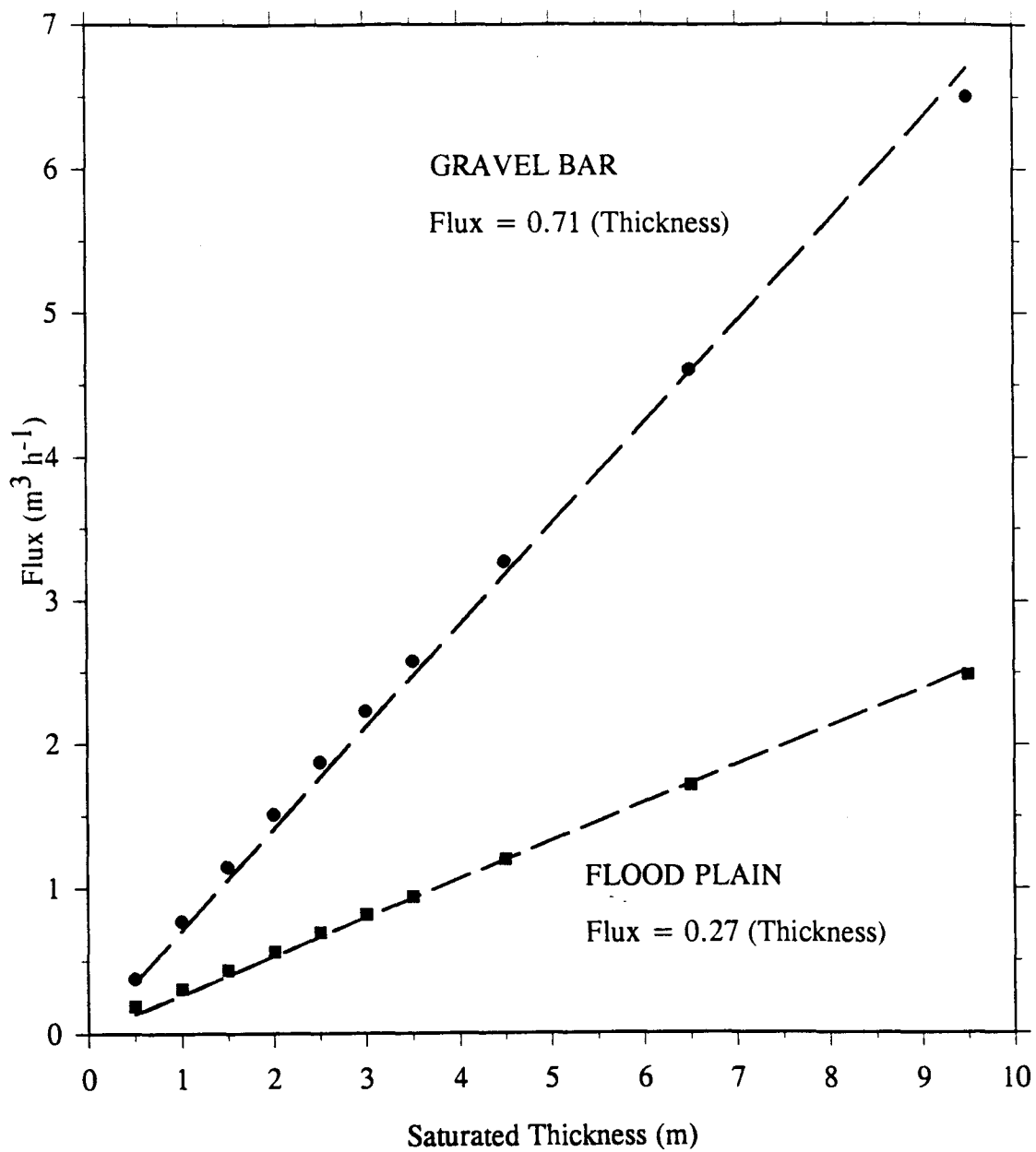
The transient simulation was six days in length and divided into 24, six-hour stress periods. Boundary conditions for each stress period were defined as described above, using field data collected during the storm. Observations were unavailable to define boundary conditions for several stress periods, because head and stream stage data were not collected at six hour intervals. In these cases, stream stage and heads were interpolated from observations collected before and after the stress period for which data were unavailable. These interpolated "data" were used to define the boundary conditions for that stress period. Precipitation rates were assumed to be constant within a stress period and equal to the average hourly precipitation rate observed over that 6 hour period.

In general, the model predicted the overall gradient of the water table (Fig. II.9) and changes in water table elevations during this storm very well (Fig. II.10). The average of all the means of the residuals (MR) calculated for each observation data set was < 1 cm and the average of all the MARs was 16 cm. The predicted heads in wells along the lower part of the floodplain, especially along the terrace boundary (PA51 & PE30), were consistently underestimated. In contrast, the predicted heads in wells located on the gravel bar (PA07) were always very close to observed values (Fig. II.9 & II.10).

Averaging precipitation inputs over a six-hour period was an additional source of error in the model predictions. For example, eleven hours after the start of the storm event, the predicted heads underestimated the observed values by an average of 20 cm, and the MAR reached a maximum for the simulation of 33 cm. The simulated precipitation rate was 0.17 cm h^{-1} for hours 7 -12 of the transient simulation, while the observed precipitation rate during the eleventh hour of the simulation was 0.50 cm h^{-1}. Inputs of water to the aquifer during short periods of intense precipitation exceed subsurface flow rates and the water table rises as this water is stored in the aquifer. These short-term responses were not well simulated when precipitation was averaged over a 6-hour stress period.

Fig. II.9. Comparison between observed and predicted heads for 36 observation wells for the 6-day transient simulation. The dashed line shows the regression between the observed and predicted values.

Predicted = 0.99(Observed) + 0.01

$r^2 = 0.97$

Predicted Head (m)
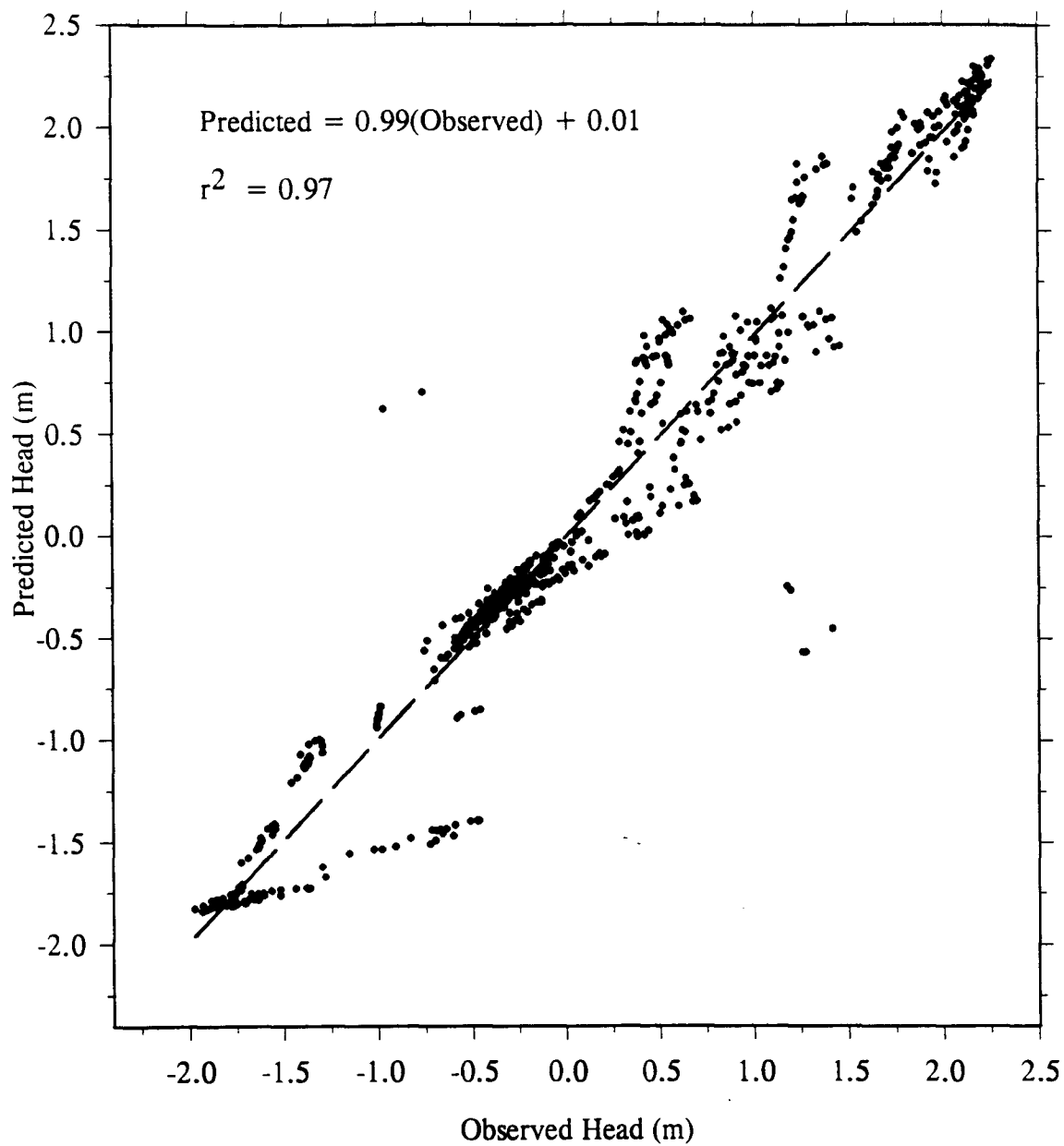
Observed Head (m)

Fig. II.10. Comparison of observed versus predicted head in 5 wells over the course of the 6-day transient simulation.
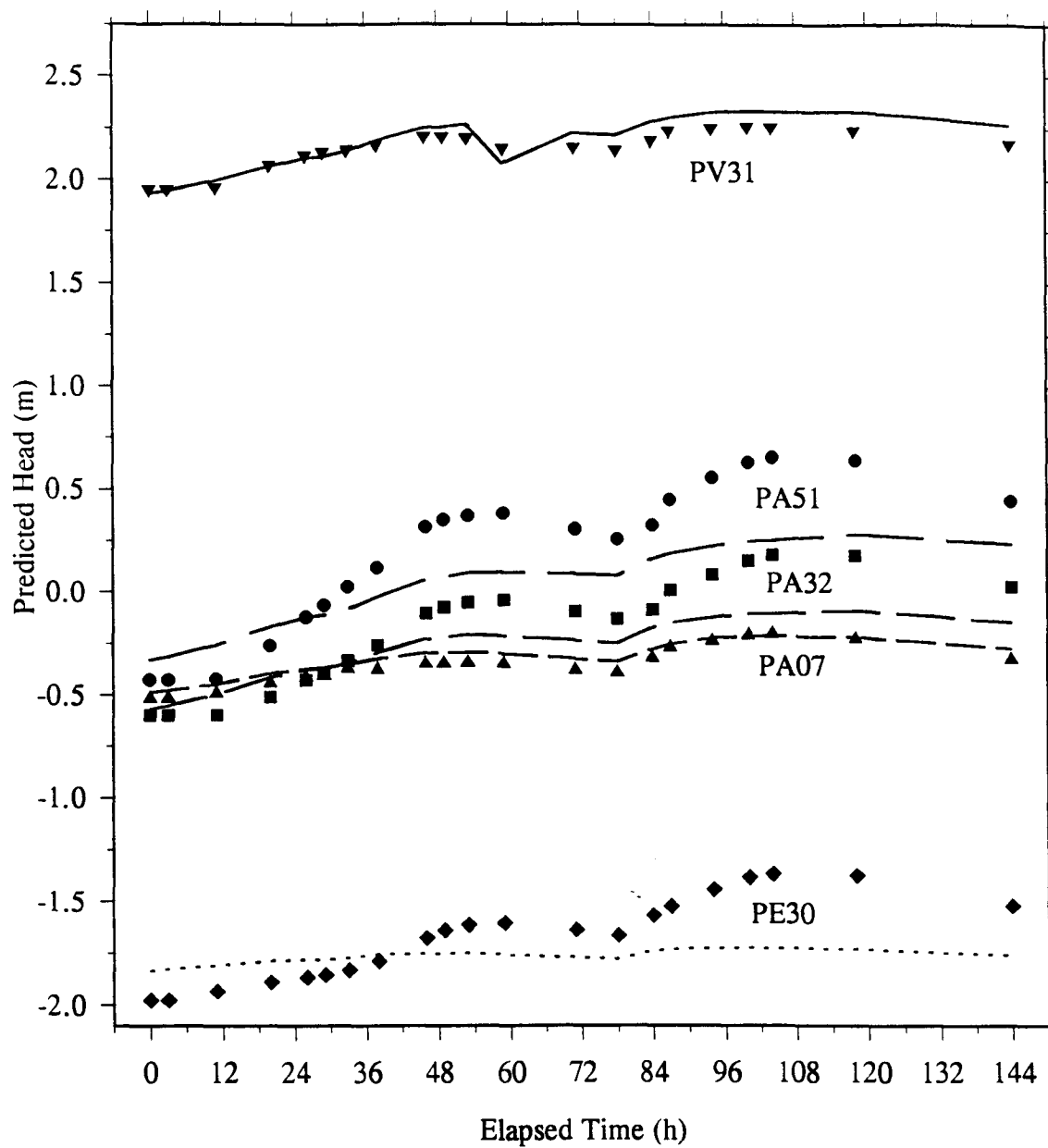
Model limitations

Subsurface flows cannot be measured directly. Attempts to estimate the rate of exchange flows between the stream and the subsurface, or the flow of ground water through the shallow aquifer, are hampered by the lack of geohydrologic data at the appropriate scale and by the complexity of the flow system. The predicted heads agree with the observed data reasonably well for conditions ranging from a steady state following months without significant precipitation to a large storm lasting several days. However, this does not mean that the subsurface fluxes predicted by the model are realistic. Subsurface flux is proportional to the **k** specified in the model, and estimates of *k* from single-well slug tests are intrinsically crude. The volume of precipitation input during the storm event was the only independent estimate of flux available. In this case, the precipitation flux was large relative to the rates of ground water flow predicted by the model for base-flow conditions. The close match between observed and predicted head, and the rate at which water table elevations returned to steady-state levels after the storm, suggest that the model predictions were realistic.

Model predictions were also limited by the lack of detailed geohydrologic data for the study site. I assumed that horizontal flux should predominate because sediment layers within the aquifer are horizontally continuous, and because the alternating layers of fine and coarse sediment characteristic of alluvial deposits would restrict vertical flux. However, no data are available on the stratigraphy of the floodplain or the depths to impermeable layers. The assumed aquifer thickness (3 m) seems reasonable given that sediment layers exposed in stream banks, soil pits and auger holes within the Lookout Creek catchment seldom exceeded this thickness. Still, the predicted ground water fluxes are sensitive to the aquifer thickness, and the long history of fluvial disturbance and sedimentation and width of the valley floor in this stream reach suggest that the total thickness of sediment deposits greatly exceed 3 m. Much additional work, including the drilling of much deeper wells, would be necessary to decipher the

ways in which water in the upper 3 m of the aquifer interacts with water in deeper sediment layers.

Finally, both the flow of ground water and the distribution of head are influenced by small-scale heterogeneity of the porous media that may not be simulated by the model, even at very small nodal spacings (Gelhar 1986). The head distribution observed in the well network is always incomplete, consequently, ground water fluxes predicted by a model calibrated to the available head data are uncertain.

Given that the sources of uncertainty in this model are large, I believe that the model predictions of the head distributions, especially during the transient simulation, are good, and suggest that the flux estimates are reasonable. Even so, the sensitivity analysis shows that the flux estimates are directly proportional to both k and the aquifer thickness. Consequently, these predictions should be considered as only initial estimates. Additional work and data would be required to rigorously validate these model predictions.

Results and Discussion

Ground Water Flux During Base Flow

Gravel bar. The predicted flows of subsurface water through the gravel bar and the floodplain varied linearly with stream discharge over the observed range of base flow (Fig. II.11). Predicted flow rates of advected channel water through the gravel bar ranged from 2.5 m^3 h^{-1} during the dry season when stream discharge was only 400 m^3 h^{-1}, to 3.5 m^3 h^{-1} during the winter when stream discharge exceeded 1,000 m^3 h^{-1}. The head gradient between the relic and main channels was steep and advected channel water flowed through the gravel bar under all observed conditions. The head gradients indicate that flow of advected channel water from the stream and of ground water from the floodplain converged along the relic channel (Fig. II.12). Surface flow in this relic channel was intermittent in late summer at the end of the dry season and increased during the winter rainy season when predicted subsurface fluxes also increased.

Floodplain. Predicted flow rates through the aquifer underlying the floodplain ranged from 1.3 m^3 h^{-1} during the dry season to 1.7 m^3 h^{-1} during the winter. The predicted inputs of ground water from GHB cells along the terrace boundary were positively correlated to stream discharge and ranged from 0.3 m^3 h^{-1} to 0.7 m^3 h^{-1} between summer and winter base flow, respectively (Fig. II.11). The predicted inputs of ground water from GHB cells along the floodplain boundary were constant at approximately 0.6 m^3 h^{-1} during base-flow periods and were not well correlated to stream discharge. Near the head of the gravel bar, there was a small zone where 0.2 m^3 h^{-1} of advected channel water flowed into the floodplain. This zone was widest during the summer and narrowed as ground water flow through the floodplain from other sources increased (Fig. II.12).

Fig. II.11. Relationship between subsurface flux from each source and stream discharge, for the gravel bar and the floodplain, predicted from 8 model runs bracketing the range in base flow conditions.
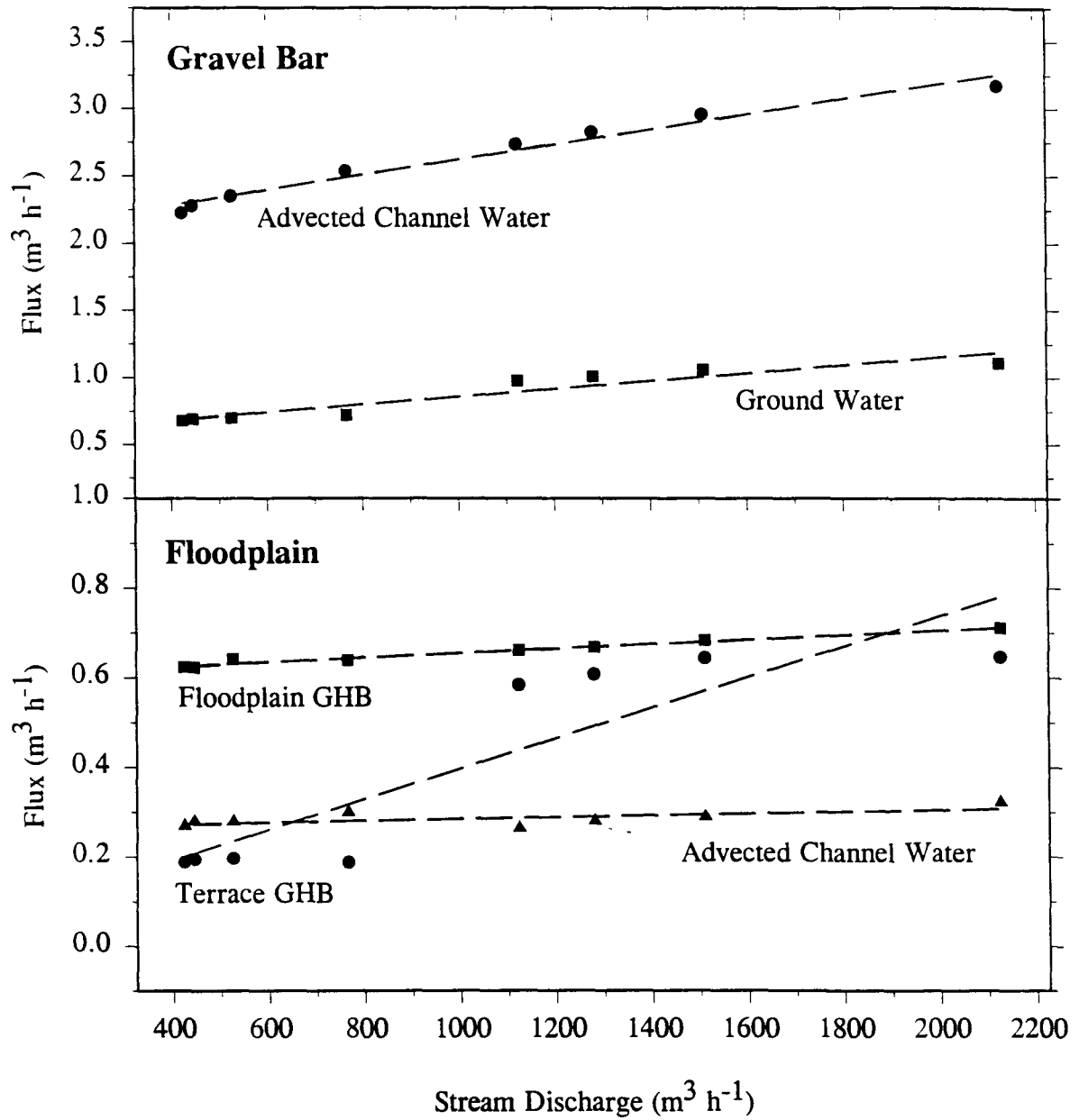
Fig. II.12. Piezometric surface predicted from model simulation for a) summer base flow, b) winter base flow, and c) peak storm flow. Equipotential interval is 0.1 m.

53
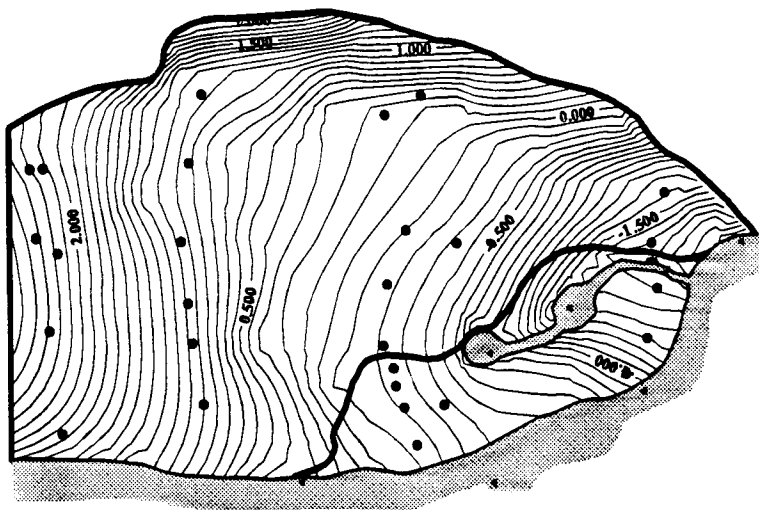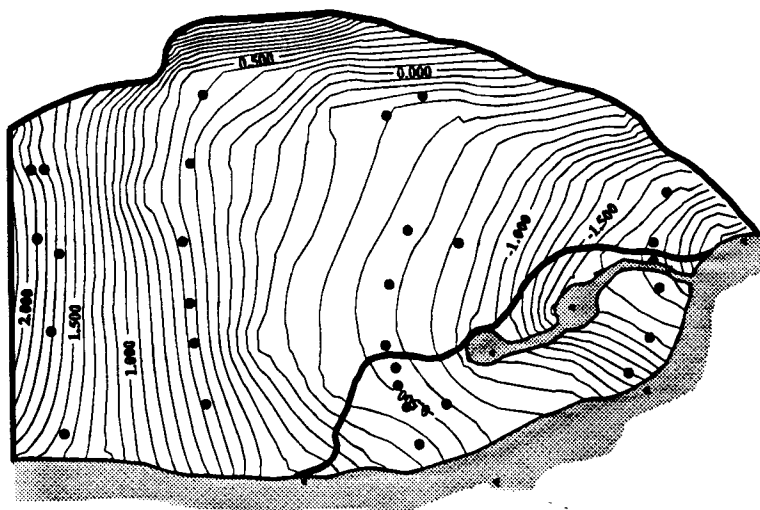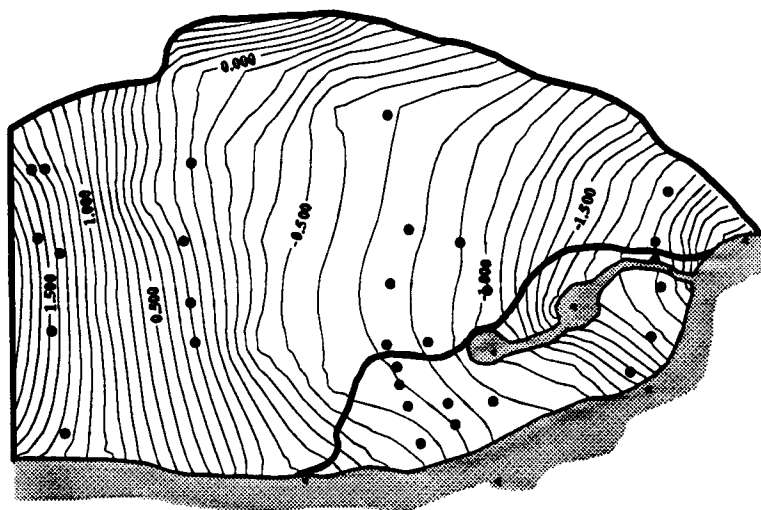
A. Summer Base Flow   **B. Winter Base Flow**   **C. Peak Storm Flow**

Ground Water Flux During Storms

Gravel bar. Predicted flows of advected channel water through the gravel bar decreased from 3.5 m^3 h^{-1} prior to the storm to approximately 2.5 m^3 h^{-1} during peak storm discharge and then increased again after the storm (Fig. II.13). This pattern is opposite that predicted for base flow when stream discharge and the flow of advected channel water were positively correlated as predicted by Meyer et al. (1988), but this difference is easily explained. First, the gradient from the main channel to the relic channel does not increase much during storms (Fig. II.12). Water levels in the relic channel are nearly constant, changing less than 5 cm between summer low flow and peak storm discharge. During base-flow periods, stage increases linearly with stream discharge (observed stage -0.008 to 0.200 m). However, at stages higher than 0.200 m, the relationship between stage and discharge is exponential (Fig. II.14). Therefore, the stage during peak storm discharge is little higher than at winter base flow. Second, precipitation inputs account for nearly 30% of the total subsurface flow through the gravel bar at peak storm discharge. These precipitation inputs replace some of the flows of advected channel water that would have been predicted from the relationship between stream stage and subsurface flow under base-flow conditions (Fig. II.11).

Precipitation inputs drained rapidly from the gravel bar so that water table elevations returned quickly to steady-state levels after the storm. Similarly, flow through the gravel bar had nearly returned to pre-storm rates within 24 hours following the last precipitation from this storm (Fig II.13). At this time the water table was only slightly elevated above steady-state levels and drainage of this stored water accounted for <5% of the total flow through the gravel bar.

Floodplain. Water flow through the floodplain was dominated by precipitation throughout the transient simulation. By the end of the storm, precipitation alone accounted for 2.0 m^3 h^{-1} of subsurface flow and represented

Fig. II.13. Average hourly precipitation rate for each 6 hour stress period of the
6-day transient simulation (bottom). The predicted flux of advected
channel water through the gravel bar; the predicted discharge of ground
water from the floodplain into the gravel bar; and the predicted subsurface
flux from precipitation (change in storage minus precipitation inputs) for
times at which head data were observed from the well network (middle).
The proportion of total predicted ground water flow from each source.
Area between the curves is proportional to the percent of the subsurface
flow contributed by that source (top).
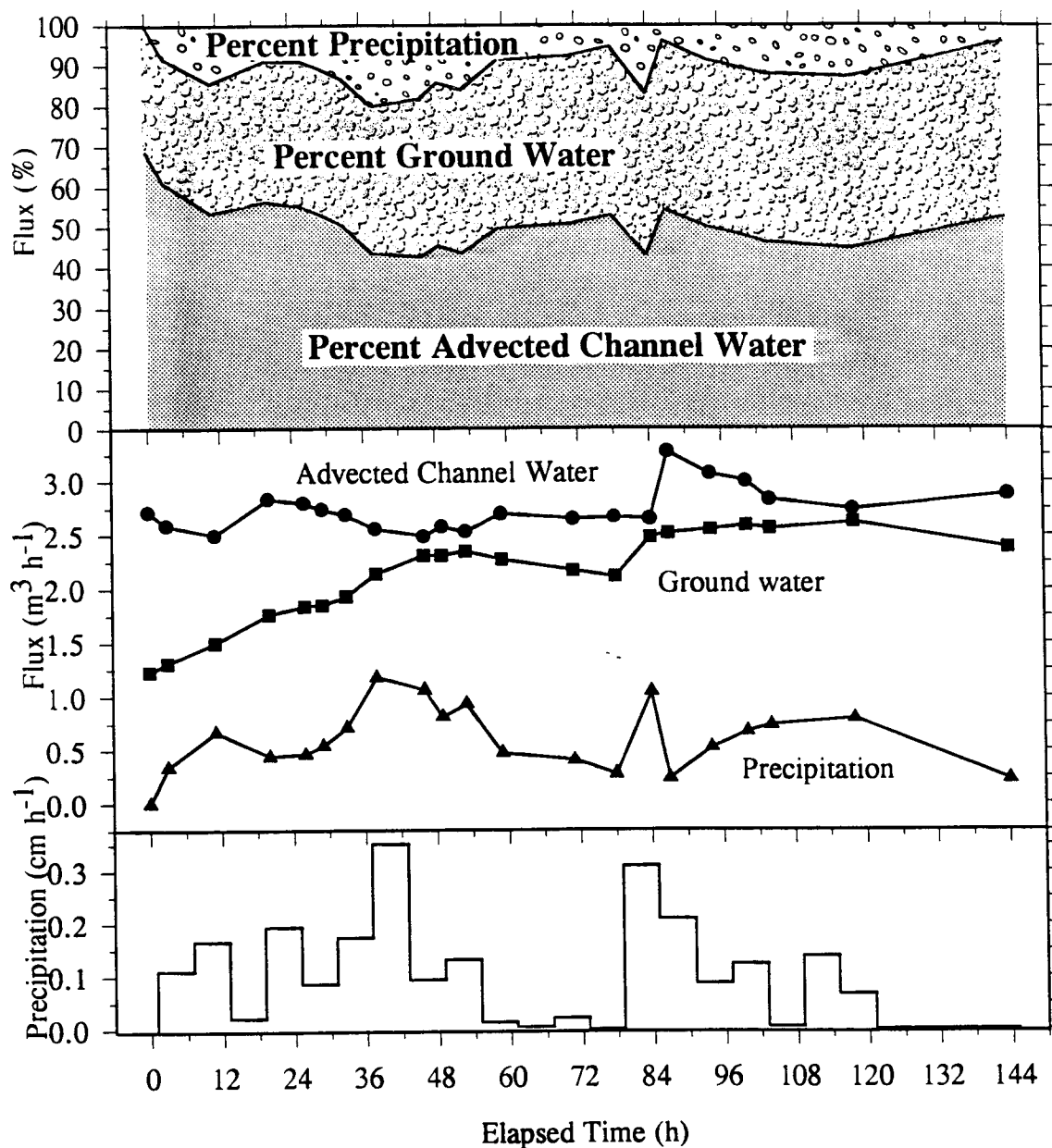
Fig. II.14. Observed stage height versus estimated discharge for McRae Creek.

Discharge $= 1154 + 7229(\text{Stage}) + e^{30.23(\text{Stage})}$

$r^2 = 0.91$

Estimated Discharge ($m^3 \ h^{-1}$)

Stage (m)
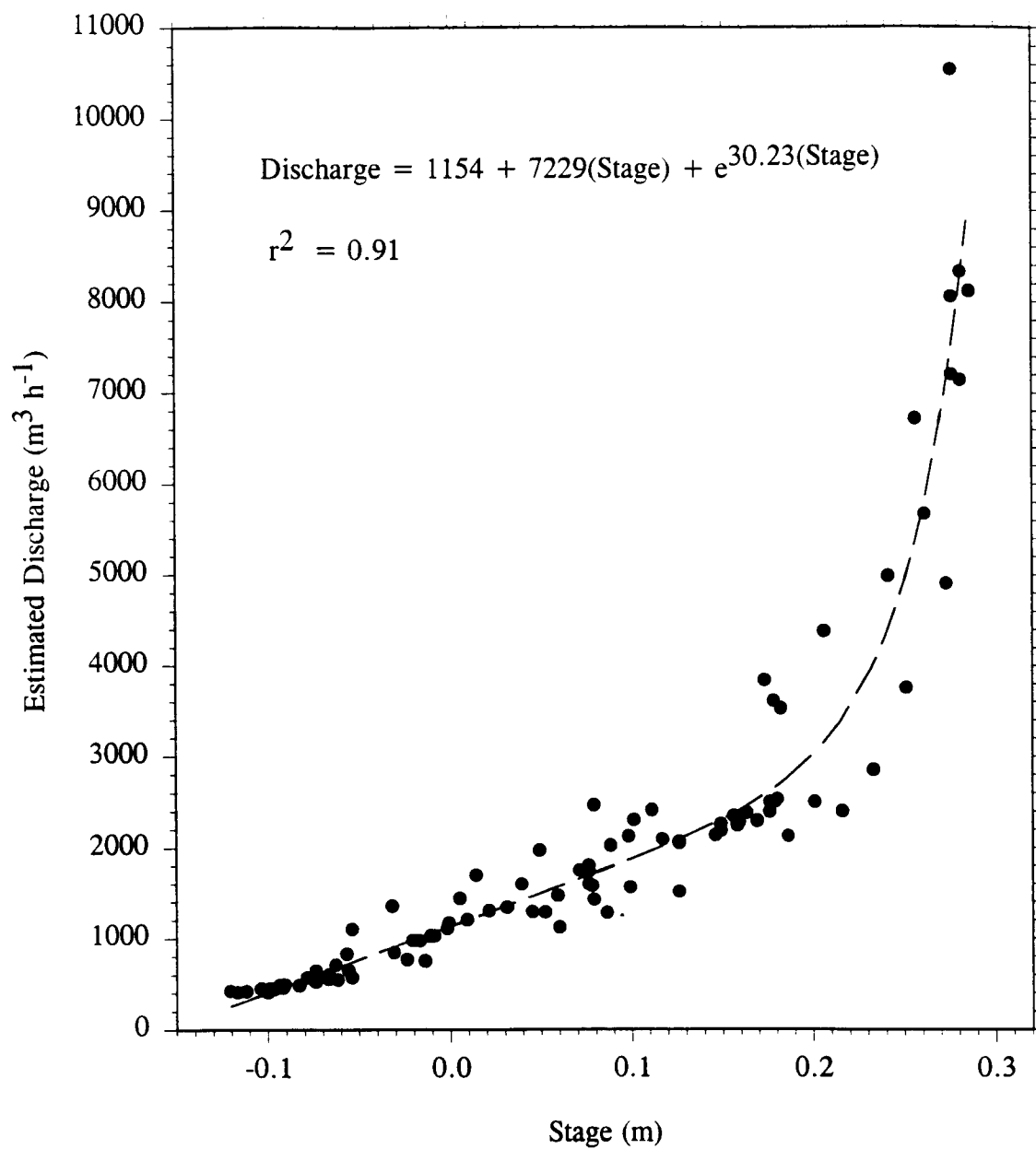
more than 50% of the total subsurface flow through the floodplain (Fig. II.15). Precipitation exceeded subsurface flow rates, consequently the water table elevations increased as water was stored within the aquifer. The hydraulic conductivities in the finer sediments of the floodplain were lower than those of the gravel bar and resulted in greater storage within the floodplain aquifer, and much slower return to steady state conditions after the storm. A linear extrapolation based on the rates at which water drained from the aquifer during the final 24 hours of the transient simulation, or the period between 54 and 78 hours when little precipitation fell, suggest that ground water fluxes through the aquifer would take at least 5 more days to return to steady state.

Predicted flows of ground water from both the floodplain and the terrace GHB cells were small relative to precipitation during the simulation. The predicted flow from the terrace peaked at 0.8 m^3 h^{-1} at the peak of the storm (Fig. II.15), which was only 15% greater than winter base flow inputs from this source. Surprisingly, the model predicted that inputs from GHB cells at the head of the floodplain decreased by 50% at the peak of the storm (Fig. II.15). The decreased inputs resulted from a decrease in the head gradient from 0.078 to 0.052 m m^{-1} in the region adjacent to this boundary (Fig. II.12). Although this result is counter intuitive, it is consistent with the observed head data which also show a decrease in the head gradient from pre-storm to peak flow.

Fig. II.15. Average hourly precipitation rate for each 6 hour stress period of the 6-day transient simulation (bottom). The predicted flux of advected channel water through the floodplain: the predicted flux of water into the floodplain from GHB cells along the boundary at the head of the floodplain and along the terrace: and the predicted subsurface flux from precipitation (change in storage minus precipitation inputs) for times at which head data were observed from the well network (middle). The proportion of total predicted ground water flow from each source. Area between the curves is proportional to the percent of the subsurface flow contributed by that source (top).
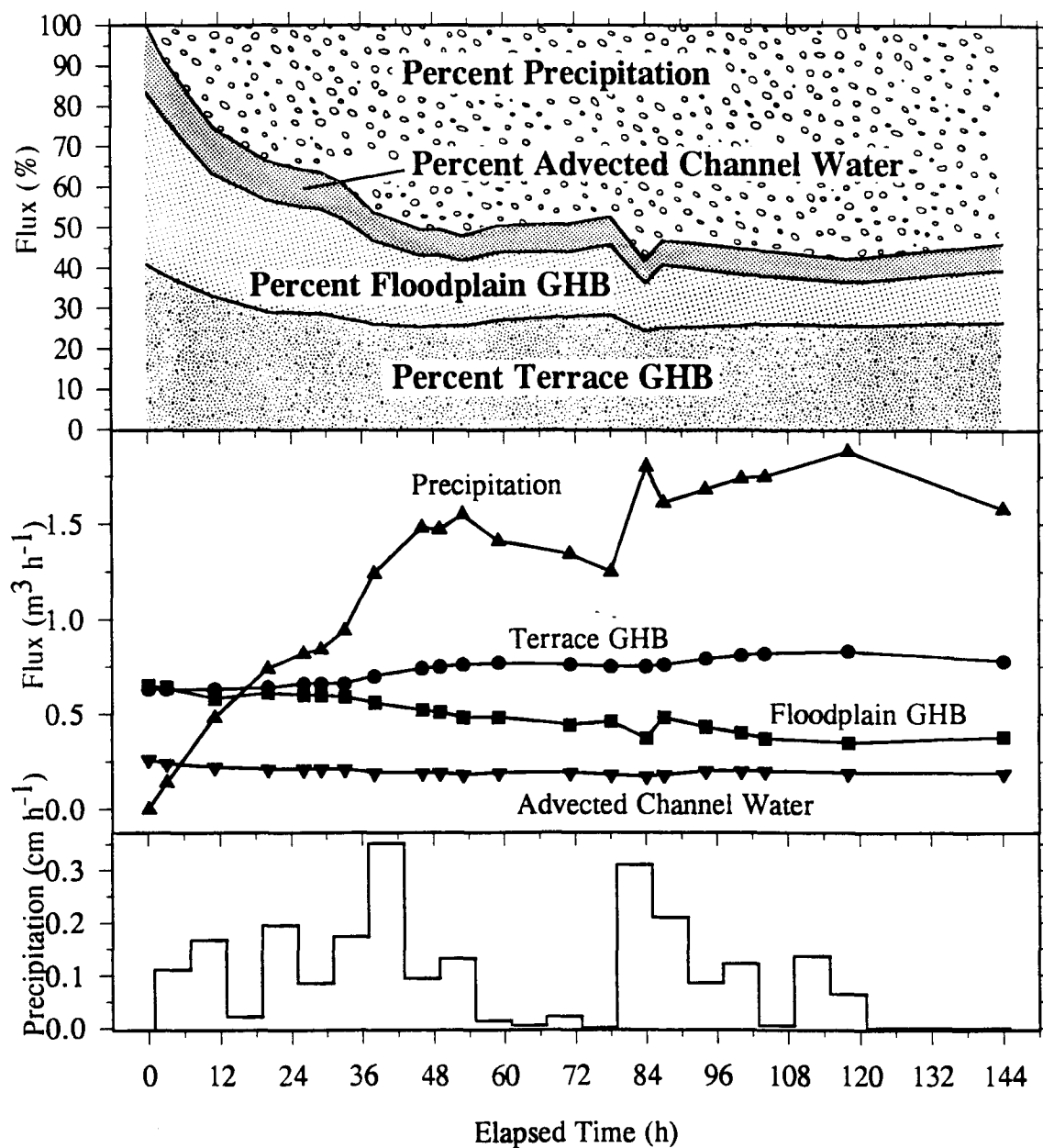
Conclusions

The dominant source of water flowing through the gravel bar during all seasons of the year and during storm events was advected channel water. The dominate source of water flowing through the floodplain during summer base flow was ground water from the floodplain GHB cells, while water from the terrace GHB cells equaled inputs from the floodplain GHB cells during winter base flow. Unlike the gravel bar, ground water flows through the floodplain were dominated by precipitation during storms.

The overall pattern of subsurface flow changed little over the course of the year, even though the relative flux from each source changed among seasons and during storms. Apparently the longitudinal gradient of the main valley floor, the location and stage of the main stream, and the influence of the relic channel all influence the pattern of subsurface flow. Changes in the flux from each source result in local steepening of head gradients and increase water table levels, but do not change patterns of subsurface flow.

The interface between the advected channel water and the ground water may be sharp, and stationary through time where relic or back channels create zones of convergent flow. This situation existed along the lower half of the relic channel where subsurface water is discharged. Little mixing of advected channel water and ground water occurred, even within 2 or 3 meters of the relic channel. There may be a relatively large mixing zone other locations which shifts location depending on the size of the fluxes of advected channel water and ground water. There was a small region near the head of the gravel bar where advected channel water flowed into the aquifer beneath the floodplain and mixed with ground water. This zone exceeded 10 m in width during summer low flow, but was narrower in other seasons of the year when ground water fluxes through the floodplain were greater.

CHAPTER 3:
NITROGEN DYNAMICS IN THE SHALLOW AQUIFER ADJACENT TO A FOURTH-ORDER MOUNTAIN STREAM: SEASONAL AND STORM DYNAMICS

Introduction

Primary productivity in third-order, and larger streams in the Cascade Range, Oregon, is nitrogen limited (Gregory 1979). Consequently, stream productivity is regulated by the rate at which nitrogen is cycled through the stream ecosystem and by the rate at which nitrogen is added to the stream from adjacent riparian ecosystems. The chemical transformations involved in the cycling of nitrogen within ecosystems are mediated primarily by living organisms. In small, mountain streams, most bacteria and algae are not suspended within the water, but live on sediment surfaces (Hynes 1970, Vannote et al. 1980, Minshall et al. 1983, Wallis et al. 1981). Many studies have shown the importance of benthic communities to biochemical transformations (Hynes 1970, Dahm 1980, Bott et al. 1984, Loch et al. 1984, Pringle and Bowers 1984, Pringle 1987). However, subsurface epilithic communities also play important roles in stream ecosystems (Hynes 1983, Mickleburgh et al. 1984, Grimm and Fischer 1984, Loch et al. 1984). Consequently, it seems reasonable to expect that the rates of biogeochemical transformations of nitrogen should be a function the surface area of sediment and the residence time of water in contact with sediment.

In high gradient mountain streams where the streambed is armored by cobbles, the total surface area of sediment on the streambed is small. In comparison, surface area of sediment in the subsurface is large because there is a lower density of cobbles and the spaces between the cobbles are typically filled with sand and gravel. Therefore the flow of water between the stream and the subsurface and the residence time of the water in the subsurface may be major factors regulating nitrogen cycling within stream ecosystems, reducing spiraling

lengths (Elwood et al. 1983, Newbold et al. 1983) and contributing to tight cycling of nitrogen.

The hyporheic zone has long been known to be biologically active (Coleman and Hynes 1970). Nitrogen in the stream water is transported with advected channel water into the hyporheos where it may be transformed by biochemical processes (Grimm & Fisher 1984, Stanford and Ward 1988, Duff and Triska 1990). The hyporheic zone is typically well aerated (Triska et al. 1989), which allows mineralization of organic carbon (Triska et al. 1990) and nitrification of ammonium (NH_4^+-N). Inorganic forms of nitrogen may be taken up by plants, immobilized by microorganisms, or returned to the stream wherever advected channel water is discharged from the aquifer. In contrast ground water is typically anaerobic and either organic-N or NH_4^+-N is the dominant form of dissolved nitrogen. Nitrate (NO_3^--N) is not abundant because it is usually removed from ground water via denitrification (Coats et al. 1976, Rhodes et al. 1985, Peterjohn and Correll 1984, Pinay and Décamps 1988). Where ground water and advected channel water mix, NH_4^+-N supplied in the ground water is rapidly nitrified (Triska et al. 1990).

If additional sources of nitrogen were available to the stream, they could also be a major factor regulating stream productivity. Red alder is a nitrogen-fixing, early-successional species (Worthington 1965, Bollen and Lu 1968) that colonizes frequently flooded or recently disturbed surfaces along the margins of larger streams. Flows of advected channel water beneath these alder stands could leach nitrogen from the riparian zone and transport it to the stream. The sites along constrained stream reaches colonized by alder are typically narrow and discontinuous, seldom exceeding a few meters in width. In contrast, the valley floor is wide in unconstrained stream reaches and in these locations gravel bars are extensive, often exceeding 10 m in width. Lateral bars are present along either or both sides of the channel for much of its length, and it is common to find bars within the active channel. In most cases, these gravel bars are dominated by red alder.

Published estimates of nitrogen fixation rates using acetylene reduction method indicates that red alder may fix as much as 60 to 70 kg N ha^{-1} yr^{-1} (Tripp et al. 1979, Bormann and Gordon 1984), and studies based on chronosequences suggest that the accumulation rates of nitrogen in the forest floor and mineral soil beneath red alder stands are high, ranging from 85 kg ha^{-1} yr^{-1} (Cole et al. 1978) to 320 kg ha^{-1} yr^{-1} (Newton et al. 1968). Bormann and DeBell (1981) estimated a mean annual accumulation rate of 100 kg ha^{-1} yr^{-1}, with 15% accumulating in the forest floor, 35% in the surface soil horizons between 0 and 20 cm, 30% between 20 and 50-cm depth, and the remainder in biomass. However, these estimates were made in deep, well drained forest soils. In contrast, the soils of the gravel bars colonized by alders are young and poorly developed, with very high contents of cobble, gravel and coarse sand, without appreciable accumulation of organic material on the surface and with relatively shallow depths to the aquifer. Rates of nitrogen fixation have not been estimated for riparian environments, but there is no reason to expect that they would be dramatically different than in uplands. Further, since the soils of the gravel bar environments are poorly developed, it seems reasonalble that leaching in this environment would at least equal losses from deep, well developed, upland soils.

The objective of this study was to monitor changes in dissolved nitrogen concentrations in subsurface water among seasons and within storms. These data are used to infer the effect of both leaching and biochemical transformations on nitrogen concentrations, and to quantify the effect of subsurface flows on the transport of nitrogen between the riparian forest and adjacent stream ecosystem. The conceptual model presented above (Chapter #1) predicts that the magnitude of subsurface flows, relative to stream discharge, would be largest in unconstrained third- or fourth-order streams, and that nitrogen fixed by red alder in this location may be a significant source of nitrogen to the stream. Therefore, I choose a study site along a fourth-order unconstrained, stream reach in the Lookout Creek catchment, H. J. Andrews Experimental Forest, Oregon (Fig. I.1).

Methods

Site Description

The study site (Fig. I.1) is located along McRae Creek, a fourth-order stream within the Lookout Creek catchment and the H.J. Andrews Experimental Forest in the western Cascade Mountains of Oregon (44° 10' N, 122° 15' W). Most of the area is in primary Douglas-fir forest (*Pseudotsuga menziesii* (Mirbel) Franco.) and western hemlock (*Tsuga heterophylla* (Raf.) Sarg.) forest. A network of logging roads was constructed within the catchment and approximately 24% of the area has been clearcut and regenerated in Douglas-fir plantations since 1950. Primary logging roads continue to be maintained within the catchment to provide research access.

The drainage area above the study site is 1,400 ha, and elevation within the catchment ranges from 600 m at the study site to 1,600 m along the drainage divide. At elevations above 1,000 m snow accumulates during the winter; at lower elevations, snow falls during cold winter storms but is melted during warmer rain storms so that in most winters the ground is not permanently snow covered. Average annual precipitation is approximately 2,500 mm, falling mainly between November and March (Bierlmaier and McKee 1989). Stream discharge was highly variable over the study period, ranging from a low of 400 m^3 h^{-1} during September or October, to 2,200 m^3 h^{-1} during base flow periods throughout the winter, and with peak flows during fall and winter storms exceeding 20,000 m^3 h^{-1} .

The instrumented study site is 250 m long and 80 m wide. It is located along the eastern bank of an unconstrained stream reach in which the entire valley floor exceeds 100 m in width (Fig. II.1). Within this reach alluvial sediment has been reworked by lateral channel migration. A layer of rounded, stream-worked cobbles underlies the entire floodplain. However, the depth to this layer varies depending on the thickness of overbank deposits. A complex of landforms is present within the study site, including recently formed gravel bars, older

floodplain surfaces, relic channels, and terraces. The variety of landforms and the recent history of forest disturbance from flooding and associated lateral channel migration has resulted in a heterogenous forest. Red alder, an early-successional, nitrogen-fixing, deciduous tree (Worthington 1965, Bollen and Lu 1968) occupies areas recently disturbed by fluvial processes adjacent to the stream channel. Conifer-dominated stands cover the rest of the study site.

The study site was staked on a 10 x 10 m grid, and used as a base for mapping the major surface features of the valley floor and boundaries between the valley floor and adjacent alluvial fans, terraces and hillslopes. The locations of all wells were mapped (Fig. II.1) and the elevation of the top of the well casing and the ground level at each well was surveyed. Elevations for the stream boundary were surveyed by stretching a measuring tape down the center of the stream and surveying the elevation of the stream bed and recording the depth of water at 1 m intervals. All elevations for the entire study site were referenced to an arbitrary bench. Maps of the landforms and well locations were digitized in ARC/INFO.

Well Network

There is no road access to the study site so all wells had to be driven by hand. Because of the presence of large cobbles throughout the study site, the deepest wells penetrate only 2.5 m below the surface. All attempts to nest wells of differing depths failed.

Two types of wells were used in this study: observation wells and sample wells. Casings for observation wells were made from varying lengths and diameters of PVC pipe. Most were 2.54 cm in diameter, but some were constructed from 3.81 or 7.62 cm diameter pipe. Well "screens" were made by drilling 0.32 cm holes into the bottom 50 cm of each PVC pipe, at an approximate density of 1 hole cm^{-2}. The bottom of each casing was plugged with a solid rubber stopper to prevent sediment from entering the bottom of the well.

All wells were capped with PVC caps to prevent contamination with foreign materials, and caps were vented to prevent the build up of back pressure when water table elevations changed.

Sample wells were constructed from 45 cm lengths of 2.54 cm diameter, porous, high density polyethylene pipe (HDPE) (Aquaculture Research / Environmental Associates, Inc., P.O. Box 1303, Homestead FL 33090). These pipes have a mean pore diameter of 20 μm, which filters sediment out of the collected samples (C. Dahm, Univ. New Mexico, personal communication). The bottom end of the well casing was closed with a 2.54 cm diameter PVC cap. A length of 2.54 cm PVC pipe was added using a PVC sleeve connection to extend the casing above the ground surface. Fittings were pressed together without glue. Sample wells were permanently sealed using a two hole rubber stopper with Pyrex tubing pressed through the holes. A Tygon evacuation tube was connected to one glass tube and extended to the bottom of the well so that water samples could be collected. The other glass tube provided an air inlet to prevent drawing a vacuum when collecting samples.

Both the HDPE and PVC pipe were scrubbed with alcohol and rinsed in tap water to remove ink and manufacturing residues. Then, the well casings and other well parts were acid washed by soaking them for 24 hr in a 0.5 M HCl bath, and then rinsed with deionized water (DI). The acid bath was changed and the well casings and other parts were soaked for another 24 hr and again rinsed with DI water. Finally, well casings and parts were soaked in DI water for 24 hours to remove the acid residue. Wells were assembled, wrapped in clean aluminum foil or plastic wrap, and transported to the field.

Initially, sample wells were paired with observation wells so that water table levels could be measured concurrently with the collection of water samples. Wherever possible, wells were placed into holes driven at least 50 cm below the surface of the water table at summer base flow. Holes were back filled with the soil originally removed, and if necessary, additional fill was taken from nearby soil pits or recent root-throw pits. Following installation of the observation wells, back fill was washed and entrained sediment removed from the well by

repeated pumping using a large diameter tube and a bilge pump. Sample wells were treated similarly, but in this case the existing Tygon evacuation tubes were used to prevent contaminating the well.

The transect of wells PA03 to PA72 was established during late summer in 1989 as part of a pilot study to monitor changes in solute concentrations of ground water across a toposequence from the hillslope to the stream (Fig. II.1). During the summer of 1990, five more transects of observation wells were added to provide a plan view of the water table within the study site. However, only four more sampling wells were added (adjacent to PX09, PX30, PE23 and PE37) because of the difficulty of driving wells into the cobbley sediment. During the summer of 1991, about half of the observation wells were retro-fitted with evacuation tubes so that water samples could be collected over a larger area. Glass tubes were bent into a "J" shape with a narrow radius so they would fit inside the 2.54 cm observation well. Tygon tubes and glass tubes were acid washed and DI rinsed, as described above, and put into the observation wells with the bend of the glass tube resting on the bottom of the well. An additional 18 observation wells were established on, and adjacent to, the gravel bar during 1991 and 1992.

Field Sampling

Sampling Protocol. Water table depths were recorded from observation wells within 24 hours of collecting base flow water samples. During 1991, dissolved oxygen and temperature were also measured in each observation well using a YSI Model 51A dissolved oxygen meter and a YSI probe. Then, both sample wells and observation wells that were retro-fitted to collect samples were pumped dry and allowed to refill before collecting samples.

Water samples were collected only from the sample wells during storms. Water samples could not be collected from observation wells because these were used to monitor changes in water table levels during storms and withdrawing

water to collect samples would have changed the water level in the wells. Twenty-four hours before a storm was forecasted, all sample wells were pumped dry and allowed to refill. Wells were not re-evacuated between sample collections during a storm.

To collect water samples, an acid washed flask was connected to the evacuation tube and a vacuum was drawn on the flask with a hand pump. A small amount of water was drawn into the flask and used to rinse the flask. The water sample was then collected. A small amount of the sample was transferred to an acid washed HDPE bottle and used to rinse the bottle. Subsequently, the remainder of the sample was transferred to the sample bottle and placed on ice. The flask was rinsed with DI water between collection of individual samples.

The sample flask could not be rinsed with sample water prior to collecting a sample from observation wells. When the vacuum was released in order to rinse the sample flask, the column of water in the evacuation tube would mix with the water in the well, suspending substantial amounts of fine sediment making the water too muddy to be filtered. Samples collected without pre-rinsing the collection flask may have been contaminated. To test this, field blanks were collected for analysis. These were prepared by pumping either DI water or stream water into the collection flask without first pre-rinsing with sample. The concentrations of dissolved nitrogen from the field blanks were compared to concentrations of nitrogen in standard samples. There was no measurable dissolved nitrogen in the DI water, nor were the stream samples measurably diluted by residual DI water in the sample flask when samples were collected this way.

Sampling Schedule. Water samples were collected from wells to compare changes in dissolved nitrogen concentrations among seasons and within storm events. Sampling was concentrated from mid-summer to early fall and during late fall storms. Samples were also collected during mid winter, in early spring, and during a single late-winter storm.

Analytical Methods

Samples were analyzed at the Cooperative Chemical Analytical Laboratory, which is located on the OSU campus, and administered jointly by the U.S.D.A. Forest Service and the Department of Forest Science, Oregon State University. Established protocol for preparation and analysis of water samples was followed to prevent errors resulting from procedural differences when comparing results of this study with long-term precipitation and stream flow data for the H. J. Andrews Experimental Forest.

Prior to analysis all samples were filtered with acid washed glass microfibre filters (Whatman GF/C, retention of 1.2 μm). The analysis for total Kjeldahl nitrogen (TKN) generally followed the Kjeldahl procedure using a H_2SO_4 digestant and $CuSO_4$/KCl catalyst, but with Nessler finish (Greenberg et al. 1980). NO_3^- and NH_4^+ were analyzed on an Technicon Autoanalyzer II. The analysis for NO_3^- (procedure 418F, Greenberg et al. 1980) was modified following Technicon's Industrial Method No. 100-70W distributed in 1973 (Technicon Industrial Systems, Tarrytown NY 10591). The analysis for NH_4^+ followed procedure 417F (Greenberg et al. 1980). Dissolved organic nitrogen (DON) was the difference between TKN and NH_4^+. Total dissolved nitrogen (TDN) was the sum between NO_3^-, NH_4^+, and DON.

Base flow samples were transported on ice to the Cooperative Chemical Analysis Laboratory at Oregon State University. Samples were filtered within 24 hours of collection and analyzed within 48 hours of collection. This was not possible during storm events since sample collections were spread over several days, thus storm samples were frozen for later analysis. Additionally, from the late fall of 1991 through the winter of 1992, the Auto-analyzer was not working and all base flow samples had to be frozen until it was possible to analyze them. Because this could have changed the nitrogen chemistry of the samples a series of samples were collected from the stream and from a sample well. One group was filtered and analyzed immediately; one group was filtered and frozen for several months, thawed and analyzed; and a final group was frozen without filtering,

thawed, filtered and then analyzed. No treatment effect was detected for either TKN or NO_3^-, although there was a loss of 4 to 5 μg l^{-1} NH_4^+-N.

Statistical Analysis

All samples were categorized by location, season, and a storm index variable. Samples from wells were grouped by landforms and grab samples from surface water were assigned to the stream, tributary, or relic channel. Seasons were defined using a combination of red alder phenology and stream discharge characteristics. Summer is a five to six month period of gradually decreasing base flow discharge that starts in June when red alders are fully leafed out and lasts until late September or early October, when red alders typically drop about 50% of their leaves. Fall is a period of increasing base flow discharge, beginning with the start of the rainy season in October or November and lasting until mid-December. The winter months, mid-December through mid-March, are characterized by frequent storms during the coldest time of year when red alders are dormant. Spring is a period with many storms, high stream discharges from melting snow at higher elevations of the catchment, followed by decreasing stream discharge in very late spring as dryer conditions prevail. The start of spring coincides with the swelling of red alder leafbuds and extends until full-leaf conditions in early summer. Each season was subdivided into periods of base flow or storm flow using hydrographs of either stream discharge or well records of water table elevations. Storms were further subdivided by the rising, crest, and falling legs of the stream hydrograph.

Dissolved nitrogen concentrations did not fit a normal distribution and were therefore *ln* transformed to fit a normal distribution. Analysis of variance was used to test data from baseflow periods (all seasons and landforms) for overall differences in dissolved nitrogen and oxygen concentrations among seasons within each landform, and among landforms within each season. Because the sampling design was unbalanced, significant differences were further analyzed

with a Least Square Means to test for significant differences between the mean concentration of dissolved nitrogen or oxygen for each pairwise combination of seasons or landforms. The same statistical analyses were used to test for differences in the mean concentration of nitrogen in samples collected during storm periods, but these analyses were grouped by season (fall or winter). Means and standard errors of the mean were back transformed for graphical presentation. Back-transformed standard errors are not evenly distributed above and below the mean, therefore, only the upper (larger) standard error is shown.

Results and Discussion

Seasonal Changes in Dissolved Nitrogen and Oxygen

Large differences in dissolved NH_4^+ and NO_3^- concentrations were observed among seasons (Fig. III.1). In general, observed concentrations of dissolved nitrogen were significantly greater in the summer and fall than in either the winter or spring. Similar trends were observed for both DON and TDN, but fewer samples were collected and the data were highly variable. Thus, these differences were not statistically significant in most cases. The pattern was reversed for dissolved O_2, with concentrations significantly greater in the winter and spring than either the summer or fall.

Differences Among Landforms

Differences in dissolved NH_4^+ and NO_3^- concentrations were observed among landforms at base flow for each season (Fig. III.1). These differences were usually greatest during the summer and fall, when concentrations of NH_4^+, NO_3^-, and TDN were also greatest. The concentration of NO_3^- was greater in samples collected from wells on the gravel bar and floodplain than in samples collected from either the tributary or main stream. DON was the dominant form of nitrogen in water samples, with a single exception, concentrations of NO_3^- were greater than DON in samples collected from gravel-bar wells during summer base flow.

Summer Base Flow. Samples locations from the stream, from a well in the streambed, from wells in the gravel bar, and from the relic channel are located along a path of advected channel water flowing through the gravel bar (Fig II.12). The mean concentration of NO_3^- was significantly greater in samples

Fig. III.1. Mean dissolved nitrogen concentrations for each landform (or location) for each season of the year. Error bars show the standard error of the mean. numbers are the sample size for each group, sample sizes are equal for NH_4^+-N and NO_3^--N, and for DON and TDN. Means and standard errors were calculated from *ln* transformed data and back transformed before graphing.
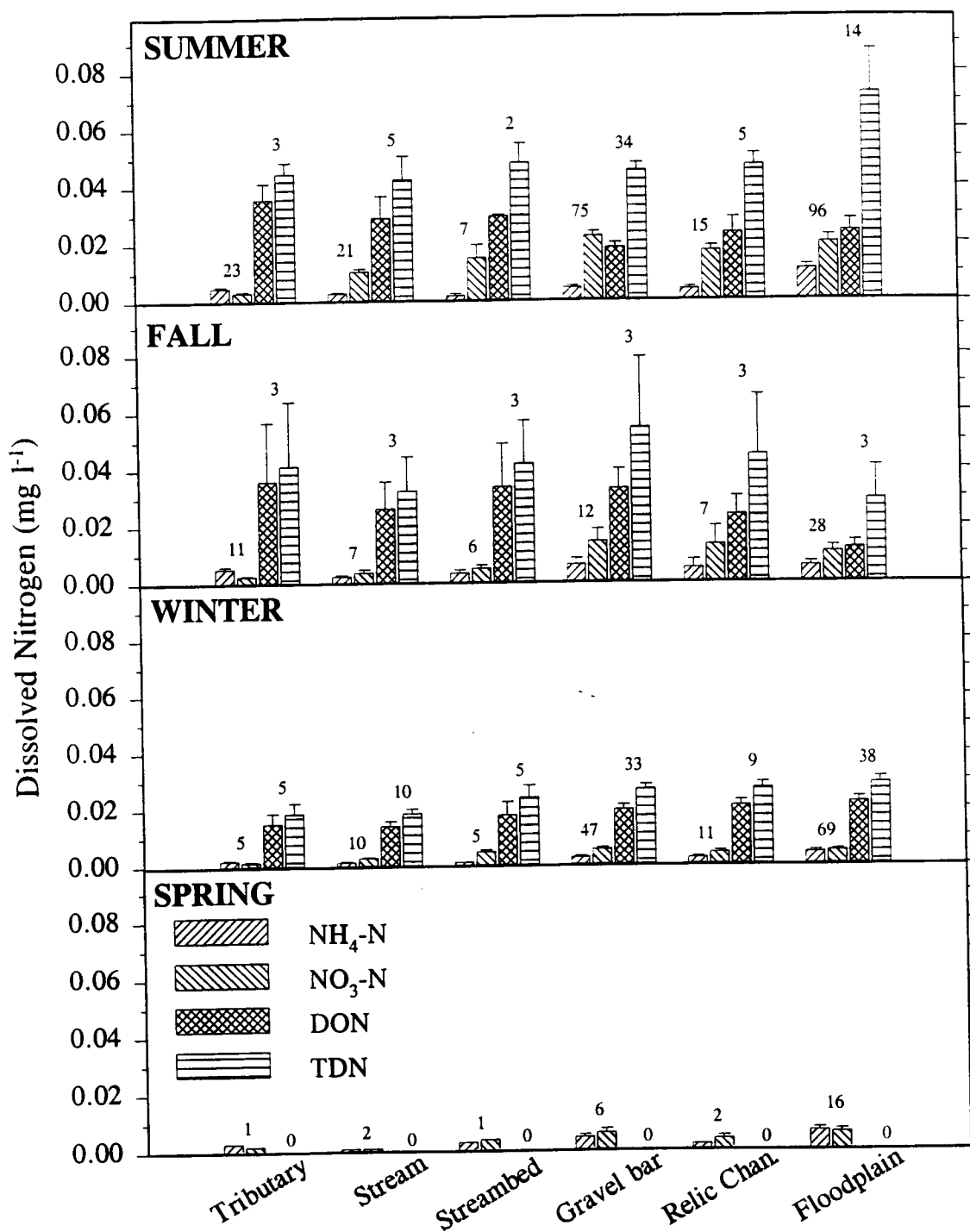
collected from the gravel bar than in the stream (Fig. III.1). There was also a trend toward decreasing concentrations of DON in samples from the gravel bar wells, although the differences between the mean concentrations among locations were not statistically significant. Mean concentrations of dissolved O_2 were significantly greater in stream water than in wells located on the gravel bar.

The increased NO_3^- concentration during summer must result from the mineralization and subsequent nitrification of organic nitrogen because there was no change in the concentration of either NH_4^+ or TDN. However, the source of the organic nitrogen is not known. The most likely source for the increased NO_3^- is the transformation of stream DON transported into the subsurface environment with advected channel water. The trend of decreasing DON but constant TDN with distance along this flow path during summer base flow and the concurrent loss of dissolved O_2 support this hypothesis. Microbial processing determines the fate of labile dissolved organic carbon in many streams, and these microbes are most commonly attached to sediment surfaces (Cummins et al. 1972, Lock and Hynes 1975 & 1976, Dahm 1980). Results from MODFLOW suggest that the mean turnover time for ground water in the gravel bar is approximately 16 days (Chapter #4). Given the length of time and the high surface area of sediment, it seems reasonable that the gravel bar was a site for the transformation of stream DON to NO_3^- during the summer.

Triska et al. (1990) documented that NH_4^+ from ground-water is nitrified in the hyporheic zone where ground water mixes with advected channel water, but this is not a likely explanation for the increased concentrations of NO_3^- observed in this study. Temperature measurements from late summer, when ground water was $5°$ C colder than stream water, and measurements of water table levels indicated that water beneath the gravel bar was entirely advected channel water. The increase in NO_3^- may also result from the transformation of organic nitrogen supplied in fine particulate organic matter (POM) transported from the stream into the subsurface, or leaching from the soil above. However, if POM is the ultimate source of the increased NO_3^-, then TDN should have also increased with distance from the stream, but this was not observed (Fig. III.1).

The floodplain at the McRae Creek study site appeared to be the primary source of nitrogen for the stream during summer low flow. The average concentrations of both NH_4^+ and TDN were significantly greater in water samples collected from floodplain wells than in samples collected from other locations (Fig. III.1). Mean concentrations of dissolved O_2 were significantly lower in wells located on the floodplain than in the stream. Triska et al. (1990) reported that potential rates of nitrification were much lower in the ground-water zone than in the hyporheic zone. This might account for the difference between the gravel bar, where NH_4^+ was never observed in high concentrations, and the floodplain wells where concentrations of NH_4^+ were often quite high during the summer.

There are three possible sources for the nitrogen in water samples collected from the floodplain. The nitrogen must come from either ground water inputs from the adjacent hillslopes, mobilization of nitrogen from organic matter deposited within the floodplain sediment, or by leaching from the soil profile overlying the aquifer. Drainage from hillslopes is a potentially important source of nitrogen to the ground water. The ground water flux into the aquifer from the hillslopes accounted for ~15% of the total subsurface flow through the floodplain during the summer (Chapter 2). The mean concentration of dissolved nitrogen measured in samples collected from floodplain wells were similar to those reported for soil water at 2 m depth, beneath the rooting zone of a nearby old-growth Douglas-fir forest (Sollins et al. 1980, Sollins and McCorison 1981).

Measurements of water table levels and the results of MODFLOW (Chapter #2) indicated that many parts of the floodplain did not recieve flow from the adjacent hillslopes (Fig. II.12). Rather, these locations received ground water from upstream portions of the aquifer. The variation in the concentration of dissolved NH_4^+ in these locations was high. This variation may result from differences in the location and amounts of organic matter deposited within the floodplain. It did not seem to be related to either the saturated hyrdraulic conductivity (k) or the concentrations of dissolved O_2, as was reported by McDowell et al. (1992).

Fall Base Flow & Storm Events. The concentrations of NO_3^- and NH_4^+ were higher in samples collected from the gravel bar than in samples collected from the stream during fall base flow.   There was also a trend towards increasing concentration of TDN but without a decrease in the concentration of DON (Fig. III.1). Differences among the observed mean concentrations of either DON or TDN among landforms/locations were not statistically significant, however, because of the high variability in the data and small sample sizes. These data suggest that the gravel bar was a source of nitrogen for the stream during the fall. Winter dormancy may reduce plant uptake of nitrogen, while relatively warm temperatures and inputs of fresh organic matter from leaf fall, and perhaps fine root turnover, might maintain high rates of microbial activity. Thus mineralization and nitrification of labile organic nitrogen could produce high levels of NO_3^-. Leaching of the soil profile would increase at the onset of the rainy season because of both percolation of precipitation through the rooting zone and increased elevation of the water table into portions of the soil profile that have not been saturated since spring. Thus, it seems reasonable that NO_3^- stored in the soil profile would be mobilized and transported in the subsurface flow.

Mean concentrations of dissolved NO_3^- in samples collected from McRae Creek and from the gravel-bar wells were significantly greater during the rising leg, crest, and falling leg than concentrations during fall base-flow periods (Fig. III.2). The observed concentration of NO_3^--N increased during the rising leg of the hydrograph, averaged 78 μg l^{-1} for the short period during peak flow, a 5-fold increase over fall base-flow concentrations, and decreased rapidly during the falling leg of the hydrograph (Fig. III.3). Even though there was increased flow through the gravel bar during peak flows, the model predictions (Chapter #2) indicate that the mean turnover time for water in the gravel bar was approximately 10 days. Consequently, a simple replacement of the nitrogen-poor water with nitrogen-rich water during storm events can not explain the rapid changes in dissolved nitrogen concentrations during peak flow. Measurements could have been biased because nitrogen concentrations in shallow wells close to the roots of red alders may have been higher for the short period at the peak of

Fig. III.2. Mean dissolved nitrogen concentrations for each landform (or location) during fall storms. Error bars show the standard error of the mean. numbers are the sample size for each group, sample sizes are equal for NH_4^+-N and NO_3^--N, and for DON and TDN. Means and standard errors were calculated from *ln* transformed data and back transformed before graphing.
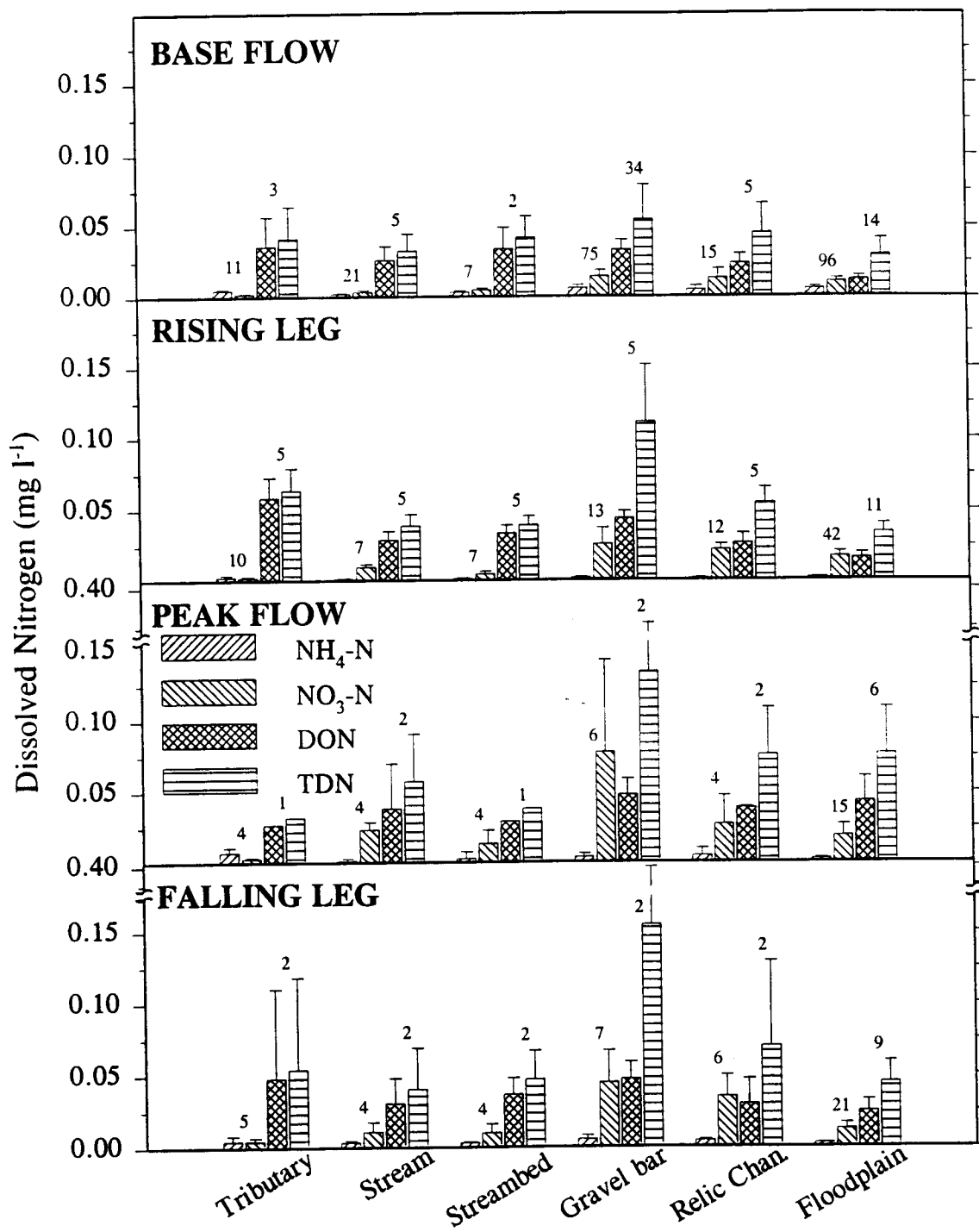
Fig. III.3. Ratio of the mean dissolved nitrogen concentrations during fall storms. relative to base flow concentrations, for each landform. The average concentration during the rising. peak. and falling portions of the hydrograph was divided by the mean concentration during fall base flow.
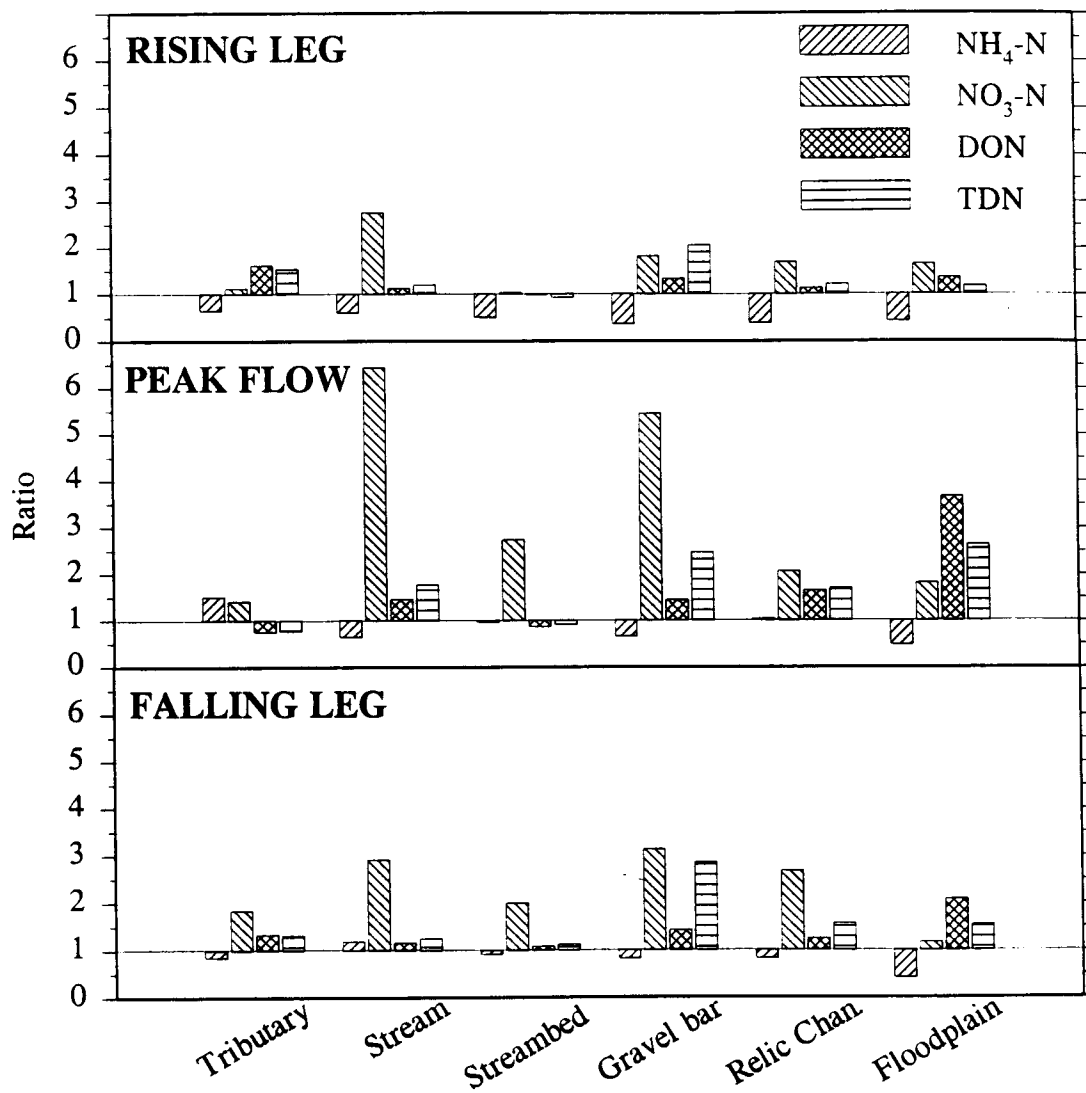
the storm, and decreased quickly as nitrogen-rich and nitrogen-poor water within the aquifer was mixed. Alternatively, a relatively small volume of water within larger pore spaces could turn over much more rapidly than the rest of the ground water within the gravel bar. Similar flow systems, in which "macropore flow" occurs, have been documented for forest soils (Bevin and Germann 1982, Seyfried and Rao 1987, Sollins and Radulovich 1988). Water flowing through macropores may be isolated from the bulk soil water (Thomas and Phillips 1979) which may influence the leaching of nutrients (Thomas and Phillips 1979, Sollins and Radulovich 1988).

In any case, gravel bars along the stream network must be an effective source of NO_3^--N, because the observed concentrations in the stream at peak flow averaged 24 μg l^{-1}, more than a six-fold increase over mean base-flow concentrations (Fig. III.3). Neither the tributary nor the floodplain are likely sources for this NO_3^-, because measured NO_3^- concentrations in these locations were always less than concentrations in stream water. The only location in which observed NO_3^- concentrations exceeded that of stream water was the gravel bar (Fig. III.2).

Nitrogen concentrations in samples collected from floodplain wells during fall base flow were lower than during the summer (Fig. III.2), and the concentration of NH_4^+ and DON changed rapidly during storms (Fig. III.3). NH_4^+ concentrations in samples collected during storms were significantly lower than during base flow. In contrast, concentrations of DON increased significantly during peak flow and rapidly decreased to pre-storm concentrations afterwards. Again, a simple replacement of nitrogen-poor water with nitrogen-rich water during storms can not explain the rapid changes in DON concentrations. The results from MODFLOW indicated that the mean turnover time of ground water in the aquifer would be approximately 30 days, far too long to cause changes during a single storm event. Measurements could have been biased because nitrogen concentrations in shallow wells may have been higher for the short period at the peak of the storm, and decreased quickly as nitrogen-rich and nitrogen-poor water within the aquifer was mixed. Alternatively, a relatively

small volume of water within larger pore spaces could turn over much more rapidly than the rest of the ground water within the floodplain.

Winter Base Flow & Storm Event. Nitrogen concentrations were much lower during the winter than during the summer or fall (Fig. III.1). As before, concentrations of NH_4^+, NO_3^-, and TDN were significantly higher in sample collected from gravel-bar wells than in samples collected from the stream. Mean dissolved nitrogen concentrations in samples collected from floodplain wells were also significantly greater than concentrations observed in samples from either stream or tributary. Dissolved nitrogen in samples from all locations was dominated by DON, which never comprised less than 70% of TDN (Fig. III.1).

Samples were collected only during a single late-winter storm event in March, 1993 (Fig. III.4). The observed concentrations of dissolved NO_3^- in samples collected at peak flow were significantly greater in the main stream, but significantly lower in the tributary, than mean concentrations observed during base flow. Otherwise, concentrations of dissolved nitrogen did not change during the storm (Fig. III.4). These data suggest that continued flushing of nitrogen pools throughout the rainy season either depleted existing pools or exceeded the rate at which mineralization and nitrification replenished these pools. Most vascular plants were dormant during the winter, so fresh inputs of labile OM from root turnover would not be expected. Further, cold temperatures should have reduced the rates of microbrial activity which produces NO_3^- and DOM. Consequently, it seems reasonable that the soil would not be a large source of nitrogen to the ground water at this time of year.

Spring Base Flow. Samples for spring base flow were collected on a single date, and samples were only analyzed for inorganic nitrogen. Concentrations of dissolved NH_4^+ and NO_3^- were quite similar to those observed during winter base flow (Fig. III.2).

Fig. III.4. Mean dissolved nitrogen concentrations for each landform (or location) during a winter storm. Error bars show the standard error of the mean. numbers are the sample size for each group. sample sizes are equal for NH_4^+-N and NO_3^--N. and for DON and TDN. Means and standard errors were calculated from *ln* transformed data and back transformed before graphing.
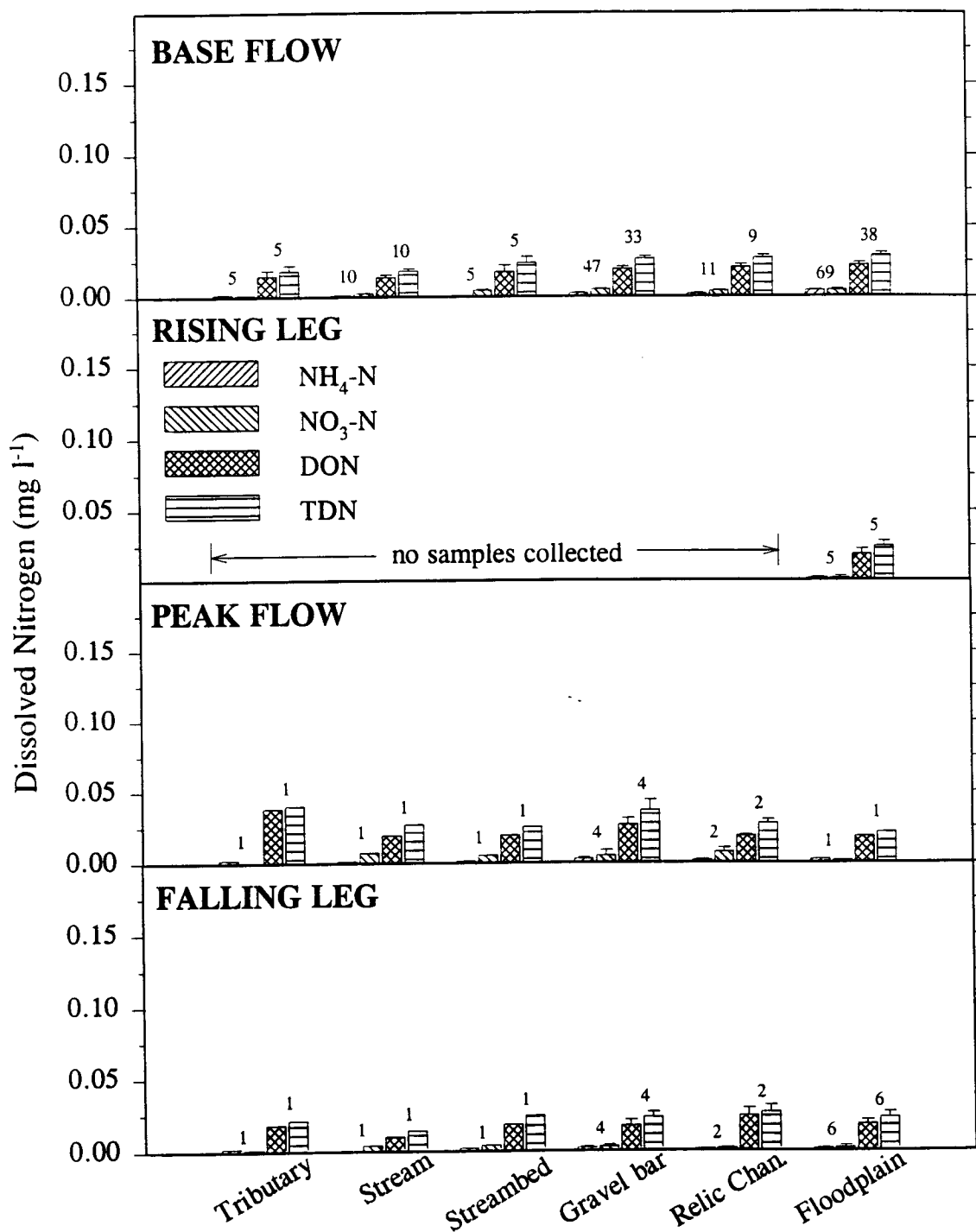
Conclusions

The floodplain appeared to be the primary source of nitrogen for the stream during summer low flow when concentrations of TDN and NH_4^+ were much higher in samples collected from the floodplain than in samples from other locations. Concentrations of NO_3^- in advected channel water flowing through the gravel bar increased and DON tended to decrease during the summer. However, there was no apparent trend in the concentration of TDN, suggesting that DON in the stream water was transported into the subsurface where it was transformed to NO_3^-.

The gravel bar appeared to be the primary source of nitrogen for the stream during fall base flow and storms. During the fall, concentrations of NO_3^- in advected channel water flowing through the gravel bar increased, and concentrations of DON and TDN also tended to increase, suggesting that the gravel bar was a net source of nitrogen. The greatest concentrations of nitrogen were observed during fall storms at the beginning of the rainy season. Concentrations of NO_3^- were five- to six-fold higher in samples collected from the stream and gravel bar during peak flow than during base flow. A similar pattern was observed in samples collected from the floodplain where concentrations of DON were threee-fold higher durng fall storms than during fall base flow.

In general, observed concentrations of dissolved nitrogen were significantly greater in the summer and fall than in either the winter or spring. Percolation of precipitation through the soil profile during fall and early winter storms appeared to flush nitrogen into both the advected channel water and the ground water. This nitrogen was then transported to the stream. Either the pool of mobile nitrogen was small, or biotic processes that produce mobile nitrogen are much slower during the winter, because nitrogen concentrations changed little during a late winter storm.

No location within the gravel bar was anaerobic, and ground water at most locations within the floodplain was also areobic. Because concentrations of

dissolved NO_3^--N were low within the floodplain, and since little of the aquifer was anaerobic, denitrification is probably not a significant pathway for nitrogen loss in this environment.

CHAPTER 4:
THE TRANSPORT OF WATER AND DISSOLVED NITROGEN THROUGH THE FLOODPLAIN OF A FOURTH-ORDER MOUNTAIN STREAM: SEASONAL AND ANNUAL BUDGET

Introduction

Interest in valley-floor ground-water systems has increased dramatically over the last decade due to a growing awareness that riparian areas may play an important role in catchment hydrogeochemistry (Bencala et al. 1984, Grimm and Fisher 1984, Stanford and Ward 1988, Pinay and Decamps 1988, Ford and Naiman 1989, Triska et al. 1989, Triska et al. 1990, Castro and Hornberger 1991). However, the effects of biochemical transformations occurring in the subsurface on the forms and concentration of dissolved nutrients in stream water are poorly understood. The objective of this study was to quantify the effect of subsurface flows on the transport of nitrogen between a riparian forest and an adjacent stream ecosystem. The effect of subsurface processes on stream water chemistry depends on both the rate of flow between the stream and the shallow aquifer and the rates of biogeochemical processes that transform nitrogen. The estimates of the rates of subsurface flow through a shallow aquifer in an unconstrained reach of a mountain stream were presented in Chapter #2. The patterns observed in dissolved nitrogen concentrations among seasons and within storms were presented in Chapter #3. In this chapter I use the subsurface flow rates from individual model simulations to estimate total, seasonal, subsurface water flux. I then multiply the water flux estimates by the mean dissolved nitrogen concentrations to estimate the seasonal flux of nitrogen from the aquifer into the adjacent stream.

Methods

Site Description

The study site (Fig. I.1) is located along McRae Creek, a fourth-order stream within the Lookout Creek catchment and the H.J. Andrews Experimental Forest in the western Cascade Mountains of Oregon (44° 10' N, 122° 15' W). Most of the area is in primary Douglas-fir forest (*Pseudotsuga menziesii* (Mirbel) Franco.) and western hemlock (*Tsuga heterophylla* (Raf.) Sarg.) forest. A network of logging roads was constructed within the catchment and approximately 24% of the area has been clearcut and regenerated in Douglas-fir plantations since 1950. Primary logging roads continue to be maintained within the catchment to provide research access.

The drainage area above the study site is 1,400 ha, and elevation within the catchment ranges from 600 m at the study site to 1,600 m along the drainage divide. At elevations above 1,000 m snow accumulates during the winter, at lower elevations, snow falls during cold winter storms but is melted during warmer rain storms so that in most winters the ground is not permanently snow covered. Average annual precipitation is approximately 2,500 mm, falling mainly between November and March (Bierlmaier and McKee 1989). Stream discharge was highly variable over the study period, ranging from a low of 400 m^3 h^{-1} during September or October, to 2,200 m^3 h^{-1} during base flow periods throughout the winter, and with peak flows during fall and winter storms exceeding 20,000 m^3 h^{-1}.

The instrumented study site is 250 m long and 80 m wide. It is located along the eastern bank of an unconstrained stream reach in which the entire valley floor exceeds 100 m in width (Fig. II.1). Approximately one-half of this area was selected as the model domain for a ground-water flow model, and subsurface fluxes through the model domain were estimated from model simulations (Chapter #2). The length of the stream channel within the model domain was 119 m. The gravel bar had an area of 825 m^2 and the floodplain had an area of 4106 m^2.

Ground Water Flow Predictions

To estimate the total ground water flux for each season of the year it was necessary to scale up from the rates of ground water flux predicted from individual simulations. Regression equations were developed (Chapter #2) to relate estimated subsurface flow to stream discharge under base-flow conditions. However, McRae Creek was not gauged, so I used records from Mack Creek which is 4.5 km away, with a catchment area of 875 ha (Fig. I.1) and a similar elevation range. Assuming that the unit area discharges would be similar for the two catchments, I multiplied Mack Creek discharge by the ratio of the areas of the two catchments (1.6) to estimate McRae Creek discharge. Observed stream stage at McRae Creek was graphed against the estimated discharge for each observation to test the relationship between these variables (Fig. II.14).

Graphs of stream discharge for Mack Creek were examined to separate periods of base flow from periods of storm flow. Stream discharge at the Mack Creek stream gauge is not recorded at fixed intervals, rather sampling rates are proportional to discharge. In general, periods of storm flow were characterized by rapidly changing stream discharge so that changes between consecutive measurements could be used to identify storm events. I initially searched the 13 yr (1979-1992) record of stream discharges using a simple computer program. After several tries, I found that changes in stream discharge greater than 0.035 m^3 s^{-1} identified most storms within the record. I then searched the discharge records by hand for any storms that had been missed or incorrectly classified.

The number of days with storm discharge in each season for the 13 year period of record were averaged and subtracted from the total number of days in each season to estimate the average number of days of base flow discharge. A base-flow hydrograph of the water year was constructed by averaging the daily mean discharge (storm days excluded) for each day within the period of record (for example: 1/1/79, 1/1/80, 1/1/81, ... 1/1/92; and so on for each day of the year). The daily average base-flow discharge at Mack Creek was then multiplied by 1.6 to estimate the corresponding discharge at McRae Creek. The regression

equations relating subsurface flux to stream discharge (Fig. II.11) were then used to estimate the mean, daily, subsurface-water flux through the study site for each day of the year under base flow conditions.

Scaling up estimates of subsurface flux during storms to estimate total annual storm flux was problematic. Only one storm event was simulated, however, this six-day period was a sequence of smaller, closely-spaced storms (Fig. IV.1) and could be treated as three separate storms. These storms varied in intensity and duration and were used to represent the flow conditions that may occur over a range in storm sizes. I used graphs of precipitation and ground water fluxes to divide the six-day period into small, intermediate, and large storm classes. The small storm class included only the first 12 hours of rainfall, and lasted for a total of 84 hours. The intermediate storm class included the first 54 hours of rainfall, and lasted 163 hours. The large storm class included all the precipitation for the entire period, and lasted for 248 hours. I further subdivided each of these events into a rising leg, crest, and falling leg, to match the times at which water samples were collected during storms. Water sample data indicated that peak nitrogen concentrations lasted for a period of only a few hours at the peak of storm discharge. Yet, hydrographs showed that the storm crest lasted longer during larger storms. To be consistent across all storm classes, I assumed that peak discharge lasted for 25% of the total time between the start of the storm and the time of peak instantaneous discharge. There was not a clear peak in subsurface dischargefrom the floodplain for the small storm class, so the inflection point was used as the crest of the storm instead of the peak in discharge. There was a near linear decrease in subsurface flow rates from the both the gravel bar and floodplain between 54 and 78 hours, and between 118 and 144, hours. I extended these lines until they reached the subsurface flow rates estimated for base-flow periods to estimate the length of time that subsurface flows were influenced by precipitation. I then calculated the area under the curve to estimate the total subsurface flux for the rising, crest and falling legs of the hydrograph within each storm class.

Fig. IV.1. Partitioning a six-day storm event into small. intermediate. and large storm classes. R, C, and F refer to rising leg, crest and falling leg of the hydrograph, respectively.
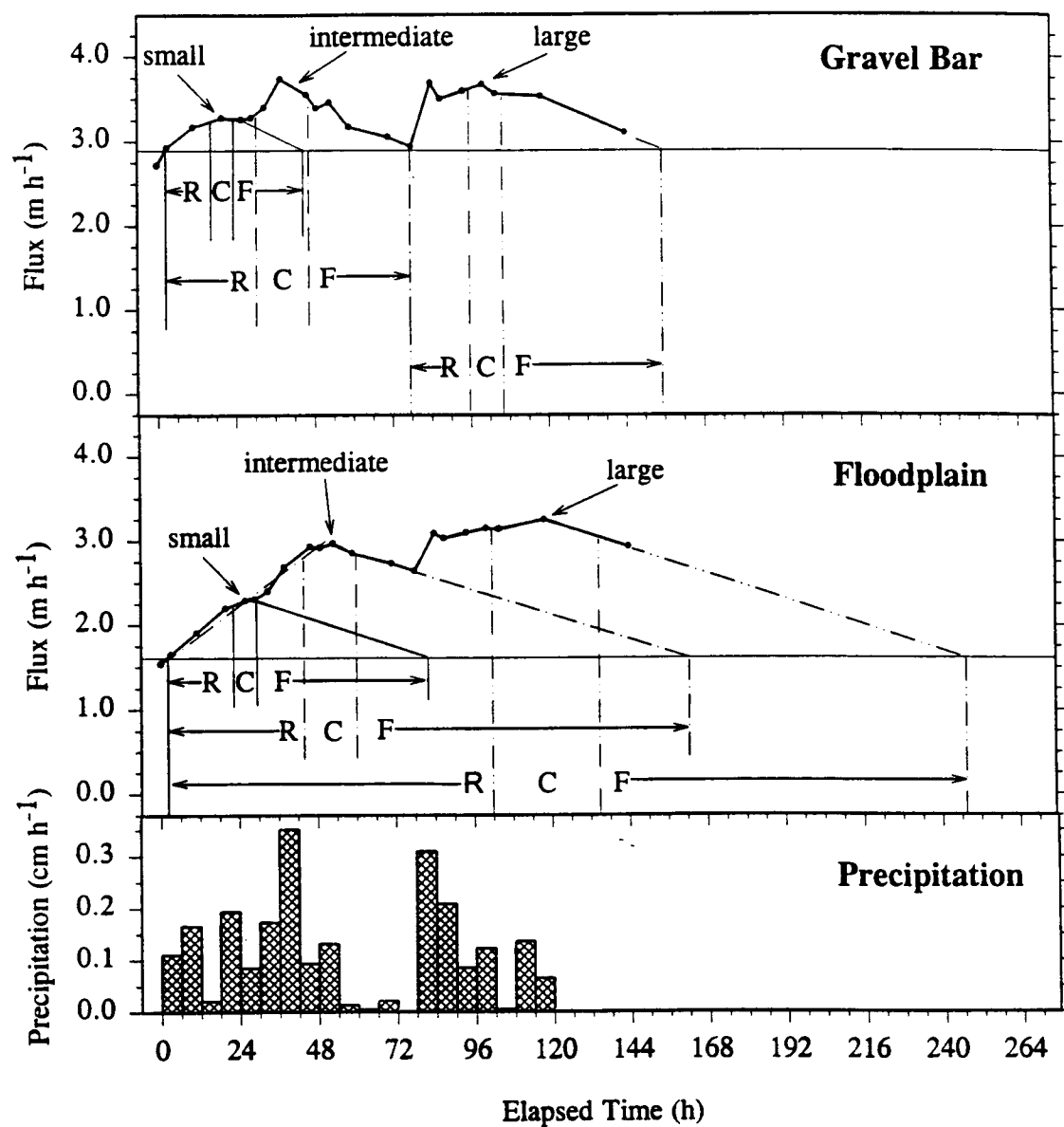
To estimate the total subsurface flux occuring during storms for each season of the year, the frequency of storms in each class was multiplied by the subsurface fluxes calculated for each of the three storm classes. Storm sizes and frequencies were calculated from stream discharge records for Mack Creek between 1979 and 1992 as described above. A consecutive string of days with storm discharge was considered a storm event, and the average number of storm events within each season was recorded. The length, peak instantaneous stream discharge, and the total event discharge were also recorded for each storm event. These variables were then used to rank all the storm events in each season during the period of record. The total event discharge recorded at Mack Creek for the three storm classes described above was $32,200$ m^3 of water for the small class, $68,700$ m^3 for the intermediate class, and $348,600$ m^3 for the large class. Thus, the list of storms was divided into three storm classes, with each class centered on these total event discharges. I then calculated the proportion of all storm events falling within each class during each season of the year. To estimate total subsurface flux, the proportion of storms in each class was multiplied by the number of storms in each season and by the subsurface flux estimated for storms of each class. Separate estimates were made each season of the year and for the rising, crest, and falling legs of the hydrograph.

Nitrogen Flux Estimates

Nitrogen concentrations were multiplied by the estimated subsurface flux of water to estimate the flux of nitrogen through the subsurface. Separate estimates were made for NH_4^+, NO_3^-, DON, and TDN; for samples collected from the floodplain and from the gravel bar; and for both base-flow periods and storm-flow periods in each season of the year. Additionally, separate estimates were made for the rising leg, crest, and falling leg of the hydrograph. The mean concentration of each form of nitrogen in the stream water was subtracted from the corresponding concentration in the advected channel water to correct for

transport into the subsurface by advective flow. The estimated nitrogen fluxes were standardized to unit area and unit time, or unit channel length and unit time, to compare between landforms and seasons.

Results and discussion

Subsurface Flux

Regression equations were used to estimate the rate of water flux through the aquifer during base flow. Stream discharge was highly correlated $(0.65 < r^2 < 0.99)$ to the estimated flux of water through the aquifer during base flow (Fig. II.11). The stream discharge estimated for McRae Creek tracked the seasonal trends in climate, reaching a mean low discharge in late summer of 750 m^3 h^{-1}. Discharge increased during the fall, following the onset of the rainy season, and averaged 2,000 m^3 h^{-1} during base flow periods through the end of the rainy season in late spring or early summer (Fig. IV.2). The model predictions had been validated over this range (Chapter #2), so the regression equations were appropriate to estimate the rate of water flux through the aquifer.

The seasonal storm frequencies were used to estimate water flux during storms. The analysis of stream discharge records from Mack Creek showed that, on averager, storm discharge occurred on 40% of the days during fall, 31% of the days during spring, and 28% of the days during winter. During these seasons, storms were nearly evenly distributed into small, intermediate, and large storm classes. Storm discharges were recorded for only 5% of the days during the summer, and most summer storms were small (Table IV.1). Estimates of water flux were weighted by the proportion of storms in each class and multiplied by the average number of storms during each season.

Gravel Bar. Flow of advected channel water through the gravel bar increased linearly with stream discharge during base-flow periods. Subsurface flows ranged from a low of 2.50 m^3 h^{-1} in late summer when stream discharge was 750 m^3 h^{-1} to a high of 3.25 m^3 h^{-1} during the winter and spring when stream discharge reached 2,000 m^3 h^{-1} (Fig. IV.2). These results suggest that the flow of advected channel water into the hyporheic zone depends on discharge, as was

Fig. IV.2. A) Proportion of the total subsurface flow through the gravel bar accounted for by advected channel water from the stream flowing into the gravel bar and by ground water from the floodplain flowing into the gravel bar: B) Estimated daily flux of advected channel water and ground water through the gravel bar: and C) Thirteen year average of stream discharge for McRae Creek.
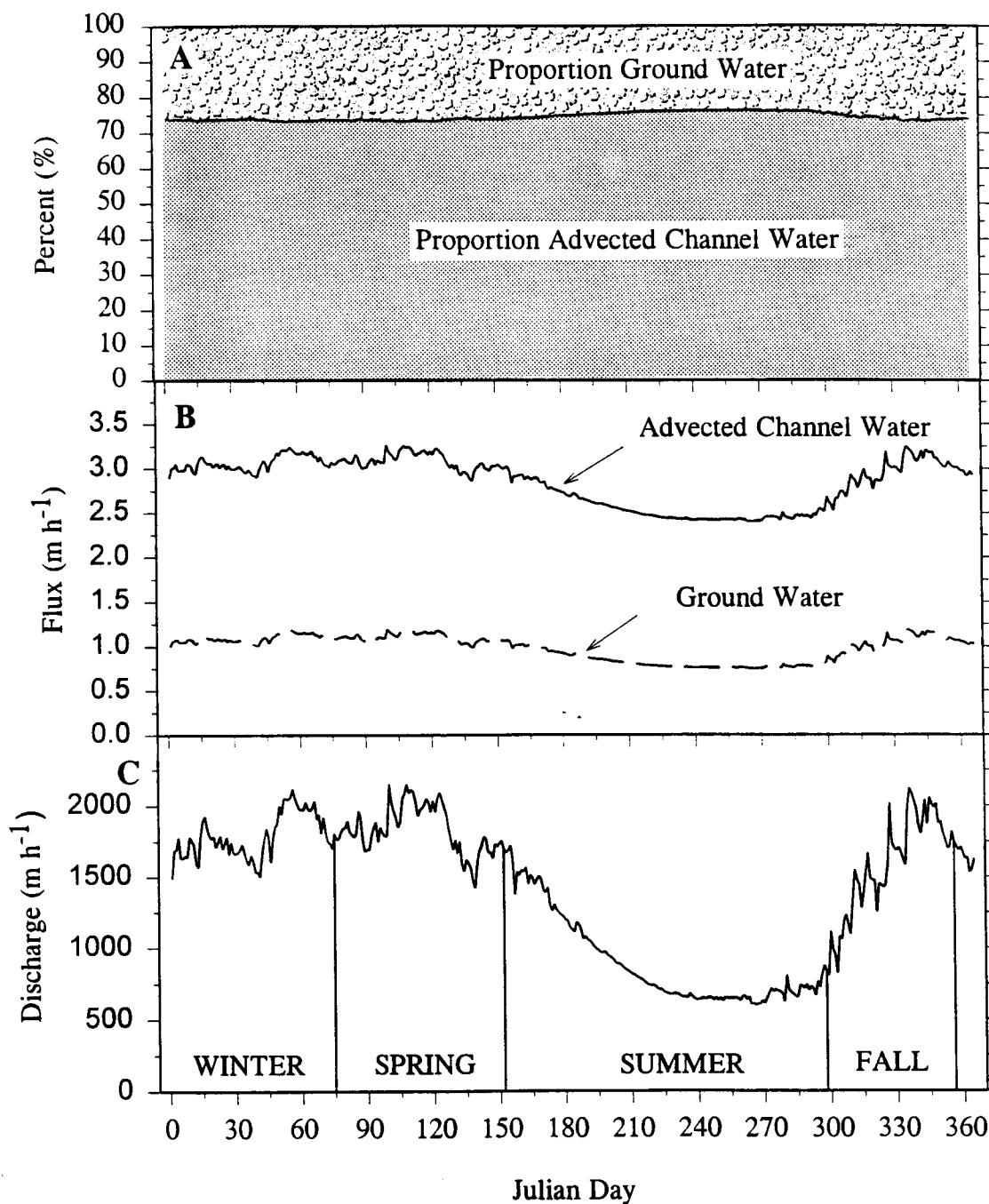
Table IV.1. Number of storms and storm days for each season of the year, and the percentage of storms in the small, intermediate and large storm classes. Data from Mack Creek stream gauge, H. J. Andrews Experimental Forest (unpublished data).

SEASON	# of STORMS	# of STORM DAYS	% SMALL STORMS	% MEDIUM STORMS	% LARGE STORMS
Winter 84 days	6.62	25.77	27.5	35.0	37.5
Spring 77 days	7.15	21.62	24.0	37.5	38.5
Summer 146 days	4.00	7.69	61.5	22.5	16.0
Fall 58 days	6.46	23.00	31.0	31.0	38.0

speculated by Meyer et al. (1988). However, this relationship was not maintained during storms, when the estimated flow of water through the gravel bar peaked at 3.3 m^3 h^{-1}, which was only 3% higher than during winter base flow. The total seasonal flux through the gravel bar was much greater in the summer than in the other seasons of the year, because of the length of the summer (Table IV.2).

After storms, precipitation drained rapidly from the gravel bar so that water table elevations quickly returned to steady-state levels. Consequently, the increased rates of subsurface flux during the rising and falling legs of the stream hydrograph were evenly distributed around the period of peak flow, each accounting for approximately 45% of the total ground water flux during the storm. The period of peak flow accounted for the remaining 10% (Fig. IV.1). Although the fluxes are asymetrical for the large storm class they closely match the pattern of precipitation (compare to the floodplain where the hydrograph is asymetric and does not match the pattern of precipitation).

The gravel bar had a total area of 825 m^2. Assuming an average aquifer thickness of 3 m and a specific yield of 0.30 for a gravelly sand (Dawson and Istok 1991), the gravel bar would store 740 m^3 of water. Consequently, the estimated mean residence time of this ground water in the gravel bar would range from 10 to 12 days during base-flow periods, given the range in the flow rates of advected channel water among seasons. The estimated mean residence time of water in the gravel bar was 9 days during storms because subsurface flow rates increase due to precipitation inputs. Precipitation during the six-day storm (Fig. IV.1, large storm class) was equal to 12% of the volume of water stored in the gravel bar.

Floodplain. Flow of advected channel water into the floodplain, and inputs from the floodplain GHB cells at the head of the model domain (Fig. II.2), were relatively constant over the course of the year at 0.67 and 0.30 m^3 h^{-1}, respectively (Fig. IV.3). Flow through the terrace GHB cells was more variable,

Table IV.2. Mean and total seasonal flux of stream water (McRae Creek); advected channel water through the gravel bar (Gravel bar); and ground water through the floodplain (Floodplain) for winter, spring, summer and fall during periods of base flow.

WINTER	BASEFLOW		58.2 days
22 Dec - 15 Mar	McRae Creek	Gravel Bar	Floodplain
Mean (m^3 h^{-1})	1773	3.05	1.66
Total (m^3)	2.48 x 10^6	4.26 x 10^3	2.31 x 10^3
SPRING	BASEFLOW		55.4 days
16 Mar - 31 May	McRae Creek	Gravel Bar	Floodplain
Mean (m^3 h^{-1})	1837	3.09	1.68
Total (m^3)	2.44 x 10^6	4.11 x 10^3	2.24 x 10^3
SUMMER	BASEFLOW		138.3 days
1 June - 23 Oct	McRae Creek	Gravel Bar	Floodplain
Mean (m^3 h^{-1})	901	2.57	1.30
Total (m^3)	3.43 x 10^6	8.53 x 10^3	4.32 x 10^3
FALL	BASEFLOW		35.0 days
24 Oct - 21 Dec	McRae Creek	Gravel Bar	Floodplain
Mean (m^3 h^{-1})	1571	2.94	1.57
Total (m^3)	1.32 x 10^6	2.47 x 10^3	1.32 x 10^3

Fig. IV.3. A) Proportion of the total subsurface flow through the floodplain accounted for by advected channel water from the stream flowing into the floodplain. and by ground water from the GHB cells at the head of the model domain (Floodplain GHB) or along the terrace boundary (Terrace GHB) flowing into the floodplain: B) Estimated daily flux of advected channel water, ground water from floodplain GHB cells, and ground water from terrace GHB cells flowing through the floodplain: and C) Thirteen year average of stream discharge for McRae Creek.
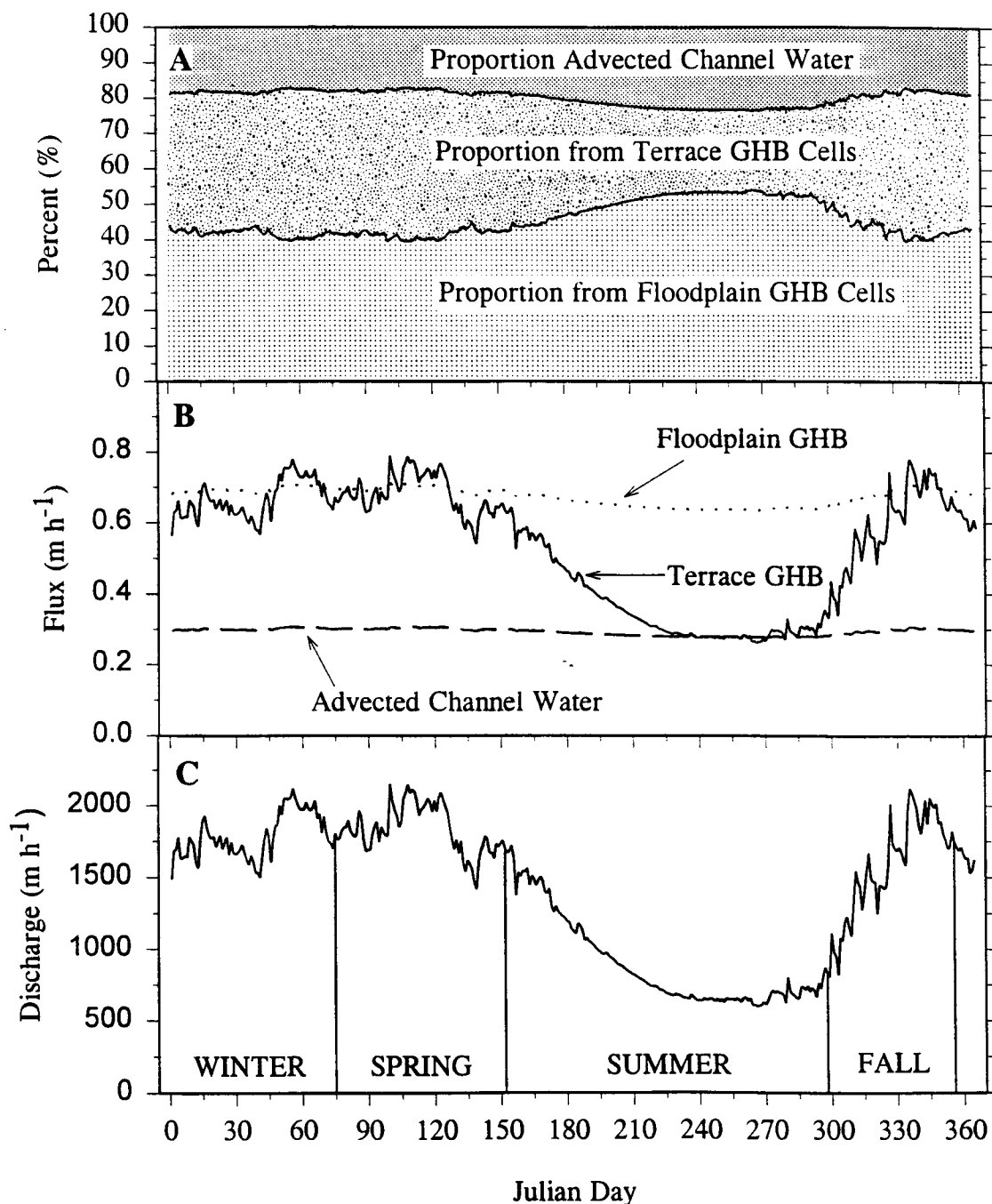
Table IV.3. Mean and total seasonal flux of stream water (McRae Creek); advected channel water and precipitation through the gravel bar (Gravel bar); and ground water and precipitation through the floodplain (Floodplain) for winter, spring, summer and fall during periods of storm flow.

WINTER	STORM		25.8 days
22 Dec - 15 Mar	McRae Creek	Gravel Bar	Floodplain
Mean (m^3 h^{-1})	5871	3.34	2.76
Total (m^3)	3.64 x 10^6	2.13 x 10^3	2.68 x 10^3
SPRING	STORM		21.6 days
16 Mar - 31 May	McRae Creek	Gravel Bar	Floodplain
Mean (m^3 h^{-1})	4312	3.34	2.76
Total (m^3)	2.24 x 10^6	2.35 x 10^3	2.97 x 10^3
SUMMER	STORM		7.7 days
1 June - 23 Oct	McRae Creek	Gravel Bar	Floodplain
Mean (m^3 h^{-1})	2352	3.34	2.76
Total (m^3)	0.43 x 10^6	0.92 x 10^3	1.10 x 10^3
FALL	STORM		23.0 days
24 Oct - 21 Dec	McRae Creek	Gravel Bar	Floodplain
Mean (m^3 h^{-1})	4353	3.34	2.76
Total (m^3)	2.40 x 10^6	2.07 x 10^3	2.58 x 10^3

accounting for more than 40% of the total ground water flux during the winter, but less than 15% during summer base flow. During storms the average of the estimated ground water flux was 2.8 m^3 h^{-1}, nearly double the flux through the floodplain during winter base flow periods (Table IV.3).

Water flow through the floodplain was dominated by precipitation throughout the simulated storm (Fig. II.15). Precipitation exceeded subsurface flow rates, consequently the water table levels rose as water was stored within the aquifer. The hydraulic conductivities in the finer sediments of the floodplain were lower than those of the gravel bar, resulting in greater storage within the floodplain aquifer, and much slower return to steady state conditions after the storm. A linear extrapolation based on the rates at which water drained from the aquifer during the final 24 hours of the transient simulation, or the period between 54 and 78 hours when little precipitation fell, suggests that it would take at least 5 days without rain for ground water fluxes to return to steady state (Fig. IV.1). Drainage of water from the aquifer during the falling leg of the hydrograph accounted for approximately 60% of the total ground water flux during the storm. Thirty percent of the total ground water flux occurred during the rising leg, and the period of peak flow accounted for the remainder, 11%.

The total flux of ground water through the floodplain was much less than the flow of advected channel water through the gravel bar under base flow conditions for every season of the year (Table IV.2). The floodplain had an area of 4000 m^2. Assuming an average aquifer thickness of 3 m and a specific yield of 0.20 for silt or sandy clays (Dawson and Istok 1991), the floodplain could store 2500 m^3 of water. The estimated mean residence time of this water varies from 57 to 87 days, given the range in the estimated subsurface flows among seasons. The estimated mean residence time of water in the floodplain was 31 days during storms because subsurface flow rates increase due to precipitation inputs. Precipitation during the six-day storm (Fig. IV.1, large storm class) was equal to 23% of the volume of water stored in the floodplain.

Nitrogen Flux

Subsurface flow through the aquifer adjacent to the stream was a net source of nitrogen to the stream in all seasons of the year and during storms. These fluxes may be standardized to a unit length of stream channel (stream perspective), or to a unit area of terrestrial forest (soil or forest perspective). The conifer-forested floodplain supplied the greatest amount of the nitrogen per unit length of stream - accounting for approximately two-thirds of the estimated inputs of nitrogen (Fig. IV.4). But, the area of the floodplain was five-time larger than that of the gravel bar. Consequently, on a per unit area basis, the gravel bar supplies more nitrogen to the stream than the floodplain during all seasons of the year (Fig. IV.5). The rates of nitrogen inputs are always greater during storms than during base flow, and the highest rate estimated was from the gravel bar during fall storms.

Gravel bar. Flow of advected channel water through the red-alder-dominated gravel bar and back to the stream supplied approximately one-third (340 g yr^{-1}) of the total estimated flux of nitrogen into the stream (Table IV.4). Storm inputs were approximately double base flow inputs during the fall. In other seasons, storm inputs were less than those estimated for base flow periods (Table IV.4). Biochemical processes in the subsurface of the gravel bar also transformed approximately 90 g of DON to NO_3^{-1}-N over the summer. These values translate to an estimated annual loss of nitrogen from the gravel bar to the stream of 4.2 kg ha^{-1} yr^{-1}, and an input of 1.1 kg ha^{-1} yr^{-1} of inorganic nitrogen from the transformation of DON.

The estimated annual loss of nitrogen from the gravel bar to the stream (4.2 kg ha^{-1} yr^{-1}) is approximately one-tenth of the estimated leaching losses from red alder stands in upland sites (Van Miegroet and Cole 1984; Binkley et al. 1994). However, leaching losses may be related to both the pool size of nitrogen in the soil and the rate of nitrogen fixation in the red alders. Neither the pool size or the rate of fixation is known. Most of the nitrogen fixed in upland red alder stands appears to accumulate in the soil (Bormann and DeBell 1981). The soils of the gravel bar are

Fig. IV.4. Nitrogen flux (per unit channel length) into the stream from the gravel bar, the floodplain, and from both landforms combined (total). Estimates are for base-flow periods (base), storms, or the entire season (season).
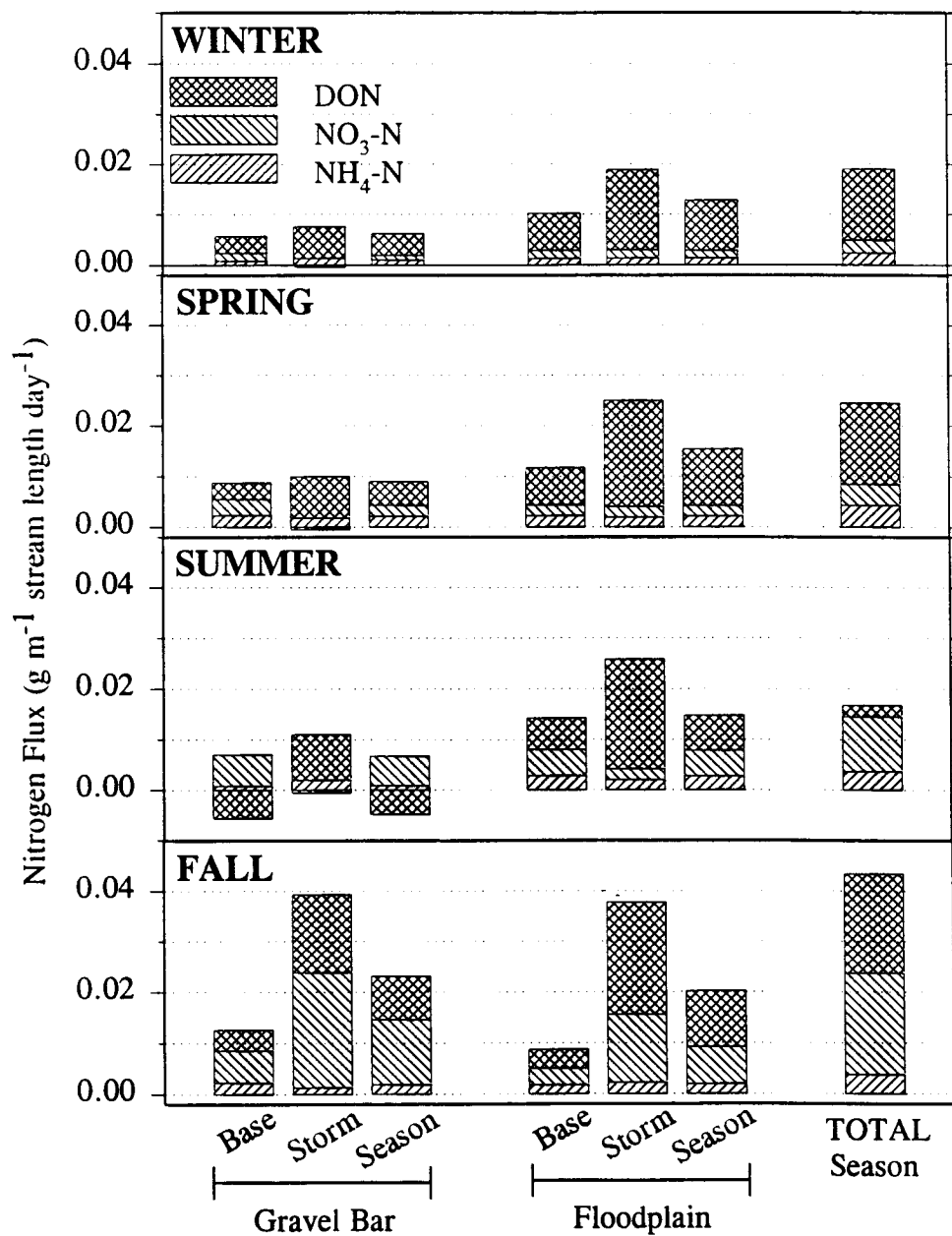
Fig. IV.5. Nitrogen flux (per unit land area) into the stream from the gravel bar, the floodplain, and from both landforms combined (total). Estimates are for base-flow periods (base), storms, or the entire season (season).
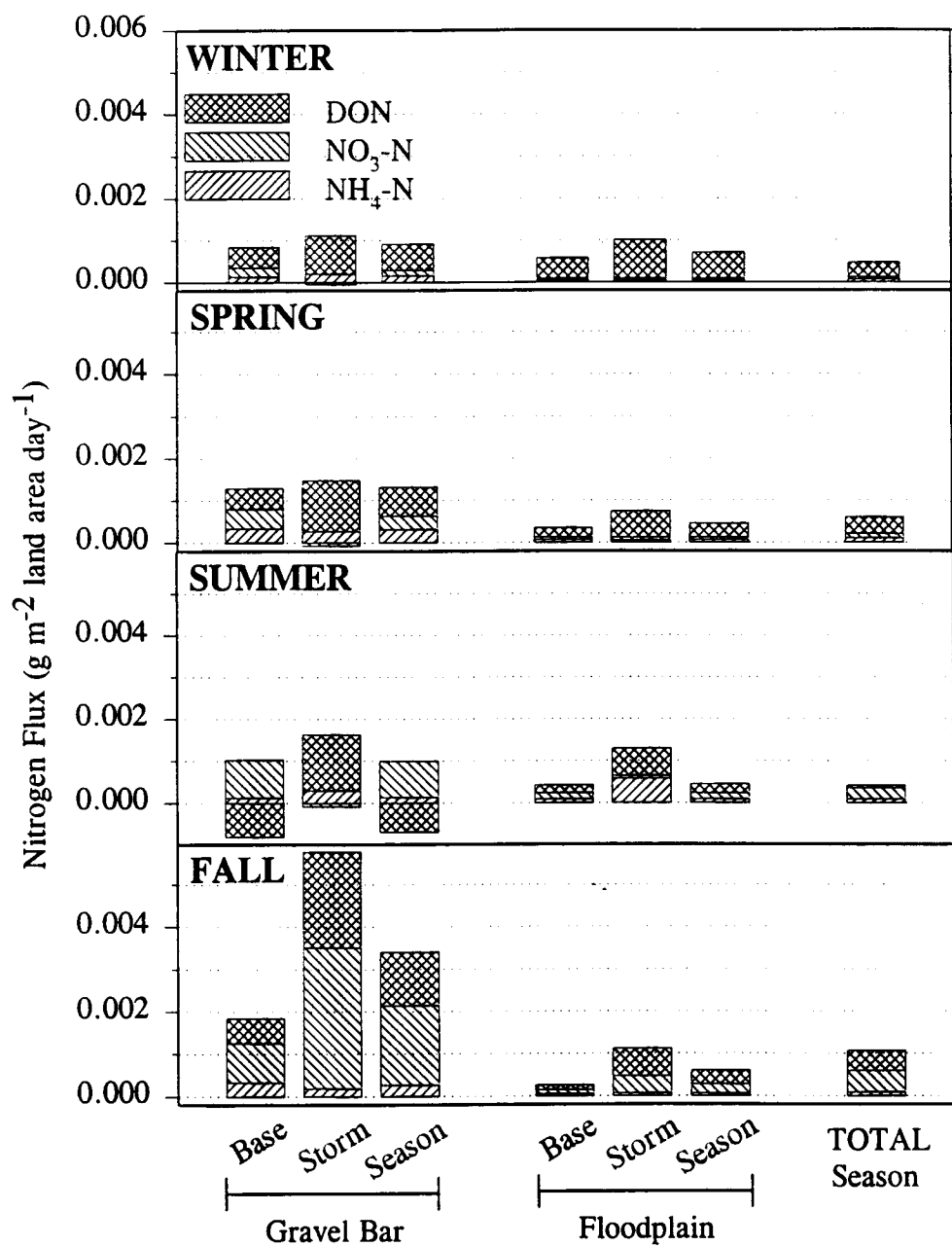
Table IV.4. Estimated inputs of nitrogen (g yr^{-1}) to the stream from the gravel bar and the floodplain for each season of the year during periods of base flow (base) and storm flow (storm).

WINTER	BASE		STORM	
	GRAVEL BAR	FLOOD PLAIN	GRAVEL BAR	FLOOD PLAIN
NH4-N	5.97	9.48	4.20	4.40
NO3-N	10.67	10.40	-1.17	4.94
DON	23.04	50.63	19.22	48.60
TDN	39.67	70.52	22.25	57.93
SPRING				
NH4-N	14.79	14.76	4.63	4.87
NO3-N	20.96	13.64	-1.29	5.46
DON	22.19	48.97	21.18	53.82
TDN	57.94	77.37	24.52	64.15
SUMMER				
NH4-N	13.63	46.08	1.82	1.80
NO3-N	102.25	85.71	-0.51	2.02
DON	-91.17	102.51	8.32	19.90
TDN	24.71	234.30	9.64	23.72
FALL				
NH4-N	9.14	7.13	3.40	5.98
NO3-N	26.19	13.61	61.85	36.61
DON	17.05	15.46	42.33	60.82
TDN	52.39	36.20	107.59	103.41

coarse textured and poorly developed, with little accumulation of organic matter at the surface. Nitrogen fixation rates may also be proportional to stocking density (Bormann and Gordon 1984). The gravel bar within the study site was poorly stocked with red alder, and most trees were young and quite small which might account for the small leaching losses observed in this study. Alder stands on other gravel bars along McRae Creek, and through out the west slope of the Cascade Range, are often older and with higher densities. If leaching losses from these gravel bars equaled leaching losses estimated for upland stands, gravel bars colonized by red alder and located along the stream network may be more important to the stream nitrogen budget than this study would indicate.

Studies have consistently shown that subsurface processes may be important to stream ecosystem functions (Hynes 1983, Mickleburgh 1984, Grimm and Fischer 1984, Grimm 1987, Triska et al. 1989, Valett et al. 1990, Vervier and Naiman 1992). I estimated that biochemical processes within the gravel bar mineralized approximately 1.1 kg of DON to NO_3^{-1}-N ha^{-1} yr^{-1}. However, I did not design this study to measure the extent to which these transformations may also occur within the sediments of the streambed. Chemical transformations are rate dependent processes and neither the rate at which mineralization occurs nor the residence time of advected channel water in the streambed is known. Certainly, large volumes of exchange flow would be expected in mountain stream because sediments are coarse textured and streambeds have a stepped morphology (Vaux 1962, Grant et al 1990, Harvey and Bencala 1993). Thus, if the rates of nitrogen mineralization are high in the sediments of the streambed, the total amount of DON transformed to NO_3^{-1} in the hyporheic zone may be much larger than I estimated.

Floodplain. The greatest single source of nitrogen to the stream water was the floodplain, which supplied approximately two-thirds (670 g yr^{-1}) of the total inputs of nitrogen (Table IV.3). The dominant form was DON, and the largest fluxes occurred during the summer. This suggests an input of 1.7 kg ha^{-1} yr^{-1}, approximately the same nitrogen flux to ground water as was reported by Sollins et al. (1980) for

leaching below the rooting zone ($>$2-m depth) in an upland, old-growth Douglas-fir forest. However, my estimate includes both direct losses from the terrestrial ecosystem on the floodplain as well as the nitrogen lost from hillslope locations and transported through the floodplain. A trend towards increasing concentrations of TDN, with distance along flow paths through the floodplain, would be expected if nitrogen was being leached into the ground water. This was not observed, suggesting that either little leaching occurs or that plant uptake, immobilization, or denitrification prevent accumulation of nitrogen in the ground water along these flow paths. It was not possible to separate the effect of nitrogen inputs from the adjacent hillslopes from the effect of biochemical processes occurring within the floodplain because the total source area for ground water inputs was unknown and because wells were not located at the hillslope boundary.

Conclusions

Subsurface flows at the McRae Creek study site were dominated by the flow of advected channel water through the gravel bar. Subsurface flows through the gravel bar did not increase during storms. Ground water flows through the aquifer beneath the floodplain were small during base flow, but nearly doubled during storm events. The mean residence time of water stored within the aquifer was long, exceeding 10 days for the gravel bar and 30 days for the floodplain. Even though precipitation inputs to the aquifer during storms equaled 12% of the water stored in the gravel bar and 23% of the water stored in the floodplain, the mean residence time of water remained long.

Subsurface flow through the aquifer adjacent to the stream was a net source of nitrogen to the stream in all seasons of the year and during storms. Flows of water through the conifer-forested floodplain supplied most of the nitrogen per unit length of stream - accounting for approximately two-thirds of the estimated flux. Even though stands of red alder growing on recently disturbed sites along the stream channel fix nitrogen, the gravel bar was not the primary source of nitrogen for the stream, because the area of gravel bar is quite small relative to the total size of the floodplain. However, on a unit area basis, flows of water through the red alder dominated gravel bar supplied approximately 2.5 times more nitrogen to the stream than did the floodplain, and NO_3^- was the dominant form. Since the advected channel water is highly oxygenated, little denitrification losses would be expected, so most of the nitrate would be returned to the stream.

The rates of nitrogen inputs are always greater during storms than during base flow, and the highest rate estimated was from the gravel bar during fall storms. The highest rates of subsurface water flow occurred during storms, and appeared to flush nitrogen stored within the soil into the aquifer. However, leaching losses of nitrogen during storm events were large only during the fall, at the beginning of the rainy season. Either the pool of mobile nitrogen is quite small, or the rates of biotic processes that produce mobile nitrogen are much reduced during the winter.

Both ground water and advected channel water were enriched in nitrogen, relative to the stream. However, flows of water through the aquifer adjacent to McRae Creek were always many orders of magnitude smaller than stream discharge. Therefore, only a small amount of nitrogen is transported into the stream via subsurface flow. If the McRae Creek study site is representative of the mix of landforms and forest types in unconstrained stream reaches along the stream network; then I estimate that 2 kg ha^{-1} yr^{-1} are leached from riparian forests into the aquifer, and transported to the stream in the subsurface flow. The study site covered only one-half of the valley floor. Assuming that similar fluxes occurred from the opposite side of the valley, I estimate that 17 g of nitrogen yr^{-1} m^{-1} channel length are input to the stream. The stream is approximately 10 m wide, thus these inputs equal 1.7 g N m^{-2} streambed yr^{-1}.

The fluxes of nitrogen estimated in this study are much lower than I expected given the presence of red alders on the gravel bar, published leaching rates for red alder stands, and the framework of the conceptual model presented in Chapter #1. The estimated nitrogen inputs to the stream are also small relative to expected nitrogen inputs from other sources, and both pools sizes and the rate of nitrogen cycling within the stream. Triska et al. (1984), estimated that annual inputs of nitrogen to a steam in a nearby, headwater chatchment were 11 g m^{-2} in subsurface water flow and 1.3 g m^{-2} in litterfall. The particulate organic nitrogen pool in this stream was 12 g m^{-2}, and the stream lost 8.8 g m^{-2} yr^{-1} of dissolved nitrogen to downstream transport, most of which was DON. For comparison, I estimate the flux of nitrogen dissolved in the stream water, flowing past any point in the stream channel at the McRae Creek study site was approximately 1.2 x 10^{-3} g yr^{-1}. However, the dominant form of nitrogen in the water of McRae Creek is DON, and much of this may be in complex organic compounds not readily transformed by biochemical processes (Dahm 1980).

The influence of the hyporheic zone on the stream nitrogen budget may be much larger than this study would indicate. First, biochemical processes occurring in the aquifer beneath the gravel bar transformed DON to NO_3^{-1} during the summer. I did not design this study to quantify the effect of biochemical transformations

occurring that may occur within the sediments of the streambed. Thus, if the rates of nitrogen mineralization are high in the sediments of the streambed, the total amount of DON transformed to NO_3^{-1} in may be larger than I estimated. Similarly, the gravel bar within the study site was poorly stocked with red alder, and most trees were young and quite small. Alders are often older and grow in higher densities on other gravel bars along McRae Creek. If leaching losses from these gravel bars equaled leaching losses estimated for upland stands, gravel bars colonized by red alder and located along the stream network may be more important to the stream nitrogen budget than this study would indicate.

LITERATURE CITED

Anderson, M. P., and W. W. Woessner. 1992. Applied Ground Water Modeling: Simulation of Flow and Advective Transport. Academic Press, Inc. 381 pp.

Bencala, K. E., Kennedy, V. C., Zellweger, G. W., Jackman, A. P., Avanzino, R. J. 1984. Interactions of soulutes and streambed sediment: 1. An experimental analysis of cation and anion transport in a mountain stream. Water Resources Research 20:1797-1803.

Bevin, K., and P. Germann. 1982. Macropores and water flow in soils. Water Resources Research 18:1311-1325.

Bierlmaier, F. A., and A. McKee. 1989. Climatic summaries and documentation for the primary meteorological station, H.J. Andrews Experimental Forest, 1972 to 1984. USDA Forest Service, General Technical Report, Portland, OR.

Binkley, D., K. Cromack, Jr., and D. D. Baker. (1994). Nitrogen fixation by red alder: Biology, rates, and controls. *In*: D. Hibbs, D. DeBell, and R. F. Tarrant (eds.) Biology and management of alder. Oregon State University Press, Corvallis OR.

Bollen, W. B., and K. C. Lu. 1968. Nitrogen transformations in soils beneath red alder and conifers. pp. 141-148. *In*: J.M. Trappe, J.F. Franklin, R.F. Tarrant, and G.M. Hansen (eds.). *Biology of Alder*. U.S.D.A. Forest Service, Portland OR.

Bormann, B. T., and D. S. DeBell. 1981. Nitrogen content and other soil properties related to age of red alder stands. Soil Science Society of America Journal 45:428-432.

Bormann, B. T., and J. C. Gordon. 1984. Stand density effects in young red alder plantations: Productivity, photosynthate partitioning, and nitrogen fixation. Ecology 65:394-402.

Bott, T. L., L. A. Kaplan, and F. T. Kuserk. 1984. Benthic bacterial biomass supported by streamwater dissolved organic matter. Microbial Ecology 10:335-344.

Bouwer, H. 1989. The Bouwer and Rice slug test - an update. Ground Water 27:304-309.

Bouwer, H., and R. C. Rice. 1976. A slug test for determining hydraulic conductivities of unconfined aquifers with completely or partially penetrating wells. Water Resources Research 12:423-428.

Castro, N. M., and G. M. Hornberger. 1991. Surface-subsurface water interactions in an alluviated mountain stream channel. Water Resources Research 27:1613-1621.

Coats, R. N., R. L. Leonard, and C. R. Goldman. 1976. Nitrogen uptake and release in a forested watershed, Lake Tahoe basin, California. Ecology 57:995-1004.

Cole, D. W., S. P. Gessel, and J. Turner. 1978. Comparative mineral cycling in red alder and Douglas-fir. Pages 327-336 *In*. D. G. Briggs, D. S. DeBell, and W. A. Atkinson (eds.) Utilization and management of alder. USFS General Technical Report PNW-70.

Coleman, M. J. and H. B. N. Hynes. 1970. The vertical distribution of the invertebrate fauna in the bed of a stream. Limnol. Oceanogr. 15:31-40.

Cummins, K.W. 1975. Macroinvertebrates. Pgs. 170-198. *In*: M.A. Whitton (ed.) River Ecology. University of California Press, Berkley, CA.

Cummins, K. W., M. J. Klug, R. G. Wetzel, R. C. Peterson, K. F. Suberkropp, B. A. Manny, J. C. Waycheck, and F. O. Howard. 1972. Organic enrichment with leaf leachate in experimental lotic ecosystems. BioScience 22:719-722.

Dahm, C. N. 1980. Studies on the distribution and fates of dissolved organic carbon. Ph.D. Thesis. Oregon State University.

Dawson, K. J. and J. D. Istok. 1991. Aquifer Testing. Design and Analysis of Pumping and Slug Tests. Lewis Publ.

Duff, J. H., and F. J. Triska. 1990. Denitrification in sediments from the hyporheic zone adjacent to a small forested stream. Canadian Journal of Fisheries and Aquatic Sciences.

Elwood, J. W., J. D. Newbold, R. V. O'Neill, W. Van Winkle. 1983. Resource spiraling: An operational paradigm for analizing lotic ecosystems. Pages 3-27. In: W. T. Fontaine III, and S. M. Bartell (eds.) Dynamics of Lotic Ecosystems. Ann Arbor Science Publishers, Ann Arbor, MI, USA.

Ford, T. E., and R. J. Naiman. 1989. Groundwater - Surface water relationships in boreal forest watersheds: Dissolved organic carbon and inorganic nutrient dynamics. Canadian Journal of Fisheries and Aquatic Science 46:41-49.

Frissell, C. A., W. J. Liss, C. E. Warren, and M. D. Hurley. 1986. A hierarchical framework for stream habitat classification: Viewing streams in a watershed context. Environmental Management 10:199-214.

Grant, G. E., F. J. Swanson, and M. G. Wolman. 1990. Pattern and origin of stepped-bd morphology in high-gradient streams, Western Cascades, Oregon. Geological Society of America Bulletin. 102:340-352.

Gelhar, L. W. 1986. Stochastic subsurface hydrology from theory to applications. Water Resources Research (Supplement) 22:135S-145S.

Greenberg, A. E., J. J. Connors, and D. Jenkins (eds). 1980. Standard methods for the examination of water and wastewater. American Public Health Association, Washington D.C. 15th edition. 1134 p.

Gregory, S. V. 1979. Primary production in Pacific Northwest streams. Ph.D. dissertation. Oregon State University, Corvallis. 96 p.

Gregory, S.V., F.J. Swanson, A. McKee, and K.W. Cummins. (1991). An ecosystem perspective on riparian zones. BioScience 41:540-551.

Grimm, N. B. 1987. Nitrogen dynamics during succession in a desert stream. Ecology 68:1157-1170.

Grimm, N. B., and S. G. Fisher. 1984. Exchange between interstitial and surface water: Implications for stream metabolism and nutrient cycling. Hydrobiologia 111:219-228.

Harvey, J. W., and K. E. Bencala. 1993. The effect of streambed topography on surface-subsurface water exchange in mountain catchments. Water Resources Research 29:89-98.

Hynes, H. B. N. 1970. The ecology of running waters. Liverpool University Press, Liverpool, 555 p.

Hynes, H. B. N. 1983. Groundwater and stream ecology. Hydrobiologia 100:93-99.

Jordan, T. E., D. L. Correll, and D. W. Weller. 1993. Nutrient interception by a riparian forest receiving inputs from adjacent cropland. Journal of Environmental Quality 22:467-473.

Larkin, R. G., and J. M. Sharp, Jr. 1992. On the relationship between riber-basin geomorphology, aquifer hydraulics, and ground-water flow direction in alluvial aquifers. Geological Society of America Bulletin 104:1608-1620.

Loch, M. A., and H. B. N. Hynes. 1975. The dissapearance of four leaf leachates in a hard and soft water stream in south western Ontario, Canada. Int. Rev. Ges. Hydrobiol. 60:847-855.

Loch, M. A., and H. B. N. Hynes. 1976. The fate of "dissolved" organic carbon derived from autumn-shed maple leaves (*Acer saccharum*) in a temperate hardwater stream. Limnology and Oceanography 21:436-443.

Loch, M. A., R. R. Wallace, J. W. Costerton, R. M. Ventullo, and S. E. Charlton. 1984. River epilithon: toward a structural-functional model. Oikos 42:10-22.

McDonald, M. G. and A. W. Harbaugh. 1988. A modular three-dimensional finite-difference ground-water flow model. U.S.D.I., United States Geological Survey, Reston, VI.

McDonald, M. G., A. W. Harbaugh, B. R. Orr, and D. J. Ackerman. 1991. A method of converting no-flow cells to variable-head cells for the U.S. Geological Survey modular finite-difference ground-water flow model. U.S.G.S. Open-File Report 91-536.

McDowell, W. H., W. B. Bowden, and C. E. Asbury. 1992. Riparian nitrogen dynamics in two geomorphically distinct tropical rain forest watersheds: Subsurface solute patterns. Biogeochemistry 18:53-75.

Mickleburgh, S., M. A. Lock, and T. E. Ford. 1984. Spatial uptake of dissolved organic carbon in river beds. Hydrobiologia 108:115-119.

Minshall, G. W., R. C. Petersen, K. W. Cummins, T. L. Bott, J. R. Sedell, C. E. Cushing, and R. L. Vannote. 1983. Interbiome comparison of stream ecosystem dynamics. Ecological Monographs 53:1-25.

Meyer, J. L., W. H. McDowell, T. L. Bott, J. W. Elwood, C. Ishizaki, J. M. Melack, B. L. Peckarsky, B. J. Peterson, and P. A. Rublee. 1988. Elemental dynamics in streams. Journal of the North American Benthological Society 7:410-432.

Newbold, J. D., J. W. Elwood, R. V. O'Neill, and A. L. Sheldon. 1983. Phosphorus dnamics in a woodland stream ecosystem: A study of nutrient spiralling. Ecology 64:1249-1265.

Newton, M., B. A. El Hassan, and J. Zavitkovski. 1968. Role of red alder in western Oregon forest succession. Pgs. 73-84. *In*: J. Trappe, J. Franklin, R. Tarrant, and G. Hansen (eds.) Biology of Alder. US Forest Service, Portland OR.

Peterjohn, W. T. and D. L. Correll. 1984. Nutrient dynamics in an agricultural watershed: Observations on the role of riparian forest. Ecology 65:1466-1475.

Pinay, G., and H. DeCamps. 1988. The role of riparian woods in regulating nitrogen fluxes between the alluvial aquifer and surface water: A conceptual model. Regulated Rivers: Research and Management 2:507-516.

Pringle, C. M. 1987. Effects of water and substratum nutrient supplies on lotic periphyton growth: an integrated bioassay. Canadian Journal of Fisheries and Aquatic Sciences 44:619-629.

Pringle, C. M., and J. A. Bowers. 1984. An in situ substratum fertilization technique: diatom colonization on nutient-enriched, sand substrate. Canadian Journal of Fisheries and Aquatic Sciences 41:1247-1251.

Prudic, D. E. 1989. Documentation of a computer program to simulate stream-aquifer relations using a modular, finite difference ground-water flow model. USGS, Open-File Report 88-729. 113 pp.

Rhodes, J., C. M. Skau, D. Greenlee,and D. L. Brown. 1985. Quantification of nitrate uptake by riparian forests and wetlands in an undisturbed headwaters watershed. In:Riparian ecosystems and their management: Reconciling conflicting uses. First North American Riparian Conference. University of Arizona, Tucson, AZ. April 16-18, 1985. pgs. 175-179.

Savant, S. A., D. D. Reible, and L. J. Thibodeaux. 1987. Convective transport within stable river sediments. Water Resources Research 23:1763-1768.

Sedell, J. R., J. E. Richey, and F. J. Swanson. 1989. The river continuum concept: A basis for the expected ecosystem behavior of very large rivers? p. 49-55. In: D. P. Dodge (ed.) Proceedings of the international large river symposium. Canadian Special Publication of Fisheries and Aquatic Sciences 106.

Schumm, S. 1977. The fluvial system. John Wiley, New York.

Seyfried, M. S., and P. S. C. Rao. 1987. Solute transport in undisturbed columns of an aggregated tropical soil: Preferential flow effects. Soil Science Society of America Journal 51:1434-1444.

Sollins, P., C. C. Grier, F. M. McCorison, K. Cromack, Jr., R. Fogel, and R. L. Fredriksen. 1980. The internal element cycles of an old-growth Douglas-fir ecosystem in western Oregon. Ecological Monographs 50:261-285.

Sollins, P., and F.M. McCorison. 1981. Nitrogen and carbon solution chemistry of an old-growth coniferous forest watershed before and after cutting. Water Resources Research 17:1409-1418.

Sollins, P. and R. Radulovich. 1988. Effects of soil physical structure on solute transport in a weathered tropical soil. Soil Science Society of America Journal 52:1168-1173.

Stanford, J. A., Ward, J. V. 1988. The hyporheic habitat of river ecosystems. Nature 335:64-66.

Stoertz, M.W., and K.R. Bradbury. 1989. Mapping recharge areas using a ground-water flow model - a case study. Ground Water 27(2):220-229.

Swanson, F. J., R. L. Fredriksen, and F. M. McCorison. 1982b. Material transfer in a western Oregon forested watershed. pp. 233-266. *In*: R.L. Edmonds (ed.) Analysis of coniferous forest ecosystems in the western United States. US/IBP Synthesis Series 14. Hutchinson Ross Publ. Co., Stroudsburg, PA.

Swanson, F. J., S. V. Gregory, J. R. Sedell, and A. G. Campbell. 1982a. Land-water interactions: The riparian zone. pp. 267-291. *In*: R.L. Edmonds (ed.) Analysis of coniferous forest ecosystems in the western United States. US/IBP Synthesis Series 14. Hutchinson Ross Publ. Co., Stroudsburg, PA.

Swanson, F. J., and R. E. Sparks. 1990. Long-term ecological research and the invisible place. BioScience 40:502-508.

Thomas, G. W., and R. E. Phillips. 1979. Consequences of water movement in macropores. Journal of Environmental Quality 8:149-152.

Tripp, L. N., D. F. Bezdicek, and P. E. Heilman. 1979. Seasonal and diurnal patterns and rates of nitrogen fixation by young red alder. Forest Science 25:371-380.

Triska, F. J., J. H. Duff, and R. J. Avanzino. 1990. Influence of exchange flow between the channel and hyporheic zone on nitrate production in a small mountain stream. Canadian Journal of Fisheries and Aquatic Science 47:2099-2111.

Triska, F. J., V. C. Kennedy, R. J. Avanzio, G. W. Zellweger, and K. E. Bencala. 1989. Retention and transport of nutrients in a third-order stream in northwestern California: Hyporheic processes. Ecology 70:1893-1905.

Triska, F. J., J. R. Sedell, and K. Cromack Jr. 1984. Nitrogen budget for a small coniferous forest stream. Ecological Monographs 54:119-140.

Valett, H. M., Fisher, S. G., and Stanley, E. H. 1990. Physical and chemical characteristics of the hyporheic zone of a Sonoran desert stream. Journal of the North American Benthological Society 9:201-215.

Vannote, R. L., G. W. Minshall, K. W. Cummins, J. R. Sedell, and C. E. Cushing. 1980. The river continuum concept. Canadian Journal of Fisheries and Aquatic Sciences 37:130-137.

Van Miegroet, H., and D. W. Cole. 1984. The impact of nitrification on soil acidification and cation leaching in a red alder ecosystem. Journal of Environmental Quality 13:586-590.

Vaux, W. G. 1962. Interchange of stream and intragravel water in a salmon spawning riffle. USDI, US Fish and Wildlife Service, Special Scientific Report -- Fisheries No. 405 405:1-12.

Vaux, W. G. 1968. Intragravel flow and interchange of water in a streambed. Fisheris Bulletin. 66:479-489.

Vervier, P., and R. J. Naiman. 1992. Spatial and temporal fluctuations of dissolved organic carbon in subsurface flow of the Stillaguamish River, (Washington, USA). Archiv f. Hydrobiologie 123:401-412.

Wallis, P. M., H. B. N. Hynes, and S. A. Telang. 1981. The importance of ground-water in the transportation of allochthonous organic matter to the streams draining a small mountain basin. Hydrobiologia 79:77-90.

Waring, R. H. and W. H. Schlesinger. 1985. Forest ecosystems: Concepts and management. Academic Press, Inc., New York.

Worthington, N. P. 1965. Red alder (*Alnus rubra* Bong.). pp. 83-88. *In*: H.A. Fowells (ed.). Silvics of forest trees in the United States. U.S.D.A., Agricultural Handbook 271.